



**UNIVERSITÀ DEGLI STUDI DI MILANO**

**DIPARTIMENTO DI SCIENZE PER GLI ALIMENTI, LA  
NUTRIZIONE, L'AMBIENTE**

**DOTTORATO IN FOOD SYSTEMS**

**CICLO XXX**

**New integrated approaches for the development of  
biocatalytical processes**

Docente guida: Prof. Francesco Molinari

Direttore del corso di dottorato: Prof. Francesco Bonomi

Tesi di Dottorato di:

Valerio De Vitis

Matricola n. R10868

Anno Accademico 2017/2018



This PhD project has been structured into three parts preceded by a general introduction on basic biocatalysis concepts.

Part 1: The recombinant preparation coupled with biochemical and structure characterization a thermostable carboxylesterase (BCE) from *Bacillus coagulans* NCBI 9365. This enzyme showed high enantioselectivity towards different 1,2-*O*-isopropylidenglycerol esters (acetate, butyrate and benzoate). Both enantiopure of 1,2-*O*-isopropylidenglycerol (IPG or solketal), a chiral equivalent of glycerol, are building blocks for the synthesis of  $\beta$ -blockers, glycerophospholipids and prostaglandins.

Part 2: An insight on the biocatalytic potential of Acetic Acid Bacteria (AAB), a group of bacteria well-known for the ability to oxidize primary and secondary alcohols into partially oxidized organic compounds (aldehydes, carboxylic acids and ketones) as end-products. This part collect three chapters:

- the stereoselective desymmetrisation of achiral 2-alkyl-1,3-diols performed by oxidation of one of the two enantiotopic primary alcohol moieties by means of *Acetobacter aceti* MIM 2000/28 free whole cells to afford the corresponding chiral 2-hydroxymethyl alkanolic acids in batch system
- Chemoenzymatic flow synthesis of enantiomerically pure captopril, a widely used antihypertensive drug, with the particular focus on the enzymatic step carried on with immobilized cells of *Acetobacter aceti* MIM 2000/28 used in a continuous flow reactor.
- Productivity and stability of the air-liquid flow system setted up in the previous work, has been studied and optimized, through the use of immobilized form *Acetobacter aceti* MIM 2000/28 in the oxidation of 2-methyl-1,3-propanediols. To verify the real efficiency of the system, the experiment with other substrate will be carried out.

Part 3: Hydroxylation of (*R*)-limonene into (*R*)-perillyl alcohol studied using recombinant whole cells harbouring an optimized redox gene operon (CYP153A6) which encodes a cytochrome P450, a ferredoxin, and a ferredoxin reductase from *Mycobacterium* sp. HXN-1500-

Questa tesi di Dottorato è stata strutturata in tre parti, una per ogni tipo di attività enzimatica trattata, preceduta da una breve introduzione riguardante i principi fondamentali della biocatalisi.

Parte 1: Sono state studiate le caratteristiche strutturali e biochimiche dell'esterasi (BCE) prodotta per via ricombinante da *Bacillus coagulans* NCBI 9365. Questo enzima mostra un elevato grado di selettività nei confronti degli esteri (acetato, butirato e benzoato) dell'1,2-*O*-isopropilidenglicerolo (IPG) un acetale equivalente chirale del glicerolo, che in entrambe le configurazioni, è un utile prodotto di partenza per la sintesi di molecole naturali biologicamente attive di interesse alimentare e farmaceutico come gliceridi, glicerofosfolipidi,  $\beta$ -bloccanti ed antiipertensivi

Parte 2: Sono state studiate le potenzialità biocatalitiche di batteri acetici, microrganismi noti per la loro capacità di accumulare prodotti di ossidazione (aldeidi, chetoni e acidi carbossilici) dati dalla trasformazione di alcoli primari e secondari. Questa parte risulta ulteriormente suddivisa in tre capitoli:

- La desimmetrizzazione stereoselettiva di dioli achirali diversamente sostituiti, è stata eseguita ottenendo i corrispettivi acidi chirali utilizzando, cellule intere di *Acetobacter aceti* MIM 2000/28
- È stata studiata la sintesi chemo-enzimatica della forma enantiopura del captopril, noto farmaco utilizzato per il trattamento dell'ipertensione. Particolare attenzione è stata dedicata allo step enzimatico catalizzato da cellule immobilizzate di *Acetobacter aceti* MIM 2000/28 utilizzate in un sistema in continuo di "flow chemistry".
- La produttività e la stabilità del sistema di ossidazione "flow chemistry" è stato studiato e ottimizzato attraverso l'utilizzo del 2-metil 1,3 propandiolo. Per testare la reale efficienza del sistema in continuo messo a punto, sono in corso di studio le prove effettuate con ulteriori substrati.

Parte 3: L'idrossilazione del (R) -limonene in (R)-alcol-perililico è stata studiata attraverso l'utilizzo di cellule intere ricombinanti di *E. coli* trasformate con l'operone sintetico

ottimizzato che codifica per una citocromo P450 monossigenasi (CYP153A6), una ferredossina e una ferredossina riduttasi isolate dal ceppo *Mycobacterium sp.* HXN-1500



---

**INTRODUCTION** **11****CIRCULAR ECONOMY AND BIOECONOMY** **12****THE ROLE OF GREEN CHEMISTRY** **15****BIOPROCESSES AND BIOECONOMY** **17****MODERN BIOCATALYSIS** **17**Screening of biocatalyst 18Biocatalyst form 19Biocatalyst characterization 21Protein and metabolic engineering 22Process engineering 22**EXAMPLE OF BIOCATALYTICAL PROCESS: FOS PRODUCTION** **25****REFERENCES** **27**

---

**AIM OF THE PROJECT** **31****CHARACTERIZATION AND CRYSTAL STRUCTURE OF A STEREOSELECTIVE****CARBOXYLESTERASE FROM *BACILLUS COAGULANS*** **33****ABSTRACT** **34****INTRODUCTION** **35****MATERIALS AND METHODS** **37****RESULTS** **41****DISCUSSION** **60****CONCLUSION** **63****REFERENCES** **64****SYNTHESIS OF ENANTIOMERICALLY ENRICHED 2-HYDROXYMETHYLALKANOIC ACIDS BY  
OXIDATIVE DESYMMETRISATION OF ACHIRAL 1,3-DIOLS MEDIATED BY *ACETOBACTER******ACETI*** **69**

---

<b>ABSTRACT</b>	<b>70</b>
<b>INTRODUCTION</b>	<b>71</b>
<b>EXPERIMENTAL SECTION</b>	<b>73</b>
<b>RESULTS AND DISCUSSION</b>	<b>81</b>
<b>CONCLUSIONS</b>	<b>90</b>
<b>REFERENCES</b>	<b>92</b>

### **CHEMOENZYMATIC SYNTHESIS IN FLOW REACTORS: A RAPID AND CONVENIENT**

<b><u>PREPARATION OF CAPTOPRIL</u></b>	<b><u>97</u></b>
--	------------------

<b>ABSTRACT</b>	<b>98</b>
<b>INTRODUCTION</b>	<b>99</b>
<b>EXPERIMENTAL SECTION</b>	<b>101</b>
<b>RESULTS AND DISCUSSION</b>	<b>106</b>
<b>CONCLUSIONS</b>	<b>112</b>
<b>REFERENCE</b>	<b>113</b>

### **BIOPROCESS INTENSIFICATION USING FLOW REACTORS: STEREOSELECTIVE OXIDATION**

<b><u>OF ACHIRAL 1,3-DIOLS WITH IMMOBILIZED <i>ACETOBACTER ACETI</i></u></b>	<b><u>115</u></b>
--	-------------------

<b>ABSTRACT</b>	<b>116</b>
<b>INTRODUCTION</b>	<b>117</b>
<b>MATERIAL AND METHOD</b>	<b>119</b>
<b>RESULTS</b>	<b>121</b>
<b>CONCLUSIONS</b>	<b>125</b>
<b>REFERENCES</b>	<b>126</b>

### **BIOTRANSFORMATION OF LIMONENE FROM CITRUS PEEL INTO FOOD RELEVANT**

<b><u>ADDITIVES</u></b>	<b><u>129</u></b>
-------------------------	-------------------



<b>ABSTRACT</b>	<b>130</b>
<b>INTRODUCTION</b>	<b>131</b>
<b>MATERIAL AND METHOD</b>	<b>135</b>
<b>RESULT AND DISCUSSION</b>	<b>137</b>
<b>CONCLUSION AND FUTURE PERSPECTIVES</b>	<b>140</b>
<b>REFERENCES</b>	<b>142</b>
<b>PRODUCTS</b>	<b>145</b>
<hr/>	
<b>LIST OF PUBLICATION</b>	<b>146</b>
<b>CONGRESS PROCEEDINGS</b>	<b>148</b>



# Introduction





*Fig. 2 Schematic representation of circular economic model*

The circular economy is based on three principles (Fig 3):

- Principle 1: Preserve and enhance natural capital
- Principle 2: Optimise resource yields
- Principle 3: Improve system effectiveness

The circular economy is a model built to “auto-regenerate”. The key point is composed by the biological and technical cycle, which include all processes that are able to add value to waste materials. It is also a kind of economy able to “restore” because is based on the used renewable energy and sources in order to minimize the waste production and uses of polluting substances. Moreover, the circularity of economy not only concerns about the possibility to re-use, recycle and regenerate the waste material (defined “leakages” of the different stage of production), but also the possibility to prevent the leakages accumulation, reducing and regulating the flow and the quantity of raw material incoming in economic system<sup>2</sup>.

PRINCIPLE

1

Preserve and enhance natural capital by controlling finite stocks and balancing renewable resource flows  
 ReSOLVE levers: regenerate, virtualise, exchange



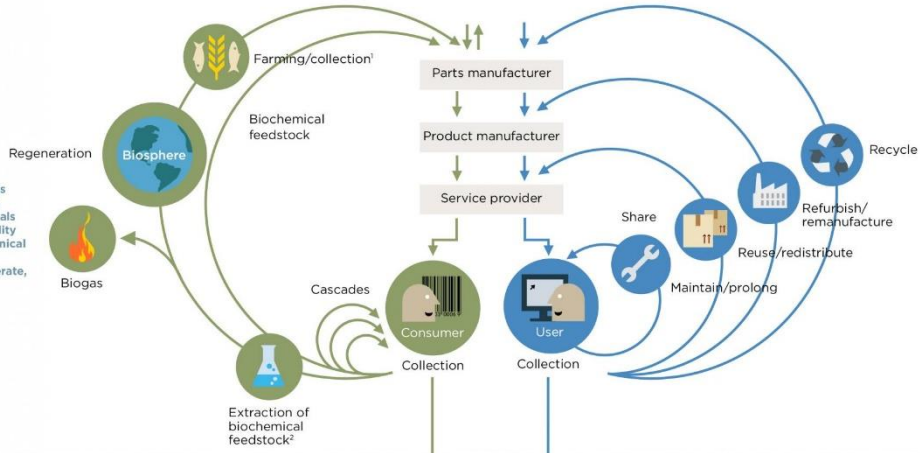
Renewables flow management

Stock management

PRINCIPLE

2

Optimise resource yields by circulating products, components and materials in use at the highest utility at all times in both technical and biological cycles  
 ReSOLVE levers: regenerate, share, optimise, loop



PRINCIPLE

3

Foster system effectiveness by revealing and designing out negative externalities  
 All ReSOLVE levers

Minimise systematic leakage and negative externalities

1. Hunting and fishing  
 2. Can take both post-harvest and post-consumer waste as an input  
 Source: Ellen MacArthur Foundation, SUN, and McKinsey Center for Business and Environment; Drawing from Braungart & McDonough, Cradle to Cradle (C2C).

Figure 3 Outline of a circular economy approach

Bioeconomy is defined by John Bell, Director of Bioeconomy Directorate of the European Commission, as the “biological heart” of circular economy<sup>3</sup>. If the circular economy focuses for the most part on the efficient use of all kind of resources and ensures that those are reused and recycled as long as possible, the bioeconomy deals with the use of renewable biological resources. In particular, this model refers to the use of biomass for the production of biomaterials and bioenergy. In this contest biomass is considered as the biodegradable fraction of products, waste and residues of biological origin from agriculture (including plant and animal substances), forestry and related industries, including fisheries and aquaculture, as well as the biodegradable part of industrial and urban waste. The principle of the circular economy is thus complementary to the renewable character of the bioeconomy, contributing to create a sustainable economic growth

According to the vision of this economic model, biorefining represents a great way to obtain large-scale and sustainable development of biomass use, resulting in the production of biobased materials and bioenergy with optimal socio-economic and environmental impacts<sup>4</sup>. Among the several definition of “biorefinery”, the most exhaustive was recently performed by the IEA Bioenergy Task 42 :“Biorefining is the sustainable processing of biomass into a spectrum of marketable products and energy”<sup>5</sup>. More in detail, we can consider the biorefinery system as an industrial facility or a network of facilities that use a broad range of technologies able to run the full sustainable transformation of biomass resources into their building blocks, which can be converted to value added products, biofuels and chemicals. Moreover, the system has to be able to combine the material flows in order to reach a complete utilization of all biomass components. In this context, the residue from one bio-industry (*e.g.* lignin from a lignocellulosic ethanol production plant) becomes an input for other industries, giving rise to integrated bio-industrial systems in order to obtain full optimization of renewable resources<sup>6</sup>.

A forward looking approach is the stepwise conversion of large parts of the global economy/industry into a sustainable biobased society having bioenergy, biofuels and biobased products as main pillars and biorefineries as the basis. Such a replacement of limited resources with renewable one will require some breakthrough changes in the today’s production of goods and services: biological and chemical sciences will play a leading role in the generation of future industries and new synergies of biological, physical, chemical and technical sciences must be developed<sup>6</sup>.

## The role of green chemistry

The use of green chemistry principles and low environmental impact technologies into biorefineries is mandatory<sup>7</sup>. We can consider the green chemistry as the area of chemistry that provide the guidelines for the manufacture and application of products that aim to develop sustainable chemical synthesis strategies limiting use, or generation, of environmentally detrimental and hazardous chemicals.

The twelve principle of green chemistry (Fig.4) published from Anastas and Warner<sup>8</sup>, represent the set of concepts with the aim to optimize the following aspects of a chemical process:

- *Chemical efficiency*: reducing the waste formation, minimizing the number of reagents atoms that take part in the reaction, minimizing the number of derivatives (limiting the work up required) and using starting materials deriving from renewable sources.
- *Energetic efficiency*: with catalysts, it's possible to reduce the use of cooling and heating required during the reactions.
- *Safety*: using reagents that are less toxic and less prone to create dangerous situations, using available knowledge to predict the toxicity characteristics of the newly synthesized compounds.



Fig.4 The twelve principles of green chemistry

The overall aim of green chemistry combined with biorefinery concept is the production of “eco-friendly” and sustainable chemical products<sup>9</sup>. Green chemistry offers a protocol when developing biorefinery processes and may play an important role in facilitating production of commodity chemicals from biomass. In accordance with green chemistry principles, during chemical product manufacture, and indeed during the whole product life cycle, energy demands should be minimized, safer processes used, and hazardous chemical use and production avoided. The final product should be non-toxic, degradable into innocuous chemicals and with minimum production of waste.



# Bioprocesses and bioeconomy

A relevant role in biorefinery and green chemistry is played by biotechnological processes, where microorganisms and enzymes are used to convert residues and by-products from biomasses into molecules of interest in different areas<sup>10,11</sup>.

Bioprocesses can be classified into fermentation and biocatalysis. Fermentation usually refers to the use of growing cells to make the products of interest; biocatalysis may broadly be defined as the use of biological catalysts (biocatalysts), which can be isolated enzymes or whole cells, used in their free or immobilised form. Fermentation technologies are usually used in large molecules production, such as enzymes, peptides, therapeutic proteins (e.g. antibodies and insulin) and proteins used in the food industry (e.g. feed additives), but also small molecules, such as metabolites of fermentation processes, e.g. ethanol, 1,3-propanediol, succinic acid and butanol<sup>12</sup>. Biocatalytic processes are used for the preparation of chemicals (small molecules) such as building blocks for added-value chemicals, amino acids, agrochemicals and active pharmaceutical ingredients (APIs), often being complementary to conventional chemical processes<sup>13</sup>.

## Modern biocatalysis

New biocatalytic processes offer an increasing potential for the production of goods to meet various human needs. The driving forces in the development of the industrial enzyme technology are:

- the obtainment of new products or processes to meet these needs;
- the improvement of the quality of processes for the preparation of existing products starting from raw materials.

Both these approaches may lead to an innovative product or process that is not only competitive, but also meet sustainability criteria<sup>14</sup>.

The main advantage in the use of biocatalysts are summarized below<sup>15</sup>:

- Chemo- regio- and stereoelectivity;
- Catalytic efficiency;

- Mild reaction conditions;
- Sustainability;
- One-pot multienzymatic reactions;
- Protein ability to accept a broad range of organic molecules.

On the other hand, some of these same advantageous traits of enzymes may also constitute their limitations:<sup>16</sup>

- Narrow operational window;
- Low productivity;
- Low number of commercially available biocatalyst;
- High time required for the development of an industrial process;
- Cofactor-dependending enzymes;
- Enzyme enantiospecificity;
- Catalyst recovery and reuse.

To overcome these issues several techniques have been developed in order to obtain better biocatalytic processes<sup>17</sup>, working on the biocatalyst improvement (screening from non-conventional sources, improved recombinant systems, protein and metabolic engineering, biocatalyst immobilization) or on the process development (operation mode and reactor selection).

### *Screening of biocatalyst*

The whole process that sees the industrial application of a new enzyme usually begins with *in vivo* (using experimental assay to test the enzymatic function) or *in silico* screening (based on enzyme sequence/structure). In the last years, a large effort has been devoted to the identification of new biocatalysts from extremophile microorganisms (particularly thermophiles), since operation at high temperatures (above 45-50 °C) minimizes the risk of microbial contamination in industrial processes. Moreover, some reactions are favoured at relatively high temperatures (an example is the isomerization of glucose to fructose),

although care should be taken to avoid an operational environment that may lead by-product formation. The majority of enzymes used is of terrestrial microbial origin, and screening-efforts for isolation of promising enzyme producing strains have accordingly been performed in such background<sup>18</sup>. From some years now, marine environments have also been tapped as a source for useful enzymes from either microbial or higher organisms origin<sup>19</sup>.

### *Biocatalyst form*

According to the kind of reaction is possible to choose to use whole cells or purified enzymes as biocatalyst. Usually, the use of whole cells is favoured in reactions where the use of cofactors is necessary, since the cellular system provides cofactors and systems for their recycling, avoiding their addition to the reaction mixture. However, due to the possibility of side reactions, the use of whole-cells may require additional downstream process costs for product recovery.

Isolated enzymes are particularly interesting for synthetic routes, due to their selectivity and purity of product stream. Additionally, the use of isolated enzymes brings simplicity to the process (avoiding undesired side reactions) but the trade-off is higher upstream costs (for enzyme recovery and purification)<sup>20</sup> and therefore re-use of the enzyme is often required to design an economically competitive process.

As a balance between these trade-offs (and as a rule of thumb), the crudest possible form of the enzyme (e.g. whole-cell or lysate) should be used, without compromising the product quality<sup>21</sup>.

Large-scale biocatalytic processes require the use of immobilised biocatalyst, in order to easily recycle and reuse the biocatalyst<sup>22</sup>. The use of immobilized form of biocatalyst allows to obtain a cleaner product stream, avoiding not only undesired by-products, but also the protein contamination. Moreover, recycling and versatility in use in continuous processes is also needed for the process economic viability, in order to compensate for a costly upstream, comprising not only enzyme recovery and purification but also the immobilisation step<sup>23</sup>.

Table 1 reports the summary of possible advantages and disadvantages of the different form of biocatalysts:

*Table 1 Different advantages and disadvantages of whole cells and isolated enzyme*

<b>Biocatalyst</b>	<b>Form</b>	<b>Advantages</b>	<b>Disadvantages</b>
<b>Isolated enzymes</b>	Dissolved in water	<ul style="list-style-type: none"> <li>✓ Simple apparatus</li> <li>✓ Simple work-up</li> <li>✓ Better productivity</li> <li>✓ High substrate concentration tolerance</li> <li>✓ High catalytic activity</li> </ul>	<ul style="list-style-type: none"> <li>✓ Cofactor recycling necessary</li> <li>✓ Side reaction possible</li> <li>✓ Lipophilic substrates insoluble</li> <li>✓ Workup requires extraction</li> </ul>
	Suspended in organic solvents	<ul style="list-style-type: none"> <li>✓ Easy to perform</li> <li>✓ Simple workup</li> <li>✓ Lipophilic substrates soluble</li> <li>✓ Easy enzyme recovery</li> </ul>	<ul style="list-style-type: none"> <li>✓ Reduced catalytic activity</li> </ul>
	Immobilized	<ul style="list-style-type: none"> <li>✓ Easy enzyme recovery</li> <li>✓ Enzymatic recycling</li> <li>✓ Possibility to use continuous flow reactors</li> </ul>	<ul style="list-style-type: none"> <li>✓ Loss of activity during immobilization</li> </ul>

<b>Whole cells</b>	Growing cultures or resting cells	<ul style="list-style-type: none"> <li>✓ No cofactor recycling necessary</li> <li>✓ High activity</li> <li>✓ Simple workup</li> <li>✓ Fewer by-products</li> </ul>	<ul style="list-style-type: none"> <li>✓ Expensive equipment</li> <li>✓ Tedious workup</li> <li>✓ Low productivity</li> <li>✓ Low substrate concentration tolerance</li> <li>✓ Low organic solvents tolerance</li> <li>✓ Uncontrolled side reactions</li> </ul>
	Immobilized cells	<ul style="list-style-type: none"> <li>✓ Possible cell re-use</li> <li>✓ Use in continuous flow reactors</li> </ul>	<ul style="list-style-type: none"> <li>✓ Loss of activity during immobilization</li> </ul>

### *Biocatalyst characterization*

The characterization of biocatalyst is usually done through the investigation of enzyme kinetics parameters. In particular, activity assays are usually used to study the effect on reaction rate of changes in temperature, pH, ionic strength, enzyme and other components concentration. The results have not always been presented in a rate law, but have most often provided a useful starting point for more detailed studies by fixing some of the environmental variables such as ionic strength, pH and temperature. Experiments have usually been carried out by mixing all components together at the same time and thereafter monitoring the development of the individual component concentrations. The rate of reaction has then been defined as either the disappearance or production of a component over time. The initial testing of enzymes usually includes an investigation of the linear activity/enzyme concentration range and the optimal pH. After this has been established, enzyme concentration can be fixed to obtain subsequently measured initial rates in a reasonable time period. The pH is then also fixed in accordance with the highest activity observed, which usually also represents the most stable condition for the enzyme.

Another important feature of biocatalysts is their operational stability, which can be influenced by different parameters (temperature, pH, co-solvents, buffers with high ionic strength etc.). Immobilization is a solution for improving enzyme stability over time. Immobilized biocatalysts (either isolated enzymes or whole cells) are more resistant to destabilizing agents, since access to the enzyme is limited; moreover, immobilization introduces new interactions between the protein and the support, which may stabilize the tertiary structure of the enzyme. Loss of quaternary structure can be also partially avoided by cross-linking unbound subunits to those already bound to the support.

### *Protein and metabolic engineering*

Some of the research efforts have focused on the biochemical and molecular mechanisms underlying the stability of enzymes from extremophiles. This kind of knowledge is also particularly useful for protein engineering of known enzymes, aiming at enhancing stability, substrate specificity without compromising catalytic activity<sup>24</sup>. The upgrading of this feature is of paramount importance for implementation of industrial processes, since it allows for reducing the amount of enzyme used in the process.

Two methodologies can be used for protein engineering:

- i. The first methodology involves rational pinpoint modifications in one or more amino acids are made, where these changes are predicted to bring along the envisaged improvement in the targeted enzyme function.
- ii. The second is the directed evolution of enzymes, through random mutagenesis and recombination. This methodology, which allows for a high throughput, has been extensively applied, aiming for more efficient biocatalysts.

### *Process engineering*

Another aspect to consider in the optimization of biocatalytic process is the choice of bioprocess mode that depend on features of biocatalyst and of the reaction. It is possible distinguish three different kind of operation mode:

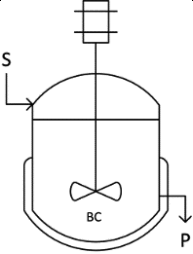
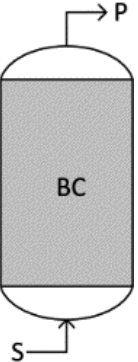
- Batch: this mode provide that all the reagents are fed into the reactor and the work up is done when the reaction is completed. However, this type of operating mode is not suitable for cases where a strong substrate inhibition is observed.

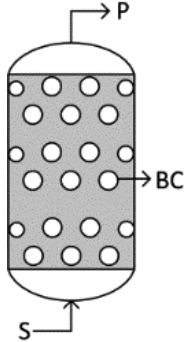
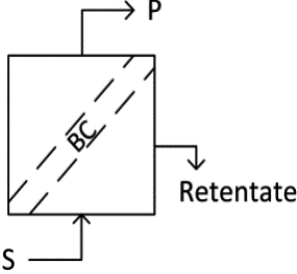
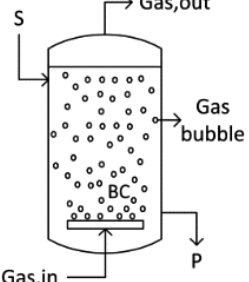
- Fed-batch: with this mode the substrate is added in a periodic or continuous way, while the product is recovered in the end of the process.
- Continuous: the reagents are continuously fed into the reactor and product is continuously recovered. This implies that the reactor is operating at the effluent substrate feed-rate.

The choice of the reactor depends on different features such as cost, space, mass transfer, kinetics, heating and cooling, easiness of operation, operation mode and reusability of the catalyst<sup>25</sup>.

In table 2 the most common reactors with their advantages and disadvantages are listed<sup>26</sup>:

*Table 2 Different reactors for multi-enzymatic processes*

Reactor type	Reactor representation	Advantages	Disadvantages
Stirred tank reactor (STR)		<ul style="list-style-type: none"> <li>Allows soluble and immobilised enzymes and whole-cell</li> <li>Multiphase media</li> <li>Good operational control</li> <li>Simple modelling</li> <li>Simple construction</li> <li>Low downtime (easy to clean)</li> </ul>	<ul style="list-style-type: none"> <li>Possible inactivation of biocatalyst</li> <li>Difficult soluble enzyme recycling</li> </ul>
Packed bed reactor (PBR)		<ul style="list-style-type: none"> <li>Allows soluble and immobilised enzymes and whole-cell</li> <li>Low enzyme damage due to shear stress</li> <li>High conversions achieved and volumetric productivities</li> <li>Shorter residence times</li> <li>Easy enzyme recycling, separation and exchange</li> <li>Low investment cost</li> </ul>	<ul style="list-style-type: none"> <li>Thermal gradient</li> <li>Difficult to control</li> <li>Complex modelling</li> <li>Mass transfer limitations</li> <li>Not suitable for multiphase reactions</li> </ul>

<p>Fluidized bed reactor (FBR)</p>		<p>Allows soluble and immobilised enzymes and whole-cell          Good enzyme mixing          Suitable for multi-phase reactions          Lower pressure drop          Uniform flow field          Good operational control          Easy enzyme recycling, separation and exchange</p>	<p>Possible inactivation of biocatalyst.          Constrained by the particle size and density</p>
<p>Membrane bioreactor (EMR)</p>		<p>Allows soluble enzymes          Low enzyme damage due to shear stress          High conversions achieved  <i>In-situ</i> separation          Retention of enzymes and cofactors          Dosing of a reagent          Compartmentalisation</p>	<p>Complex modelling          Poor control          Membrane fouling          Restrictions on the volumetric flow rate          High energy utilisation</p>
<p>Bubble column reactor</p>		<p>Simple design          High heat transfer area          Low enzyme damage due to shear stress          Low maintenance costs</p>	<p>High sparging rates are required for a turbulent flow          Bubble coalescence</p>



# Example of biocatalytical process: FOS production

FOSs are linear oligosaccharides of fructose containing a single glucose (G) moiety in which fructosyl units (F) are bound at the  $\beta(2\rightarrow1)$  position of a sucrose molecule (GF). Among 1-FOSs, 1-kestose (GF<sub>2</sub>), 1-nystose (GF<sub>3</sub>), and 1- $\beta$ -fructofuranosylnystose (GF<sub>4</sub>) represent the most studied and used compounds (family 1, Fig 5). Other FOSs families founded in commercial functional foods are 6-FOSs (family 6, Fig 5) and neo-FOSs (family neo, Fig 5)<sup>27</sup>.

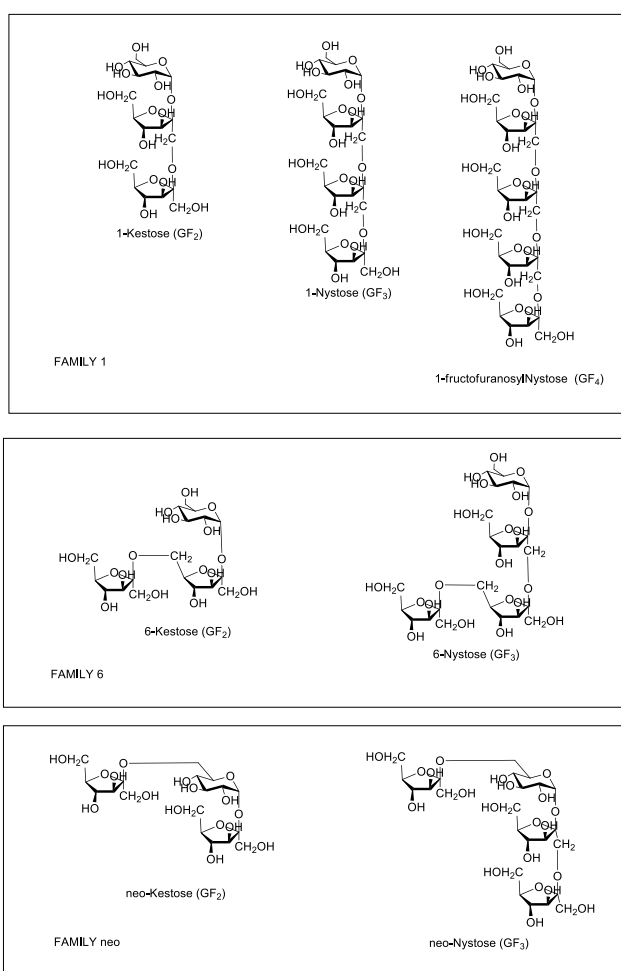


Fig.5 FOS structures (families 1, 6 and neo)

Zambelli et al.,<sup>28</sup> reported the screening of different filamentous fungi isolated from molasses and jams (kiwi and fig) for fructooligosaccharides (FOS) producing activity. Starting from 45 strains, two strains have been selected evaluating fructooligosaccharides (FOS) producing activity and considering the FOS yield and kestose/nystose ratio. In particular, using 600 g/L of sucrose, maximum FOS yield was 184 and 339 g/L for *P. sizovae* and *C. cladosporioides*, respectively. Interestingly, the highest FOS concentration with *C. cladosporioides* was reached at 93% sucrose conversion, which indicated a notable transglycosylation to hydrolysis ratio.

In a following work<sup>29</sup>, they aimed to demonstrate the advantages in the use of a flow-chemistry reactor with previously described biotransformation. With the final aim of predisposing a suitable process for the sustainable and scalable production of the desired FOS mixture, whose potential use as a novel prebiotic preparation can be easily foreseen and is at present under investigation by us. Process has been developed using a process in a continuous set-up. In particular, to this aim, a *C. cladosporioides* MUT 5506 strain was used as an immobilized mycelium in a packed bed reactor to improve the productivity, the efficiency and the scalability of the reported batch biotransformation. The innovative application of whole microbial cells into a flow chemistry reactor combines the advantages of an easy to produce biocatalyst with a process-intensification technology. Moreover, the use of a continuous-flow approach based on a packed bed reactor guarantees improved mass transfer and recyclability of the solid catalyst.

# References

1. Ellen MacArthur Foundation. Towards the Circular Economy. *Ellen MacArthur Found.* **1**, 1–96 (2013).
2. Iraldo, F. & Bruschi, I. Economia Circolare: principi guida e casi studio. (2015). doi:10.13140/RG.2.1.2493.9604
3. Bell, J. *et al.* EU ambition to build the world’s leading bioeconomy—uncertain times demand innovative and sustainable solutions. *N. Biotechnol.* (2017). doi:10.1016/j.nbt.2017.06.010
4. Cherubini, F. The biorefinery concept: Using biomass instead of oil for producing energy and chemicals. *Energy Convers. Manag.* **51**, 1412–1421 (2010).
5. IEA. Biorefineries : Adding Value to the Sustainable Utilisation of Biomass. 1–16 (2009).
6. Kamm, B. & Kamm, M. Principles of biorefineries. *Appl. Microbiol. Biotechnol.* **64**, 137–145 (2004).
7. Morais, A. R. & Bogel-Lukasik, R. Green chemistry and the biorefinery concept. *Sustain. Chem. Process.* **1**, 18 (2013).
8. P.T Anasts, J. . W. *Green Chemistry: Theory and Practise.* (1998).
9. And, K. W. & Arpe, H.-J. *Industrial Organic Chemistry.* (2003).
10. No Title. Available at: [www.europabio.org/white\\_biotech.htm](http://www.europabio.org/white_biotech.htm).
11. Gupta, M. N. & Raghava, S. Relevance of chemistry to white biotechnology. *Chem. Cent. J.* **1**, 17 (2007).
12. Chotani, G. *et al.* The commercial production of chemicals using pathway engineering. *Biochim. Biophys. Acta - Protein Struct. Mol. Enzymol.* **1543**, 434–455 (2000).
13. Panke, S., Held, M. & Wubbolts, M. Trends and innovations in industrial biocatalysis

- for the production of fine chemicals. *Curr. Opin. Biotechnol.* **15**, 272–279 (2004).
14. K. Buchhols, V. Kasche, U. T. B. *biocatalysts and enzyme technology*.
  15. Patel, R. N. *Stereoselective Biocatalysis*. (2000).
  16. Faber, K. *Biotransformations in Organic Chemistry*. (2004).
  17. Bommarius AS, R. B. *Biocatalysis*. (2004).
  18. Vieille, C. & Zeikus, G. J. Hyperthermophilic Enzymes: Sources, Uses, and Molecular Mechanisms for Thermostability. *Microbiol. Mol. Biol. Rev.* **65**, 1–43 (2001).
  19. De Vitis, V. *et al.* Marine Microorganisms as Source of Stereoselective Esterases and Ketoreductases: Kinetic Resolution of a Prostaglandin Intermediate. *Mar. Biotechnol.* **17**, 144–152 (2015).
  20. Tufvesson, P., Lima-Ramos, J., Nordblad, M. & Woodley, J. M. Guidelines and cost analysis for catalyst production in biocatalytic processes. *Org. Process Res. Dev.* **15**, 266–274 (2011).
  21. Pollard, D. J. & Woodley, J. M. Biocatalysis for pharmaceutical intermediates: the future is now. *Trends Biotechnol.* **25**, 66–73 (2007).
  22. Sheldon, R. A. Cross-linked enzyme aggregates as industrial biocatalysts. *Org. Process Res. Dev.* **15**, 213–223 (2011).
  23. Cao, L., van Langen, L. & Sheldon, R. A. Immobilised enzymes: Carrier-bound or carrier-free? *Curr. Opin. Biotechnol.* **14**, 387–394 (2003).
  24. Dalby, P. A. Engineering enzymes for biocatalysis. *Recent Pat. Biotechnol.* **1**, 1–9 (2007).
  25. Fernandes, J. F. A., McAlpine, M. & Halling, P. J. Operational stability of subtilisin CLECs in organic solvents in repeated batch and in continuous operation. *Biochem. Eng. J.* **24**, 11–15 (2005).
  26. Lima-Ramos, J. *A methodology for development of biocatalytic processes*. (2013).

27. Fernández, R. C., Maresma, B. G., Juárez, A. & Martínez, J. Production of fructooligosaccharides by  $\alpha$ -fructofuranosidase from *Aspergillus* sp 27H. *J. Chem. Technol. Biotechnol.* **79**, 268–272 (2004).
28. Zambelli, P. *et al.* Production of fructooligosaccharides by mycelium-bound transfructosylation activity present in *Cladosporium cladosporioides* and *Penicillium sizovae*. *Process Biochem.* **49**, 2174–2180 (2014).
29. Zambelli, P. *et al.* An efficient continuous flow process for the synthesis of a non-conventional mixture of fructooligosaccharides. *Food Chem.* **190**, 607–613 (2016).
30. Pfaltzgraff, L. A., De bruyn, M., Cooper, E. C., Budarin, V. & Clark, J. H. Food waste biomass: a resource for high-value chemicals. *Green Chem.* **15**, 307 (2013).



# Aim of the project

The interest in the use of biocatalysts is due to its advantages in terms of specificity, ability to operate under mild conditions of pH, temperature and pressure, high activity and turnover numbers, and high biodegradability. The whole may contribute for developing sustainable and environmentally friendly processes.

The main topic of my PhD project has been the study and the characterization the following biocatalysts activity:

- Esterase activity of a thermostable carboxylesterase from *Bacillus coagulans* (BCE) with high enantioselectivity towards different 1,2-*O*-isopropylidenglycerol esters (acetate, butyrate and benzoate);
- Oxidation activity of *Acetobacter aceti* MIM 2000/28 used to catalyse the stereoselective desymmetrisation of achiral 2-alkyl-1,3-diols;
- Hydroxylation activity of limonene monooxygenase isolated from *Mycobacterium sp. strain HXN-1500* able to product (*R*)-perillyl alcohol starting from (*R*)-limonene.



# Characterization and crystal structure of a stereoselective carboxylesterase from *Bacillus coagulans*

**Valerio De Vitis**<sup>1</sup>, Cristina Nakhnoukh<sup>2</sup>, Andrea Pinto<sup>1</sup>, Martina Letizia Contente<sup>1,3</sup>,  
Alberto Barbiroli<sup>1</sup>, Mario Milani<sup>4</sup>, Martino Bolognesi,<sup>2,5</sup> Francesco Molinari<sup>1</sup>,  
Louise J. Gourlay<sup>2\*</sup> and Diego Romano<sup>1\*</sup>.

## **Affiliations:**

<sup>1</sup> Department of Food, Environmental and Nutritional Sciences (DeFENS), Università degli Studi di Milano, Milano, Italy

<sup>2</sup> Department of Biosciences, Università degli Studi di Milano, Milano, Italy

<sup>3</sup> School of Chemistry, University of Nottingham, University Park, Nottingham, UK

<sup>4</sup> Biophysics Institute, National Research Council c/o Department of Biosciences, Università degli Studi di Milano, Via Celoria 26, 20133 Milano, Italy.

<sup>5</sup> Pediatric Research Center “Romeo ed Enrica Invernizzi”, Cryo Electron Microscopy Laboratory, University of Milano, Milano, Italy

Manuscript in preparation

# Abstract

Microbial carboxylesterases are biocatalysts that hydrolyze an extensive range of structurally different esters. Here, we report the recombinant preparation and biochemical characterization of an atypical carboxylesterase from *Bacillus coagulans* (BCE), able to enantioselectively hydrolyze different 1,2-*O*-isopropylidenglycerol (IPG or solketal) esters. In all the cases, BCE efficiently produces enantioenriched (*S*)-IPG, a versatile chiral building block usable for the synthesis of different compounds of nutritional and pharmaceutical interest (i.e.,  $\beta$ -blockers, glycerophospholipids and prostaglandins). The enzymes showed a remarkable thermophilicity, with the highest activity observed at 65° C. BCE showed a typical non-lipolytic behavior, being able to hydrolyze short-chain esters and showing no activity on laurate and palmitate esters; moreover, no interfacial activation was observed using tributyrin. The crystal structures of BCE were solved in apo- and glycerol-bound forms at resolutions of 1.9 Å and 1.8 Å, respectively. *In silico* docking studies on the BCE structure validated the experimental data, indicating that only small acyl chains (<C6) IPG esters may be hydrolyzed and that enantioselectivity may be the result of an enhanced stabilization of the tetrahedral intermediate for the *S*-enantiomer.

# Introduction

Carboxylesterases (EC 3.1.1.1) catalyze the cleavage and formation of carboxyl ester bonds, being often classified as esterases and lipases, depending on experimental data and theoretical hypotheses. Recently, it has been suggested to simply organize carboxylester hydrolases into lipolytic esterases (proposed EC: L3.1.1.1) and non-lipolytic esterases (NLEst, proposed EC: NL3.1.1.1) [1]. Databases, such as the Lipase Engineering Database (LED), the  $\alpha/\beta$ -hydrolase Fold Enzyme Family 3DM or ESTHER [2-4] are available for further classification. Carboxylesterases are useful biocatalysts, especially for the enantioselective hydrolysis or synthesis of chiral and prochiral esters [5-7].

Bacteria of the genus *Bacillus* are known for the production of carboxylesterases [8]. *B. subtilis* [9-14], *B. coagulans* [15], *B. amyloliquefaciens* [16], *B. stearothermophilus* [17], and generic *Bacillus* sp. [18] have been identified as producers stereoselective lipases and esterases.

Enantioselective hydrolysis of racemic esters of 1,2-*O*-isopropylidenglycerol (IPG or solketal) is a convenient method for producing optically pure IPG [9, 15, 19-24], a valuable chiral building block for the synthesis of  $\beta$ -blockers, glycerophospholipids, and prostaglandins [25]. However, lipases are poor enantioselective biocatalyst in the hydrolysis of IPG esters; in a screening using commercial lipases, Amano AK lipase (from *Pseudomonas* sp.) proved the only one with good enantioselectivity towards (*R,S*)-IPG octanoate, but with low yields (22% after 48 h), while ester with shorter chain gave lower enantioselectivity [25]. Other lipases, such as *Candida antartica* lipase B (Novozyme 435), were poorly enantioselective towards IPG esters [26].

A carboxylesterase from *B. coagulans* (BCE) with medium-to-high enantioselectivity towards racemic esters of IPG [5, 4] and other chiral esters [27] was previously identified and purified. The appealing thermophilicity and stereoselectivity of the enzyme led us to further investigate its biochemical and structural features.

In this context, crystal structures of BCE were solved with high resolution (1.8-1.9 Å), in its apo-form and in complex with glycerol. Our functional studies showed that BCE works as a non-lipolytic carboxylesterase and hydrolyzes C2-C8 esters, with maximum activity towards caproate (C6) esters, and catalyze the production of optically pure (*S*)-IPG from racemic

mixtures of butyrate and benzoate IPG esters. BCE showed highest activity at 65°C, showing typical Michaelis-Menten kinetics and has no apparent requirement for interfacial activation when tributyrin was used as substrate. This non-lipolytic behavior differs from structural observations that indicate the presence of a large lid domain typical of lipases. Structural analyses of this non-conventional carboxylesterase are presented in relation to its non-lipolytic catalytic function and stereoselectivity for butyrate and benzoate IPG esters.

# Materials and methods

## Production of recombinant BCE

The BCE gene coding for the full-length protein was amplified from *Bacillus coagulans* strain NCIMB 9365 genomic DNA by PCR using the following primers:

Forward: 5'-CACCATGTTGGCTTTTCAAGAGTTGAG-3';

Reverse: 5'-TGAGCTCGAGTCATTTTACGATGATCCCGTT-3'.

The amplified gene was cloned into the pET100/D-TOPO<sup>®</sup> vector (Invitrogen) in frame with a N-terminal six-histidine tag, according to the manufacturer's instructions. Correct construct sequence was confirmed by DNA sequencing.

Cultures of BL21(DE3)Star *E. coli* cells were transformed with the resulting plasmid and grown overnight at 37 °C in LB medium supplemented with 100 mg/L ampicillin. The seed culture was then diluted into 1.0 L Erlenmeyer flasks containing 100 ml Luria Broth (LB) at an initial OD<sub>600nm</sub> of 0.1. Cultivation was carried out at 37 °C with agitation at 150 rpm. Cells were grown until an OD<sub>600nm</sub> of 0.8. After cold-shock treatment, cultures were induced with 0.5 mM IPTG (isopropyl- β-D-thiogalactopyranoside) and further incubated for 16 h at 20 °C. Bacterial cells were harvested by centrifugation at 5000 rpm for 15 min, washed once with 20 mM sodium phosphate buffer at pH 7.0 and stored at -20 °C.

The cell pellet was suspended in 50 mM Tris-HCl pH 8.0 containing 100 mM NaCl, 6 mM imidazole. Bacterial cells were lysed by sonication (5 cycles of 30 s each, in ice, with 1 min interval) and the supernatant was harvested by centrifugation at 15,000 rpm for 45 min at 4 °C. BCE was purified from the supernatant by affinity chromatography with HIS-Select Nickel Affinity Gel (Sigma-aldrich) pre-equilibrated with 50 mM Tris-HCl pH 8.0, containing 100 mM NaCl, 6 mM imidazole. After a washing step with 50 mM Tris-HCl pH 8.0, 100 mM NaCl, 6 mM imidazole, His-BCE was eluted with 50 mM Tris-HCl pH 8.0, 100 mM NaCl, 250 mM imidazole.

For crystallization trials, BCE was purified from a 0.5 L bacterial culture on a 5 mL Bio-scale Mini Profinity IMAC cartridge using the Profinia Protein Purification System (Bio-rad), following standard Bio-rad protocols. Purified BCE was exchanged into crystallization buffer (10 mM Tris-HCl pH 8.0; 150 mM NaCl) using a PD10 desalting column (GE

Healthcare), according to the manufacturer's instructions and concentrated to 6.5 mg/mL, using an Amicon Ultra-15 centrifugal filter (Millipore) with a MW cut-off of 10 kDa.

### **Biotransformations and esterase activity assays**

Biotransformations of IPG esters were carried out in 5 mL screw capped tube, using 7 mU of BCE in 1 mL of 50 mM Tris-HCl pH 8.0, 100 mM NaCl. The substrates were added at the final concentration of 5 mM, dissolved in DMSO at a final concentration of 0.5%. Incubations were carried out with magnetic stirring at 30°C. Conversions and stereochemical outcomes were monitored by gas chromatography using a chiral capillary column (diameter 0.25 mm, length 25 m, thickness 0.25 µm, DMePeBeta-CDX-PS086, MEGA, Legnano, Italy) with a 0.25 mm-diameter, 25 m-length and 0.25 m-thickness, using the following temperature gradients: for IPG acetate: 10 min at 90 °C, increased to 120 °C over 15 min, maintained at 120 °C for 10 min and then increased to 180 °C over 2 min and then maintained at 180 °C for 10 min; for IPG butyrate: 10 min at 90 °C, increased to 110 °C over 5 min, maintained at 110 °C for 10 min and then increased to 180 °C over 2 min and then maintained at 180 °C for 10 min; for IPG benzoate: 10 min at 90 °C, increased to 120 °C over 3 min, maintained at 120 °C for 10 min and then increased to 180 °C over 2 min and then maintained at 180 °C for 10 min. Retention times of IPG enantiomers and esters under these conditions were: (*R*)-IPG= 8.2 min, (*S*)-IPG= 9.0 min; (*R*)-IPG acetate = 13.1 min, (*S*)-IPG acetate = 12.4 min; (*R*)-IPG butyrate = 22.3 min, (*S*)-IPG butyrate = 21.2 min; (*R*)-IPG benzoate = 27.7 min, (*S*)-IPG benzoate = 27.5 min.

Enantiomeric excesses (e.e.) were calculated using the following formulas:

$$\text{e.e.}_{\text{substrate}} = \frac{[(S)\text{-IPG ester}] - [(R)\text{-IPG ester}]}{[(S)\text{-IPG ester}] + [(R)\text{-IPG ester}]}$$

$$\text{e.e.}_{\text{product}} = \frac{[(S)\text{-IPG}] - [(R)\text{-IPG}]}{[(S)\text{-IPG}] + [(R)\text{-IPG}]}$$

Hydrolysis of IPG benzoate was also performed on semi-preparative scale: 250 mg (1.06 mmol) of substrate were dissolved in DMSO (1 mL) and added to 199 mL of 50 mM Tris-HCl pH 8.0, containing 100 mM NaCl. Upon addition of BCE (7 mU mL<sup>-1</sup>), the reaction was followed by gas-chromatography and stopped after 50 min (in correspondence to a 60% conversion). The reaction was stopped by adding 100 mL ethyl acetate (EtOAc) to recover both unreacted (*S*)-IPG benzoate and enantiomerically pure (*S*)-IPG. The aqueous phase was

extracted by repeating the addition of EtOAc twice. Organic extracts were collected, dried over sodium sulfate and the solvent removed under reduced pressure. Flash chromatography (*n*-hexane/EtOAc, 75/25) on silica gel pretreated with triethylamine afforded 52 mg of optically pure (*S*)-IPG (ee > 99% by chiral GC).

The activity of the BCE (0.036 mg mL<sup>-1</sup>) was measured spectrophotometrically using 0.015 mM *p*-nitrophenyl acetate as a substrate dissolved in 0.3% acetone, monitoring the increase in absorbance at 400 nm, corresponding to the production of *p*-nitrophenol (extinction coefficient 15000 M<sup>-1</sup> cm<sup>-1</sup>). Assays were conducted at 25°C in a microcuvette in a final volume of 1 mL of 50 mM Tris-HCl pH 8.0, 100 mM NaCl, following the reaction for 5 min. One unit of BCE corresponds to the amount of protein that produces 1 μmol of *p*-nitrophenol in 1 min.

### **Kinetic analyses of BCE activity**

The kinetic parameters were measured spectrophotometrically using different concentrations of *p*-nitrophenyl esters (acetate, butyrate, caproate, caprylate, laurate, and palmitate) at 28°C in 1 mL of 50 mM Tris-HCl pH 8.0, NaCl 100 mM (final 0.3% acetone), monitoring the increase of absorbance at 400 nm due to the production of *p*-nitrophenol (15000 M<sup>-1</sup>cm<sup>-1</sup>). Experimental data were fitted to suitable kinetic models with Origin 9.0 and kinetic parameters ( $V_{max}$ ,  $K_m$ ) were calculated with the same program.

Hydrolysis of tributyrin (in the range of 0.1-2.0 mM) was measured titrimetrically at 28 °C with a pH-stat using 30 mL of phosphate buffer 10 mM, pH 7.0.

### **BCE crystallization**

Crystallization trials of BCE (6.5 mg/mL) were prepared in 96-flat well sitting drop plates (Greiner), containing 100 μL crystallization solution of PACT Premier™Crystallization screen (Molecular Dimensions). 400 nL drops were deposited at diverse protein concentrations (30, 50 and 70 % of the stock protein solution) and crystals grew after approximately 1 week in several conditions. Data for the apo-enzyme were collected on a single crystal grown in condition 2-11 (20% PEG3350; 0.1 M sodium citrate tribasic hydrate); the crystal was cryoprotected in 50% PEG3350. Data for the glycerol-bound form of BCE were collected on a single

crystal grown in condition 42 (1.5 M ammonium sulfate, 12% glycerol and 0.1 M Tris-HCl, pH 8.0) of Hampton Crystal Screen II (Hampton Research). For cryoprotection the concentration of glycerol was raised to 25%.

### **Data Collection, model building and refinement**

X-ray diffraction Data were collected at the ID29 (glycerol-bound enzyme), ID23-1 (apo-enzyme) beamlines at the European Synchrotron Radiation Facility (ESRF, Grenoble, France). Data were processed using XDS and assigned to the hexagonal P6<sub>3</sub>22 space group using POINTLESS and scaled using AIMLESS, available in the CCP4i suite [38-40]. The 3D structure of BCE was solved *via* molecular replacement using BALBES and the protein sequence as the input; the BALBES search model was based on the structure of human monoglyceride lipase (PDB entry 3PE6) [28, 41]. The initial model was refined with PHENIX.refine, including a translational-libration-screw (TLS) option, final R<sub>gen</sub> and R<sub>free</sub> values of 21 and 24.3% (apo-BCE) and 14.7 and 16.9% (glycerol-bound BCE) were reached, respectively (**Table 3**). Both final models present ideal geometric parameters, with 97.7% (apo-BCE) and 98.1% (glycerol-bound BCE) residues assigned to the most favorable regions of the Ramachandran plot, with no outliers, according to structure validation using MolProbity under the Phenix platform (**Table 3**).

### **Circular dichroism**

Circular dichroism measurements were performed with a J-810 spectropolarimeter (JASCO Corp., Tokyo, Japan) equipped with a Peltier system for temperature control. All measurements were performed in crystallization buffer (10 mM Tris-HCl pH 8, 150 mM NaCl) at a protein concentration of 0.2 mg/mL, and in a 0.1 cm path length cuvette. Temperature ramps experiments were monitored at a wavelength of 220 nm (temperature slope 1°C/min). T<sub>m</sub>s were calculated as the maximum of the first-derivative of the traces.



# Results

## **Production of recombinant BCE**

The gene coding for BCE (accession number WP\_029142894) was amplified from *B. coagulans* NCIMB 9365 genomic DNA and cloned into the pET100/D-TOPO® bacterial expression vector. N-terminal His-tagged BCE fusion protein was produced in *Escherichia coli* BL21(DE3)Star cells, as described in the Experimental Procedures. Expression levels were determined by SDS-PAGE (data not shown) and by measuring enzyme activity (U/mg), monitoring the conversion of *p*-nitrophenyl acetate (pNPA) to *p*-nitrophenol. The highest specific activity was measured after induction with 0.5 mM IPTG for 16 h at 20°C in Luria-Bertani (LB) broth.

BCE was purified by affinity chromatography and exchanged into 50 mM Tris-HCl pH 8.0, 100 mM NaCl for activity assays, as described in the Experimental Procedures. BCE migrated on a 11% polyacrylamide gel at a molecular weight of 50 kDa, consistent with the calculated molecular mass of the full-length protein (39.2 kDa) plus the N-terminal His-tag (8.8 kDa). Under optimized conditions, 20 mU/mg of BCE was obtained, corresponding to a volumetric productivity of approximately 350 mU/L culture and to a specific productivity of 80 mU/g wet biomass.

## **BCE activity and enantioselectivity**

BCE exhibited high activity towards *p*NPA between 45 and 65°C in 50 mM Tris-HCl pH 8.0 containing 100 mM NaCl; the highest activity was observed at 65°C. BCE was active at a pH range from 7.0 to 9.0.

The ability to hydrolyze substrates with longer acyl chains was also investigated using *p*-nitrophenyl butyrate (C4), caproate (C6), caprylate (C8), caprate (C10), laurate (C12), and palmitate (C16) (**Figure 1**).

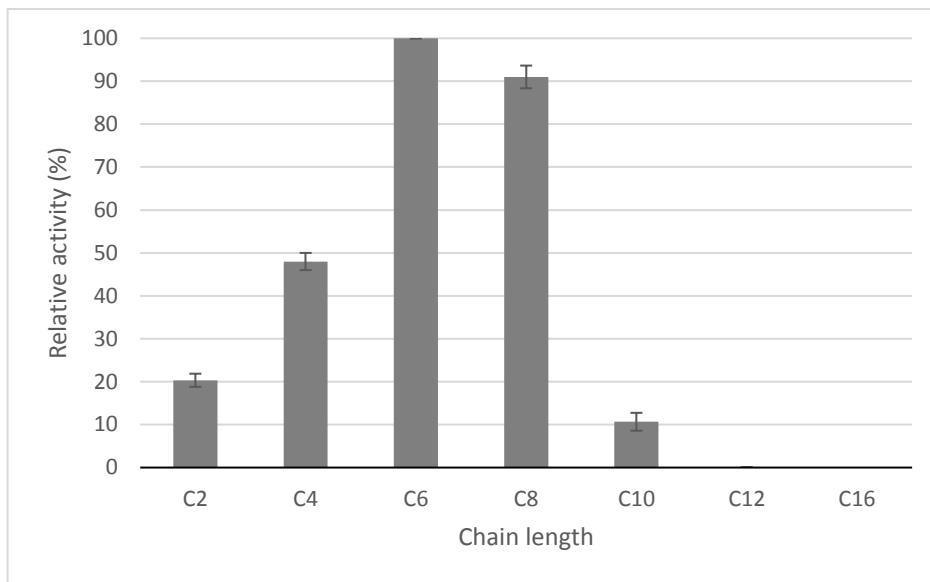


Figure 1. BCE activity towards *p*-nitrophenyl esters. Relative activity refers to the activity in presence of *p*-nitrophenyl caproate (100%) and represents the arithmetic mean and standard deviation (SD) of three measurements.

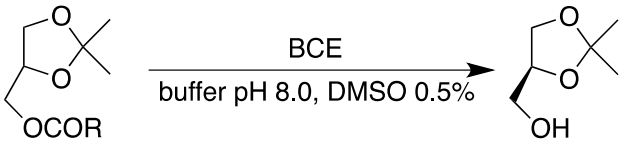
BCE showed typical non-lipolytic behavior, being able to hydrolyze C2-C8 esters following typical Michaelis-Menten kinetics, with a maximum activity towards caproate ester (see **Table 1** for kinetics data), whereas no activity was detected towards laurate and palmitate esters. The absence of interfacial activation was also confirmed by measuring the activity of BCE over a range of tributyrin concentrations (0.1-2.0 mM).

Table 1. Kinetic parameters of hydrolysis of *p*-nitrophenyl esters catalyzed by BCE.

Substrate	$k_{\text{cat}}$ ( $\text{s}^{-1}$ )	$K_{\text{M}}$ (mM)
acetate (C2)	0,621 ( $\pm$ 0.095)	0.873 ( $\pm$ 0.010)
butyrate (C4)	0.264 ( $\pm$ 0.025)	0.049 ( $\pm$ 0.006)
caproate (C6)	0.211 ( $\pm$ 0.020)	0.021 ( $\pm$ 0.005)
caprylate (C8)	0.105 ( $\pm$ 0.004)	0.003 ( $\pm$ 0.001)

The enantioselectivity of the purified recombinant BCE was assayed using three different IPG esters (acetate, butyrate, and benzoate; **Table 2**), previously tested with the wild-type enzyme [14]. Hydrolysis of butyrate and benzoate esters occurred with high reaction rates and enantioselectivity (**Table 2**), whereas the biotransformation of acetate ester was much slower and less enantioselective. Biotransformation of IPG benzoate was carried out also on semi-preparative scale (200 mL), confirming the results obtained on small scale and proving the applicability of recombinant BCE as a preparative biocatalyst.

*Table 2. Hydrolysis of IPG derivatives by BCE. E refers to the enantiomeric ratio.*

					
<b>R</b>	<b>Conversion</b>	<b>e.e.<sub>substrate</sub></b>	<b>e.e.<sub>product</sub></b>	<b>E</b>	<b>Time</b>
	<b>(%)</b>	<b>(%)</b>	<b>(%)</b>		<b>(h)</b>
CH <sub>3</sub>	46	79 ( <i>S</i> )	93 ( <i>S</i> )	67	24
(CH <sub>2</sub> ) <sub>2</sub> CH <sub>3</sub>	42	70 ( <i>S</i> )	97 ( <i>S</i> )	139	1
Ph	49	92 ( <i>S</i> )	96 ( <i>S</i> )	163	0.5

### The 3D structure of BCE

The 3D structures of ligand-free BCE and glycerol-bound BCE were solved using X-ray diffraction data collected on single hexagonal (space group P6<sub>3</sub>22) crystal (per dataset) at resolutions of 1.9 Å and 1.8 Å, respectively, as described in the Experimental Procedures. For both datasets, one BCE monomer was present in the asymmetric unit, with an estimated *w/v* solvent content of 63.1% (Matthews coefficient of 3.3 Å<sup>3</sup>/Da). Interestingly, the molecular replacement package BALBES revealed that the hexagonal BCE unit cell (a=138.1 Å, b=138.1 Å, c= 83.3 Å) is identical to that of a eukaryotic polyphosphate polymerase in complex with orthophosphate (PDB entry 3G3T); this is a coincidence since the two enzymes are completely unrelated. Both BCE structures were refined to satisfactory R<sub>free</sub> and R<sub>gen</sub> values (**Table 3**). Electron density was well-defined for almost all of the BCE

polypeptide, except for the last C-terminal residue and include an additional residue (in glycerol-bound BCE) or two (for ligand-free BCE) extra residues at the N-terminus that pertain to the cloning region of the pET100/D-TOPO bacterial expression vector.

*Table 3. Data collection, refinement and validation parameters. Data are shown for the two BCE datasets.  $aR_{merge} = \sum |I - \langle I \rangle| / \sum I \times 100$ , where  $I$  is the intensity of a reflection and  $\langle I \rangle$  is the average intensity;  $bR_{gen} = \sum |F_o - F_c| / \sum |F_o| \times 100$ ;  $cR_{free}$  was calculated from 5% of randomly selected data for cross-validation. Values in parentheses represent data belonging to highest resolution shells (Apo-BCE; 1.9-1.94 Å; glycerol-bound BCE 1.8-1.84 Å).*

	apo-BCE	BCE+glycerol
<b>Data collection</b>		
Space group	P6 <sub>3</sub> 22	P6 <sub>3</sub> 22
Cell dimensions $\square \square$		
$a, b, c$ (Å)	138.6 136.8 83.8	137.6 137.6 83.6
$\alpha, \beta, \gamma$ (°)	90, 90, 90	90, 90, 90
Resolution (Å)	40-1.9	40-1.8
$^a R_{merge}$	0.087 (0.504)	0.113 (0.598)
$I / \sigma I$	26.8 (7.8)	34.9 (8.9)
No. unique reflections	37667 (2359)	43646 (2545)
Completeness (%)	99.8 (99.5)	99.9 (99.8)
Redundancy	19.4 (20.4)	39.1 (37.6)

## Refinement

Resolution (Å)	40-1.9	40-1.8
$^bR_{\text{gen}} / ^cR_{\text{free}}$	21.6/24.3	14.7/16.9
No. atoms:		
Protein	2456	4807
Glycerol	-	18
Chloride ion	-	8
Acetate ion	-	4
Polyethylene glycol	-	6
Water	50	192
<i>B</i> -factors (Å <sup>2</sup> ):		
Protein	23.9	21.9
Glycerol	-	27.5
Chloride ion	-	44.0
Acetate ion	-	38.7
polyethylene glycol	-	56.2
Water	30	24.1
R.m.s. deviations:		
Bond lengths (Å)	0.014	0.007
Bond angles (°)	1.258	0.856

#### Ramachandran Plot (%)

Favored Regions	97.7	98.1
Allowed Regions	100	100

#### Overall 3D Fold

The overall 3D fold of both BCE structures are essentially identical (*rmsd* value 0.3 Å), displaying the canonical  $\alpha/\beta$  hydrolase fold shared by all members of this superfamily. The central  $\beta$ -sheet comprises seven parallel strands ( $\beta$ 1 and  $\beta$ 3-8) and one anti-parallel  $\beta$ -strand ( $\beta$ 2) inserted between  $\beta$ -strands 1 and 3, and contains eleven  $\alpha$ -helices and two  $3_{10}$   $\alpha$ -helices (**Figure 2**). In contrast to activity studies, which suggest that BCE is a non-lipolytic carboxylesterase, BCE presents a lipase-like 3D fold deduced by the presence of an extra so-called 'lid domain', comprising three  $\alpha$ -helices ( $\alpha$ 5,  $\alpha$ 6 and  $\alpha$ 8) that caps the entrance to the active site, housed in the canonical  $\alpha/\beta$  hydrolase core (**Figure 2**).

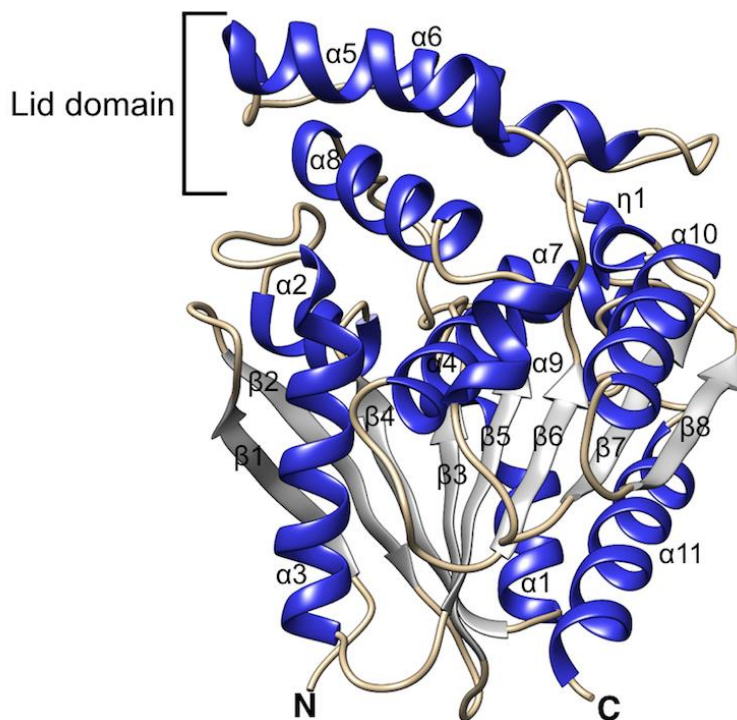
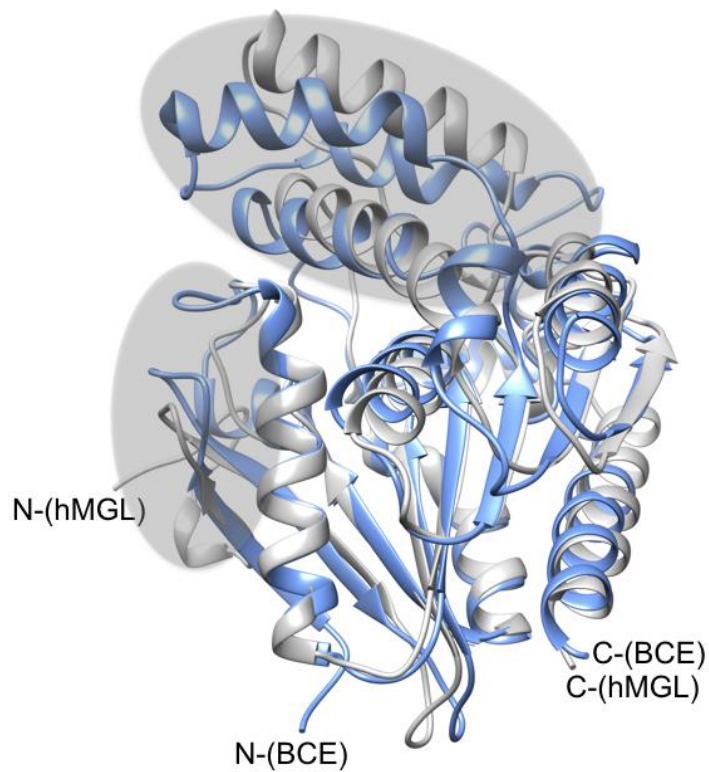


Figure 2. Ribbon secondary structure representation of the crystal structure of apo-BCE.  $\alpha$ -helices (blue) and  $\beta$ -strands (grey) and the N- and C-terminal are labeled. The lid domain comprising  $\alpha$ -helices 5, 6 and 8 is indicated.

Accordingly, despite poor sequence conservation (25.1% sequence identity), the closest structural homolog (*rmsd* value of 1.72 Å over 154/304 C $\alpha$  pairs) to BCE is human monoglyceride lipase (hMGL; PDB entry 3JWE [28]), as determined using Profunc (<http://www.ebi.ac.uk/thornton-srv/databases/profunc/>); structural conservation resides almost entirely in the  $\alpha/\beta$ -hydrolase domain and the lid domains differ significantly (**Figure 3**).



*Figure 3. Superposition of the crystal structures of apo-BCE (blue) and inhibitor-bound hMGL (grey; PDB entry 3JWE, [29]). Structural variations are highlighted in shading. All figures were generated using Chimera [31].*



hMGL, like all mono- and diacylglycerol lipases studied to date, belongs to the single  $\alpha$ -helix/loop lid lipase class [29]. If BCE were it in fact a true lipase, it would pertain to the large-lid class characteristic of thermophilic lipases, however in light of our activity data, it is likely that BCE belongs to an entirely different carboxyl esterase class all together. Additional structural differences between the two proteins occur at the N-terminus; hMGL contains an extra  $\alpha$ -helix, a shorter  $\beta$ -strand 1, and  $\alpha$ 2 in BCE is replaced by an unstructured loop in hMGL (Figure 3).

### **The BCE lid domain**

As previously mentioned, the absence of interfacial activation for catalysis is contradictory to the presence of the lipase-specific lid-domain that mediates this process. The BCE lid domain (residues 145-235) is particularly large, also with respect to the lids of the 21 other lipase members (of known structure) belonging to the large lid lipase subclass [29]. Open and closed lid conformations have been crystallized for several lipases, however the BCE lid was found in the closed conformation in all datasets collected to date, despite the absence or presence of glycerol bound at the active site.

Only two lid residues (F209 and T210), housed in a 11-residue loop that connects  $\alpha$ 7 and  $\alpha$ 8 and forms the entrance to the active site, are diversely positioned. Interestingly in apo-BCE, lid closure does not completely block entrance to the active site, and an aperture with diameter of approximately 13 Å is visible (**Figure 4**).

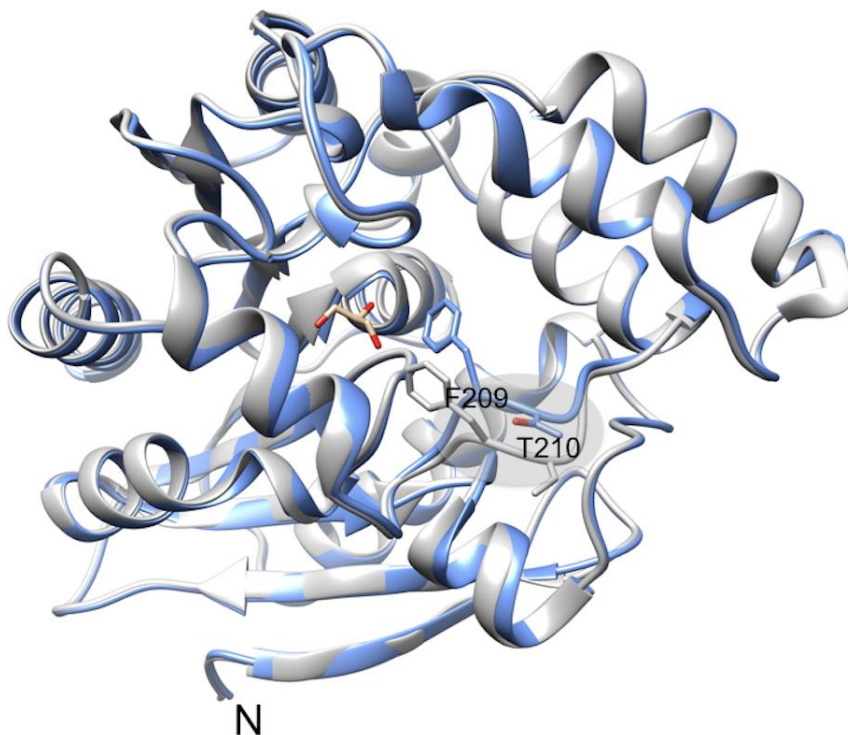


*Figure 4. Secondary structure ribbon representation of apo-BCE (grey) and glycerol-bound BCE (blue). Glycerol and residues F209 and T210 that are orientated diversely in the two structures are shown in sticks. In the glycerol-bound structure, the CZ atom of F209 is located 3.8Å away from the O3 atom of glycerol. In the ligand-free BCE structure the loop moves away from the entrance hole by 3.1 Å. The N- terminus is labeled. This figure was generated using Chimera [31].*

This aperture may permit the diffusion of small substrates directly into the active site without requiring lid repositioning. In the glycerol-bound enzyme, the repositioning of F209 and T210 is sufficient to partially close the active site aperture.

The presence of an active site aperture and the lack of classical lipolytic carboxylesterase activity, however, does not rule out the possibility of the BCE lid switching between open and closed conformations during catalysis. Accordingly, molecular dynamics calculations were made using the online server PiSQRD (<http://pisqrd.science-lab.org>) to assess BCE lid flexibility. Glycerol-free BCE was fragmented by computational simulations into two

domains that can behave as rigid units, moving independently from one another during protein structural fluctuations (in conditions of thermal equilibrium); the two domains (residues 78 to 85 (domain 1) and residues 143-227 (domain 2)) essentially represent the core  $\alpha/\beta$ -hydrolase domain and the lid domain, thus highlighting the potential dynamical role of this region of the protein [31].

### **The BCE active site**

The BCE active site contains a conserved catalytic triad (S114, H284 and D251) with the catalytic S114 being housed in the conserved GX SXG (GSHMG in BCE) motif on  $\beta 5$  that represents the nucleophilic elbow hosted in a turn that links  $\beta 5$  and  $\alpha 4$ . The oxyanion hole, which stabilizes the anionic transient tetrahedral intermediate of catalysis, is built by the backbone NH groups of M115 and G116 of the nucleophilic elbow, and by residues G37 ( $C\alpha$ ) and F38 (side-chain atoms). The active site-bound glycerol molecule observed in several of the analyzed crystals hydrogen-bonds with glycerol atom O2 and a water molecule that also interacts with the hydroxyl group of S114 and, via glycerol atom O1 with adjacent residues H113(NE2), and E285(OE2) (**Figure 5**).

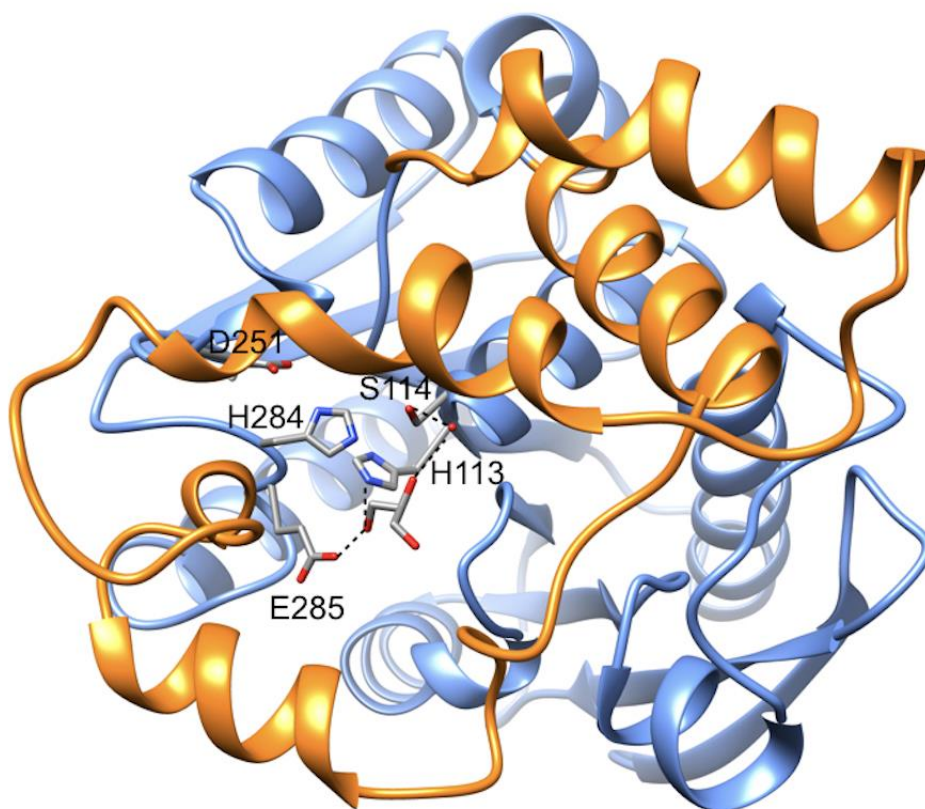


*Figure 5. View of the interaction between glycerol and BCE residues H113, E284 and a conserved water molecule (W27); hydrogen bonds are indicated by dotted lines. Interaction residues and catalytic triad (S114, H284, D251) residues are labeled and shown in sticks.*

Surface cavity analysis using CAST-P ([www. http://sts.bioe.uic.edu/castp/](http://sts.bioe.uic.edu/castp/)) and the atomic coordinates of apo-BCE, revealed the solvent-accessible active site cavity (volume = 752.3 Å<sup>3</sup>; area= 877.7 Å<sup>2</sup>), which comprises main-chain and/or side chain atoms of 34 residues (**Figure 5**) [31]. In glycerol-bound BCE, the size of this cavity increases (volume = 1028.6 Å<sup>3</sup>; area= 1370.2 Å<sup>2</sup>), however solvent accessibility decreases due to slight closure of the aperture to the active site due to the repositioning of residues F209 and T210.

#### ***In silico* docking of tested IPG ester substrates**

The BCE active site is accessible by a wide tunnel terminating in a hydrophobic cavity located after the active residue Ser114 (**Figure 6**), lined by hydrophobic residues: M118,

F143, L173, M174, M177, F221, M225. The hydrophobic cavity is quite short ( $\sim 10$  Å) and thus unable to host large aliphatic chains; this explains why BCE is inactive with compounds longer than C10 (as previously shown in **Figure 1**).

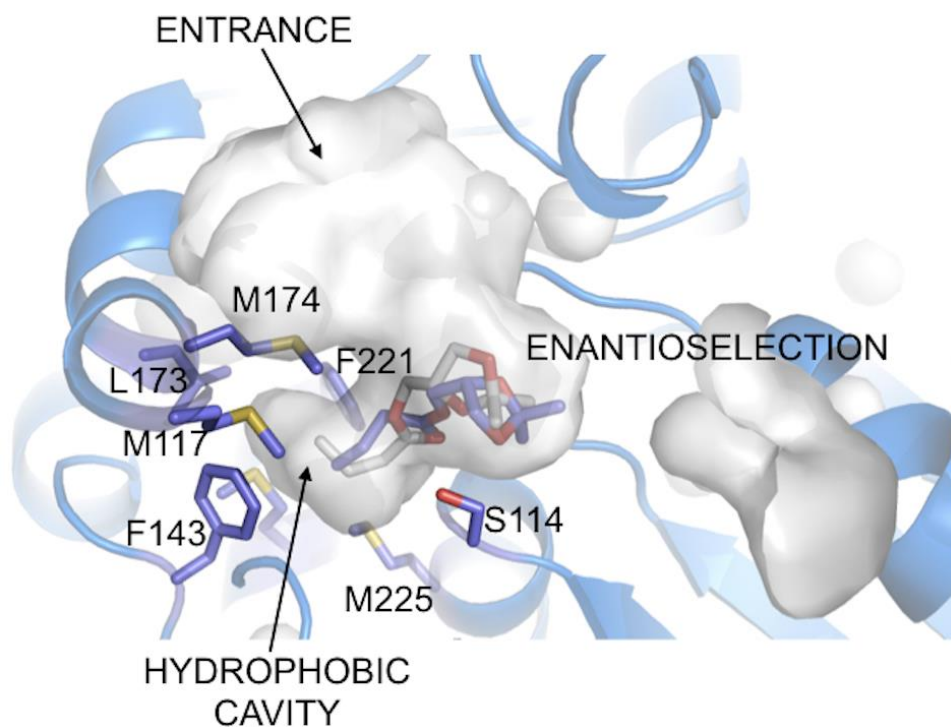


*Figure 6. Detailed view of the apo-BCE active site, highlighting the active site tunnel (surface representation); the entrance to the tunnel and the hydrophobic region of the active site are indicated. Hydrophobic residues, the catalytic S114 and the R- and S- enantiomers of butyrate-IPG (sticks) that were in silico docked in the cavity are shown;*

Analysis by *in silico* docking, using *p*-nitrophenyl compounds with different acyl chains, shows that molecules from C2 to C6 can dock into the cavity in conformations compatible with observed enzymatic activity (**Figure 7**).

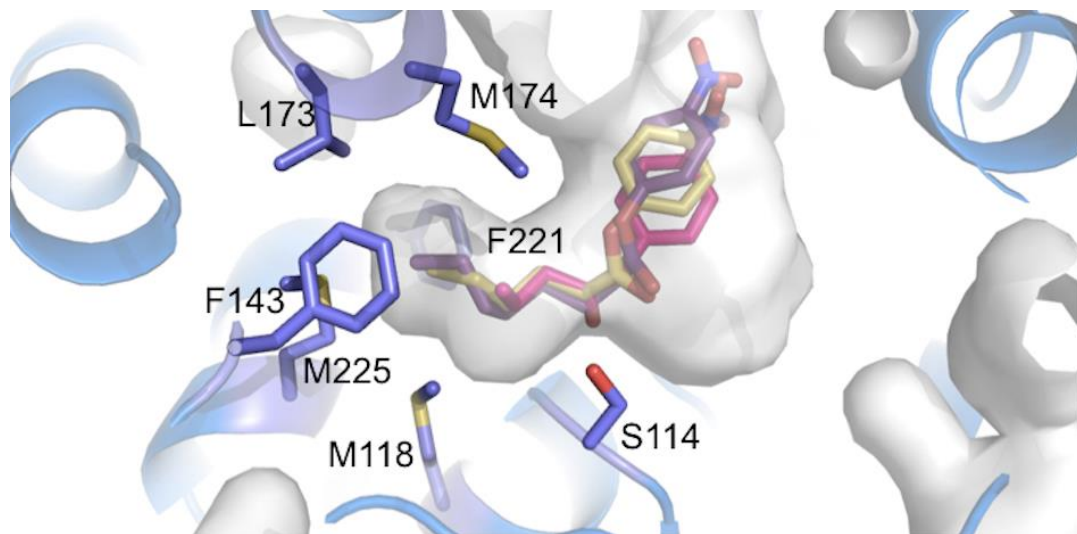


Figure 7. *in silico* docking of *p*-nitrophenyl compounds (sticks) with different acyl chains of variable lengths; C2 (pink), C4 (ochre) and C6 (purple)

On the contrary, the hydrophobic cavity is too short to host compounds bigger than C6 in their correct conformations. It is possible that the high temperature required for optimal enzymatic activity induces some structural rearrangements that allow molecules up to C10 to be processed.

We subsequently used *in silico* docking to try to gain insight into the structural bases of the enantioselectivity of BCE. The calculated dissociation constants ( $K_d$ ) for *R* and *S* enantiomers of different IPG esters (acetate, butyrate, and benzoate) are quite similar (**Table 4**), and thus does not explain the enantioselectivity observed in the experiments.

Table 4. *In silico* docking of acetate, -butyrate and -benzoate IPG esters in the active site of BCE. The calculated dissociation constants ( $K_d$ ) for the *S*- and *R*-enantiomers of the acetate, butyrate and benzoate IPG esters are shown, together with the bond length distance between H284 and the ether oxygen which stabilizes the tetrahedral reaction intermediate. Docking was carried out using Autodock 4.2 [43].

Compound	(R) $K_d$ [ $\mu$ M]	(S) $K_d$ [ $\mu$ M]	dist. O-H284 (R) (Å)	dist. O-H284 (S) (Å)
Acetate-IPG	139.2	137.6	5.0	5.0
Butyrate-IPG	41.9	43	5.0	4.3
Benzoate-IPG	9.9	7.5	5.7	5.4

To further investigate this question, the overall geometry of the chiral ligands in the active site was analyzed and found to differ, and can at least partially explain the different reaction efficiencies toward *R* or *S*-enantiomers. Among others, a parameter that is important for the enzymatic activity is the distance between the oxygen of the alcohol moiety of the esters and H284 (see **Table 4** and **Figure 8**). This distance is crucial to stabilize the tetrahedral intermediate (Step 2) formed during the reaction, as previously described [33]. In IPG acetate, the H284 distance from the oxygen of the alcohol moiety in both *R*- and *S*-enantiomers is the same, in agreement with the lower level of discrimination. On the contrary, the distance is reduced from 5.0 Å to 4.3 Å for the *R*- and *S*-enantiomers of the butyrate ester, respectively; this would suggest a higher efficiency in Step 2 towards *S*-enantiomers (**Figure 8**).

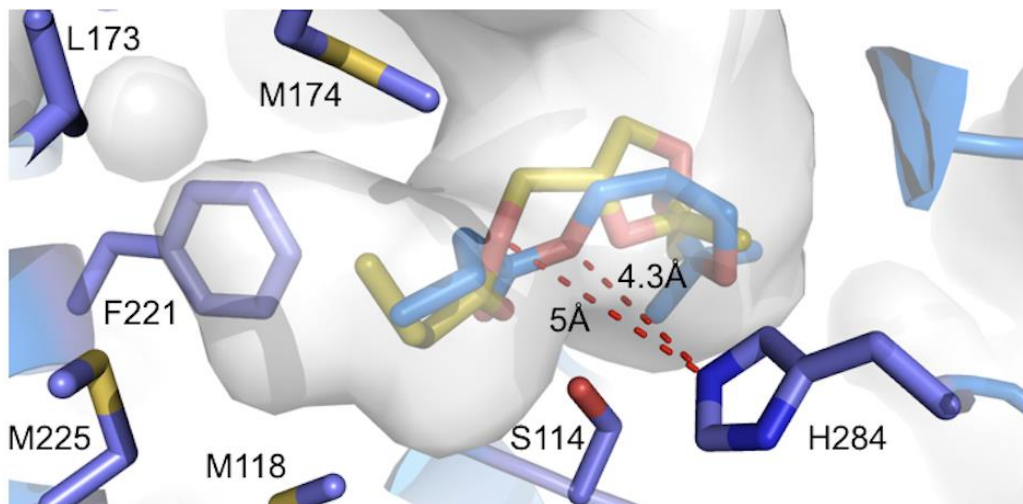


Figure 8. Illustration of the bond distances between the oxygen and H284 in R- (yellow) and S-(blue) butyrate-IPG. Docking was carried out using Autodock4.2 [43].

Overall, these observations imply that enantioselectivity may be due to a combination of different features, including the different permeation of the enantiomers toward the active site (selected by the access tunnel).

### Circular dichroism and thermal stability studies

The conformational stability of BCE in solution was characterized by circular dichroism (CD). In agreement with the crystal structure, the far-UV CD spectrum shows the typical features of  $\alpha$ -helix rich proteins: two minima at 220 and 208 nm, and an intersection at zero at about 203 nm. Thus, the thermal stability of BCE was assessed in function of increasing temperature, monitoring the ellipticity at 220 nm (reporter of  $\alpha$ -helix secondary structures) as described in the Experimental Procedures.

The BCE melting curve is biphasic, with a first minor conformational transition at 42°C ( $T_{m1}$ , 30% of the total transition) and a second main transition at 87°C ( $T_{m2}$ , 70% of the total transition) (**Figure 9**).



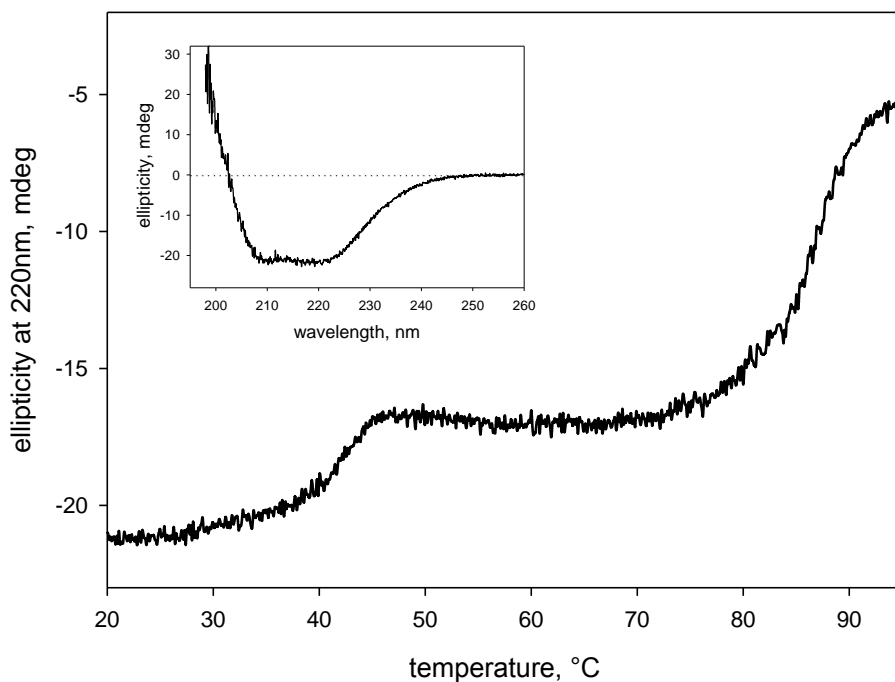


*Figure 9. Thermal unfolding of BCE monitored through far-UV CD at 220 nm as described in the Experimental procedures. The two transitions are labeled Tm1 and Tm2, respectively. Inset: BCE far-UV CD spectrum;*

The second transition triggers a macroscopic aggregation of unfolded protein that causes irreversible denaturation. The reversibility of the first transition was studied by setting-up a multistep temperature ramp experiment. A native BCE sample was heated in a first temperature ramp from 20 to 60°C and then cooled down to the starting temperature of 20°C. The same BCE sample was heated in a second temperature ramp up to 95°C (**Figure 10**).

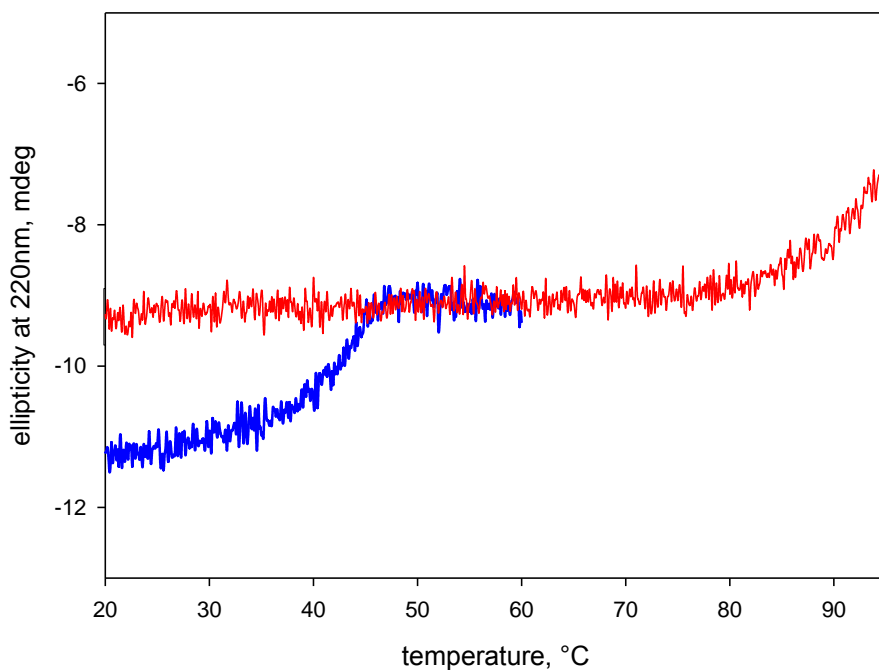


*Figure 10. The reversibility of the first conformational transition was evaluated by thermal unfolding of BCE, monitored through far-UV CD at 220 nm at protein concentration of 0.1 mg/mL. Native BCE was heated from 20°C to 60°C (blue line) and then cooled down to 20°C. The same sample was heated up to 95°C (red line). The two transitions are labeled  $T_{m1}$  and  $T_{m2}$ , respectively. In this experiment,  $T_{m2}$  occurs at higher temperature due to the lower protein concentration.*

In the second temperature ramp the first minor melting is no longer visible, whereas the second main transition is perfectly conserved, proving that the two transition are irreversible and, apparently, independent.

Although the structural regions involved in the first transition have not been identified, to gain better insight into the nature of these conformational transitions we carried-out activity assays on BCE, with and without heat-treatment at 60°C. Interestingly, also the heat-treated protein was catalytically competent, although a 90% decrease in activity was observed. According to the molecular dynamics calculations that divide the BCE structure into two independent domains (the core  $\alpha/\beta$ -hydrolase domain and the lid domain) we hypothesize

that the lid domain may be responsible for the first unfolding event, affecting the catalytic function of BCE only marginally. This hypothesis is also in good agreement with a “quantitative” analysis of the unfolding trace: the signal lost in the first transition is about 30%, thus compatible with loss of the three  $\alpha$ -helices of the lid relative to a total of the eleven  $\alpha$ -helices of the whole structure. Lid unfolding would have an effect on binding to the hydrophobic tail of the substrate, whereas binding to the oxyanion hole would be essentially unaffected.

Protein thermostability can be attributed to a number of other structural features such as the presence of disulfide bonds and intra-helical salt bridges [33]. BCE1 does not contain any disulfide bonds and in fact, only contains one non-conserved cysteine residue (C137). Using the ESPRI web server (<http://bioinformatica.isa.cnr.it/ESBRI/introduction.html>), 21 salt bridges (2.4-3.9 Å) were found in BCE, none of which are present within the lid domain, although two are formed between lid residue (D79) and residues R14(NZ) (3.2 Å) and R216(NH2) (3.1 Å (OD2) and 3.3 Å (OD1)) [34, 35]. These analyses also corroborate the theory that the  $\alpha/\beta$ -hydrolase core is stable to a greater extent than the lid domain, supporting both the MD and CD studies and reinforces the likelihood that lid unfolding is responsible for the first unfolding transition.

# Discussion

Carboxylesterases are ubiquitous enzymes that catalyze the cleavage and/or formation of carboxyl ester bonds. Their division into lipolytic (lipases) and non-lipolytic esterases is based on experimental data and theoretical hypothesis, and is often quite uncertain. All carboxylesterases share the so-called  $\alpha/\beta$  hydrolase fold, where five (or more) strands in a central  $\beta$ -sheet forming the protein core are connected by  $\alpha$ -helices; this superfamily is one of the largest families of structurally-related enzymes. Despite such elevated structural conservation,  $\alpha/\beta$ -hydrolase members catalyze a wide variety of chemical transformations, and thus are extensively used in industrial processes. Lipases are characterized by the presence of a mobile subdomain (lid), which caps and shields substrate entry to the active site. The closed-lid conformation is supposed to be preponderant in water, where most lipases are poorly active, whereas interactions with hydrophobic compounds (substrates, organic solvents) are thought to prompt a conformational change of the lid making it accessible to the substrates (open-lid). The overall phenomenon is generally referred as “interfacial activation” [36].

Due to their advantageous biochemical properties, such as high chemo-, regio- and stereo-selectivity and thermostability, microbial carboxylesterases have numerous industrial applications in a wide range of sectors [4-6]. Kinetic resolution of racemic esters of chiral alcohols *via* their enantioselective hydrolysis is among the most studied application. Optically pure (*S*)-1,2-*O*-isopropylidenglycerol (IPG) is a key intermediate for the preparation of  $\beta$ -blockers, leukotrienes, phospholipids, and prostaglandins [24]. Hydrolysis of racemic IPG esters has been explored using different carboxylesterases aiming at optically pure (*S*)-IPG; commercially available lipases are generally poorly active or scarcely enantioselective towards racemic IPG esters [25]. We previously found that BCE, a carboxylesterase from *B. coagulans*, carried out the kinetic resolution of different racemic IPG esters yielding (*S*)-IPG with high enantioselectivity [14].

To gain insight into the structure-function properties of BCE that may account for such enantioselectivity for IPG esters, we carried out the recombinant production, functional characterization and 3D structure determination of BCE (ligand-free and glycerol-bound). Recombinant BCE successfully catalyzed the enantioselective hydrolysis of different IPG

esters in providing optically pure (*S*)-IPG with good reaction rates and excellent enantiomeric ratios; the best results being obtained with butyrate (C4) and benzoate (C6) IPG esters. Activity however diminished by 10% for C8 chains and by 90% for C10 chains and was completely abolished for C12 and C16 chains. In line with these data, structure analyses show that the active site cavity may only accommodate substrates with aliphatic carbon chain lengths shorter or equal to C6. Given the activity of BCE at elevated reaction temperatures that reach as high as 65°C, it is possible that at high temperatures, a conformational change is induced, allowing expansion of the active site and permitting the hydrolysis of slightly longer substrates. In fact, CD thermal stability studies show that there are two unfolding events, with the former occurring at a  $T_M$  of 45°C. We hypothesize that this event reflects the unfolding of the lid domain, as indicated by MD studies and structural observations made that underline the presence of 21 stabilizing salt bridges in the  $\alpha/\beta$ -hydrolase core and none in the lid domain. Given that hydrophobic residues of the lid domain contribute to forming the hydrophobic cavity that binds the aliphatic carbon tail of ester substrates, it is unsurprising that substrate specificity may be altered at higher reaction temperatures.

Poor activity towards long-chain esters, together with high enantioselectivity towards IPG esters are typical features of non-lipolytic carboxylesterases. Moreover, benzoate esters, which are easily hydrolyzed by BCE, are not preferred substrates for lipases (with the exception of the very versatile *Candida antarctica* Lipase B-CALB) [37]. Such functional findings are in sharp contrast to our structural studies that highlight the presence of a lipase-typical lid domain, in addition to the canonical  $\alpha/\beta$ -hydrolase fold. Given the role of this domain for catalysis in a process termed interfacial activation, where optimal reaction rates are observed at the hydrophobic-water interface, we carried out experiments in the presence of a triglyceride layer reproduced by the addition of tributyrin. In agreement with our activity studies but in contrast to the presence of this lipase-specific domain, interfacial activation was not observed. The lack of interfacial activation and the fact that BCE was able to convert the (small) substrates used in this study in water with conventional kinetics, was also implied by the lack of lid positioning in the ligand-free and glycerol-bound structures. Interestingly, despite the observed 'closed' lid state of ligand-free BCE, access to the substrate-binding site was not completely blocked and a 13 Å mouth-opening to the active site tunnel was observed

that could easily permit the diffusion of IPG esters, as illustrated by our structural analyses. Despite non-lipase functions, we cannot rule out the lid domain switching between 'open' and 'closed' conformations; *in silico* simulations and computational analyses carried out on the BCE structure, focusing on protein flexibility and rigid body movements, detected the lid domain as a mobile entity.

In lipases, the size and structural arrangement of the lid domain varies considerably and recent attempts have been made to classify lipase sub-groups according to the size and conformation of the lid [30]. Based on 44 distinct lipase structures, three sub-groups were devised: *i*) lipases that lack a lid, *ii*) lipases that contain a lid formed by a single loop or  $\alpha$ -helix, and *iii*) lipases that contain lids comprised of two or more  $\alpha$ -helices. A link between optimum reaction temperature and lid organization was observed; large lids are correlated to catalysis at higher reaction temperatures [30]. Based on this classification, and the, were BCE, with its particularly large BCE lid (approx. 90 residues), would pertain to the third class of large lid lipases that exhibit thermostable properties[30]. This is in agreement with our findings, demonstrating that BCE remains active at high reaction temperatures.

## Conclusion

Our studies revealed that BCE is an atypical carboxylesterase characterized by non-lipolytic functionalities in contrast to a lipase-like 3D fold. With regards to the enantioselective hydrolysis of short-chain and benzoate esters of IPG, with a preference for (*S*)-IPG esters, *in silico* docking studies on the BCE structure suggest that a reduced distance between the catalytic histidine residue (H284) side chain that stabilizes the tetrahedral reaction intermediate during catalysis and the oxygen atom of the ester alcohol group, may play a role, however further studies are required. Thanks to the here-reported crystal structures, *in silico* docking may be used to identify inhibitors that may be used in co-crystallization studies to reveal the active residues that govern this specificity. Our results may pave the way for rational engineering strategies aimed at the construction of new variants with wider substrate specificities, and thus suited for different applications as stereoselective biocatalysts

## References

1. Ali, Y. B., Verger, R. & Abousalham, A. (2012) Lipases or esterases: does it really matter? Toward a new bio-physico-chemical classification, *Methods in molecular biology*. **861**, 31-51.
2. Fischer M., Pleiss J. (2003) The Lipase Engineering Database: a navigation and analysis tool for protein families. *Nucleic acids research*. **31**, 319-321.
3. Hotelier, T., Renault, L., Cousin, X., Negre, V., Marchot, P. & Chatonnet, A. (2004) ESTHER, the database of the alpha/beta-hydrolase fold superfamily of proteins, *Nucleic acids research*. **32**, D145-7.
4. Kourist, R., Jochens, H., Bartsch, S., Kuipers, R., Padhi, S. K., Gall, M., Bottcher, D., Joosten, H. J. & Bornscheuer, U. T. (2010) The alpha/beta-hydrolase fold 3DM database (ABHDB) as a tool for protein engineering, *Chembiochem : a European journal of chemical biology*. **11**, 1635-43.
5. Carvalho, A. C., Fonseca Tde, S., de Mattos, M. C., de Oliveira Mda, C., de Lemos, T. L., Molinari, F., Romano, D. & Serra, I. (2015) Recent Advances in Lipase-Mediated Preparation of Pharmaceuticals and Their Intermediates, *International journal of molecular sciences*. **16**, 29682-716.
6. Romano, D., Bonomi, F., de Mattos, M. C., de Sousa Fonseca, T., de Oliveira Mda, C. & Molinari, F. (2015) Esterases as stereoselective biocatalysts, *Biotechnology advances*. **33**, 547-65.
7. Gotor-Fernandez, V., Brieva, R and Gotor, V (2006) Lipases: Useful biocatalysts for the preparation of pharmaceuticals., *J Mol Catal*. **40**, 111-120.
8. Guncheva, M., Zhiryakova, D. (2011) Catalytic properties and potential applications of Bacillus lipases., *J Mol Catal*. **B68**, 1-21.
9. Droge, M. J., Bos, R. & Quax, W. J. (2001) Paralogous gene analysis reveals a highly enantioselective 1,2-O-isopropylidenglycerol caprylate esterase of Bacillus subtilis, *European journal of biochemistry*. **268**, 3332-8.



10. Quax, W. J. & Broekhuizen, C. P. (1994) Development of a new *Bacillus* carboxyl esterase for use in the resolution of chiral drugs, *Applied microbiology and biotechnology*. **41**, 425-31.
11. Rozeboom, H. J., Godinho, L. F., Nardini, M., Quax, W. J. & Dijkstra, B. W. (2014) Crystal structures of two *Bacillus* carboxylesterases with different enantioselectivities, *Biochimica et biophysica acta*. **1844**, 567-75.
12. Schmidt, M., Henke, E., Heinze, B., Kourist, R., Hidalgo, A. & Bornscheuer, U. T. (2007) A versatile esterase from *Bacillus subtilis*: cloning, expression, characterization, and its application in biocatalysis, *Biotechnology journal*. **2**, 249-53.
13. Steenkamp, L., Brady, D. (2008) Optimisation of stabilised carboxylesterase NP for enantioselective ester hydrolysis of naproxen methyl ester., *Process Biochem*. **43**, 1419-26.
14. van Pouderooyen, G., Eggert, T., Jaeger, K. E. & Dijkstra, B. W. (2001) The crystal structure of *Bacillus subtilis* lipase: a minimal alpha/beta hydrolase fold enzyme, *Journal of molecular biology*. **309**, 215-26.
15. Molinari, F., Brenna, O., Valenti, M., Aragozzini, F. (1996) Isolation of a novel carboxylesterase from *Bacillus coagulans* with high enantioselectivity toward racemic esters of 1,2-O-isopropylidenglycerol., *Enzyme Microb Technol*. **19**, 551-6.
16. Liu, J. Y., Zheng G.W., Imanaka, T, Xu J.H. (2014) Stepwise and combinatorial optimization of enantioselectivity for the asymmetric hydrolysis of 1-(3',4'-methylenedioxyphenyl)ethyl acetate under use of a cold-adapted *Bacillus amyloliquefaciens* esterase, *Biotechnol Bioprocess Eng*. **99**, 442-8.
17. Henke, E. & Bornscheuer, U. T. (2002) Esterases from *Bacillus subtilis* and *B. stearothermophilus* share high sequence homology but differ substantially in their properties, *Applied microbiology and biotechnology*. **60**, 320-6.
18. Fillat, A., Romea, P., Urpi, F., Pastor, F. I. & Diaz, P. (2014) Improving enantioselectivity towards tertiary alcohols using mutants of *Bacillus* sp. BP-7

esterase EstBP7 holding a rare GGG(X)-oxyanion hole, *Applied microbiology and biotechnology*. **98**, 4479-90.

19. Godinho, L. F., Reis, C.R., van Merkerk R., Poelarends G-L., Quax W.J. (2012) An esterase with superior activity and enantioselectivity towards 1,2-O-isopropylidene glycerol esters obtained by protein design., *Adv Synth Catal*. **354**, 3009-15.

20. Godinho, L. F., Reis, C. R., Rozeboom, H. J., Dekker, F. J., Dijkstra, B. W., Poelarends, G. J. & Quax, W. J. (2012) Enhancement of the enantioselectivity of carboxylesterase A by structure-based mutagenesis, *Journal of biotechnology*. **158**, 36-43.

21. Godinho, L. F., Reis, C. R., Tepper, P. G., Poelarends, G. J. & Quax, W. J. (2011) Discovery of an Escherichia coli esterase with high activity and enantioselectivity toward 1,2-O-isopropylidene glycerol esters, *Applied and environmental microbiology*. **77**, 6094-9.

22. Molinari, F., Romano, D., Gandolfi, R., Kroppenstedt, R. M. & Marinelli, F. (2005) Newly isolated Streptomyces spp. as enantioselective biocatalysts: hydrolysis of 1,2-O-isopropylidene glycerol racemic esters, *Journal of applied microbiology*. **99**, 960-7.

23. Monti, D., Ferrandi, E. E., Righi, M., Romano, D. & Molinari, F. (2008) Purification and characterization of the enantioselective esterase from Kluyveromyces marxianus CBS 1553, *Journal of biotechnology*. **133**, 65-72.

24. Romano, D., Falcioni, F, Mora, D. and Molinari, F. (2005) Enhanced enantioselectivity of Bacillus coagulans in the hydrolysis of 1,2-O-isopropylidene glycerol esters by thermal knock-out of undesired enzymes, *Tetrahedron Asymmetry*. **16**, 841-5.

25. Jurczac, J., Pikul, S., Bauer, T., (1986) *Tetrahedron Asymmetry*. **42**, 447-488.

26. Machado, A., da Silva, A., Borges, C., Simas, A, Freire, D. (2011) Kinetic resolution of (R,S)-1,2-isopropylidene glycerol (solketal) ester derivatives by lipases, *Journal of Molecular Catalysis B: Enzymatic* **69**, 42-46.

27. Romano, A., Romano, D., Molinari, F., Gandolfi, R & Costantino, F (2005) A new chemoenzymatic synthesis of D-cloprostenol. , *Tetrahedron: Asymmetry* **16**, 3279-3282.
28. Schalk-Hihi, C., Schubert, C., Alexander, R., Bayoumy, S., Clemente, J. C., Deckman, I., DesJarlais, R. L., Dzordzorme, K. C., Flores, C. M., Grasberger, B., Kranz, J. K., Lewandowski, F., Liu, L., Ma, H., Maguire, D., Macielag, M. J., McDonnell, M. E., Mezzasalma Haarlander, T., Miller, R., Milligan, C., Reynolds, C. & Kuo, L. C. (2011) Crystal structure of a soluble form of human monoglyceride lipase in complex with an inhibitor at 1.35 Å resolution, *Protein science : a publication of the Protein Society*. **20**, 670-83.
29. Bertrand, T., Auge, F., Houtmann, J., Rak, A., Vallee, F., Mikol, V., Berne, P. F., Michot, N., Cheuret, D., Hoornaert, C. & Mathieu, M. (2010) Structural basis for human monoglyceride lipase inhibition, *Journal of molecular biology*. **396**, 663-73.
30. Khan, F. I., Lan, D., Durrani, R., Huan, W., Zhao, Z. & Wang, Y. (2017) The Lid Domain in Lipases: Structural and Functional Determinant of Enzymatic Properties, *Frontiers in bioengineering and biotechnology*. **5**, 16.
31. Pettersen, E. F., Goddard, T.D., Huang, C.C., Couch, G.S., Greenblatt, D.M., Meng, E.C., Ferrin, T.E. (2004) UCSF Chimera--a visualization system for exploratory research and analysis. , *J Comput Chem*. **25**, 1065-12.
32. Aleksiev, T., Potestio, R., Pontiggia, F., Cozzini, S. & Micheletti, C. (2009) PiSQRD: a web server for decomposing proteins into quasi-rigid dynamical domains, *Bioinformatics*. **25**, 2743-4.
33. Dundas, J., Ouyang, Z., Tseng, J., Binkowski, A., Turpaz, Y. & Liang, J. (2006) CASTp: computed atlas of surface topography of proteins with structural and topographical mapping of functionally annotated residues, *Nucleic acids research*. **34**, W116-8.
34. Kumar, S., Tsai, C. J., Ma, B. & Nussinov, R. (2000) Contribution of salt bridges toward protein thermostability, *Journal of biomolecular structure & dynamics*. **17 Suppl 1**, 79-85.

35. Kumar, S. & Nussinov, R. (1999) Salt bridge stability in monomeric proteins, *Journal of molecular biology*. **293**, 1241-55.
36. Reis, P. H., K. Watzke, H. Leser. ME and Miller ,R. (2009) Lipases at interfaces: a review., *Adv Colloid Interface Sci* **147–148**, 237–250.
37. Sangeeta, N. A., B. Rakhi, S. Bhawna, M. Pritish, P. Robin, C. Jesper, B. and Allan, S. (2010) Lipases for use in industrial biocatalysis: Specificity of selected structural groups of lipases, *Journal of Molecular Catalysis B: Enzymatic*. **65**.
38. Evans, P. (2006) Scaling and assessment of data quality, *Acta crystallographica Section D, Biological crystallography*. **62**, 72-82.
39. Kabsch, W. (2010) Xds, *Acta crystallographica Section D, Biological crystallography*. **66**, 125-32.
40. Kabsch, W. (2010) Integration, scaling, space-group assignment and post-refinement, *Acta crystallographica Section D, Biological crystallography*. **66**, 133-44.
41. Long, F., Vagin, A. A., Young, P. & Murshudov, G. N. (2008) BALBES: a molecular-replacement pipeline, *Acta crystallographica Section D, Biological crystallography*. **64**, 125-32.

# Synthesis of enantiomerically enriched 2-hydroxymethylalkanoic acids by oxidative desymmetrisation of achiral 1,3-diols mediated by *Acetobacter aceti*

Elisabetta Brenna,<sup>\*,[a, b]</sup> Flavia Cannavale,<sup>[a]</sup> Michele Crotti,<sup>[a]</sup> **Valerio De Vitis**,<sup>[c]</sup> Francesco G. Gatti,<sup>[a]</sup> Gaia Migliazza,<sup>[a]</sup> Francesco Molinari,<sup>[c]</sup> Fabio Parmeggiani,<sup>[a]</sup> Diego Romano,<sup>[c]</sup> and Sara Santangelo<sup>[a]</sup>

## **Affiliations:**

<sup>[a]</sup> Prof. E. Brenna, F. Cannavale, M. Crotti, Prof. F. G. Gatti, G. Migliazza, Dr. F. Parmeggiani, S. Santangelo Dipartimento di Chimica Materiali ed Ingegneria Chimica “Giulio Natta” Politecnico di Milano Via Mancinelli 7 20131, Milano (Italy) E-mail: mariaelisabetta.brenna@polimi.it

<sup>[b]</sup> Prof. E. Brenna Istituto di Chimica del Riconoscimento Molecolare, C.N.R. Via Mario Bianco, 9 20131, Milano (Italy)

<sup>[c]</sup> V. De Vitis, Prof. F. Molinari, Dr. D. Romano University of Milan Department of Food, Environmental and Nutritional Science (DeFENS) Via Mangiagalli 25 20133, Milano (Italy)

Published on ChemCatChem, 2016

# Abstract

The stereoselective desymmetrisation of achiral 2-alkyl-1,3-diols is performed by oxidation of one of the two enantiotopic primary alcohol moieties by means of *Acetobacter aceti* MIM 2000/28 to afford the corresponding chiral 2-hydroxymethyl alkanolic acids (up to 94% ee). The procedure, carried out in aqueous medium under mild conditions of pH, temperature and pressure, contributes to enlarge the portfolio of enzymatic oxidations available to organic chemists for the development of sustainable manufacturing processes.

# Introduction

The stereoselective desymmetrisation of achiral and meso substrates is a highly effective procedure for the preparation of enantiomerically enriched compounds. The technique consists of the chemical modification of a molecule to remove one or more symmetry elements precluding chirality.<sup>[1]</sup> Typically, it is achieved by using a chiral reagent or catalyst to distinguish between two enantiotopic groups of the starting substrate and selectively promote the chemical transformation of only one of them. The huge potential of this procedure of asymmetric activation has been widely exploited for a large array of structurally diverse substrates.<sup>[2]</sup> In the last decade, enzymes have received great attention for the optimisation of desymmetrisation procedures:<sup>[3]</sup> for example, biocatalysed ester hydrolysis and transesterifications have been successfully applied to prepare enantiomerically enriched compounds starting from achiral diesters and diols. Relevant examples involving chiral active pharmaceutical ingredients (APIs) have been recently reported.<sup>[4]</sup> Among biocatalysed reactions, the oxidation of alcohols and sugars mediated by acetic acid bacteria (e.g., *Acetobacter sp.*, *Acidiphilium sp.*, *Gluconobacter sp.*) is a very powerful tool for the development of sustainable synthetic transformations.<sup>[5]</sup> This remarkable activity is powered by a peculiar respiratory chain system:<sup>[6]</sup> in acetic acid bacteria, many types of membrane-bound dehydrogenases, located on the periplasmic surface of the cytoplasmic membrane, reduce ubiquinone with concomitant substrate oxidation, then the reduced form of ubiquinone is re-oxidized by the terminal ubiquinol oxidases. Substrate oxidation occurs according to a two-step sequence, first involving the conversion of the primary alcohol into aldehyde by a pyrroquinoline quinone-dependent alcohol dehydrogenase (PPQ-ADH) and then the final transformation of the aldehyde intermediate into carboxylic acid by an aldehyde dehydrogenase. The reaction shows excellent chemo-, regio- and stereoselectivity, and it is carried out under mild conditions of temperature, pressure and pH, in non-problematic solvents, at high turnover rates.<sup>[7]</sup> Moreover, acetic acid bacteria are acidophilic microorganisms that thrive in acidic environments at pH values below 4.0, hence they are particularly naturally fit to accumulate high concentrations of carboxylic acids.<sup>[8]</sup>

All these features make this oxidation suitable for the selective modification of one enantiotopic primary alcohol moiety over another. Nonetheless, to our knowledge, the

potential of this enzymatic oxidative procedure for the desymmetrisation of achiral diols has been scarcely investigated. For 1,5-diols, only the conversion of the 3-methyl-substituted derivative into the corresponding enantiomerically enriched d-lactone was investigated, either by using *Gluconobacter roseus*[9] or by a two-step oxidation mediated by horse liver alcohol dehydrogenase.[10] The oxidative desymmetrisations of 1,3-diols reported so far are limited to those of 2-methyl and 2-butyl derivatives catalysed by acetic acid bacteria. The microbial oxidation of 2-methyl-1,3-propanediol leading to (*R*)-3-hydroxy-2-methylpropionic acid (an important building block for the synthesis of the ACE inhibitor captopril) was described in 2003, reporting 97% enantiomeric excess and 100% molar conversion of 5 gL<sup>-1</sup> within 2 h, by using *Acetobacter pasteurianus* DSM 8937.<sup>[11]</sup> More recently, *A. pasteurianus* IAM 12073 was found to produce the (*S*)-enantiomer of 2-(hydroxymethyl)hexanoic acid from 2-butyl-1,3-diol with 89% enantiomeric excess and 82% conversion after 24 h of incubation.<sup>[12]</sup> The few available sets of data on the use of acetic acid bacteria in desymmetrisation reactions prompted us to investigate more systematically their synthetic potential for the conversion of achiral 1,3-diols into chiral hydroxyalkanoic acids according to this procedure to enlarge the portfolio of enzymatic reactions available to organic chemists for the development of sustainable manufacturing processes. The results of our research are herein reported.



# Experimental Section

## General methods

$^1\text{H}$  and  $^{13}\text{C}$  NMR spectra were recorded with a 400 or 500 MHz spectrometer in  $\text{CDCl}_3$  solution at room temperature. The chemical shift scale was based on internal tetramethylsilane.

GC/MS analyses were performed by using a HP-5MS column (30 m $\times$ 0.25 mm $\times$ 0.25  $\mu\text{m}$ , Agilent). The following temperature program was employed: 60  $^\circ\text{C}$  (1 min)/6  $^\circ\text{C min}^{-1}$ /150  $^\circ\text{C}$  (1 min)/12  $^\circ\text{C min}^{-1}$ /280  $^\circ\text{C}$  (5 min).

Chiral GC analysis was performed on a Chirasil-DEX-CB (25 m $\times$ 0.25 mm $\times$ 0.25  $\mu\text{m}$ , Chrompack) column or on a DAcTBSil BetaCDX column (25 m $\times$ 0.25 mm $\times$ 0.25  $\mu\text{m}$ , Mega), installed on a gas chromatograph equipped with FID (carrier gas  $\text{H}_2$ , constant flow 3.7 mL  $\text{min}^{-1}$ ,  $t_{\text{injector}}=250$   $^\circ\text{C}$ ,  $t_{\text{detector}}=250$   $^\circ\text{C}$ ). Chiral HPLC analysis was performed on a Chiralcel OD column (4.6 mm $\times$ 250 mm, Daicel) installed on an HPLC instrument with UV detector ( $\lambda=220$  nm).

TLC analysis was performed on Merck Kieselgel 60 F<sub>254</sub> plates. All the chromatographic separations were carried out on silica gel columns.

## Microorganisms, growth and biotransformation conditions

*Acetobacter aceti* MIM 2000/28 and *Asaia bogorensis* SF2.1 from the MIM collection (Microbiologia Industriale Milano), and *Gluconobacter oxydans* DSM 50049 (Deutsche Sammlung von Mikroorganismen) were employed in the preliminary screening. All strains were routinely maintained on GYC slants (glucose 50 g  $\text{L}^{-1}$ , yeast extract 10 g  $\text{L}^{-1}$ ,  $\text{CaCO}_3$  30 g  $\text{L}^{-1}$ , agar 15 g  $\text{L}^{-1}$ , pH 6.3) at 28  $^\circ\text{C}$ . Strains, grown on GYC slants for 24 h at 28  $^\circ\text{C}$ , were inoculated into 100 mL baffled Erlenmeyer flasks containing 20 mL of liquid GLY medium (glycerol 25 g  $\text{L}^{-1}$ , yeast extract 10 g  $\text{L}^{-1}$ , pH 5, distilled water). After 24 h at 28  $^\circ\text{C}$ , 150 rpm, the entire culture was used to inoculate 2 L baffled Erlenmeyer flasks containing 200 mL of GLY medium and incubated under the same conditions. *A. aceti* MIM 2000/28 was selected for the development of the oxidative desymmetrisation reactions.

The biotransformations were performed directly inside the culture flasks according to the following procedure. The suitable neat diol **1 a–i** (200 mg) was added to the cultural broth (200 mL) and the flask was shaken at 150 rpm at 30 °C. After 72 h, the reaction mixture was centrifuged to remove the bacterial cells, the supernatant was brought to pH 2.0 with aqueous HCl and extracted with Et<sub>2</sub>O. The combined organic phases were dried over anhydrous Na<sub>2</sub>SO<sub>4</sub>. The residue was purified by column chromatography on a silica gel column, eluting with *n*-hexane and increasing amounts of ethyl acetate to obtain the corresponding hydroxy acid.

### **Characterisation of the products obtained by oxidative desymmetrisation of diols **1 a–i****

#### **(*R*)-(Hydroxymethyl)propanoic acid ((*R*)-**2 a**)**

From **1 a** (0.200 g, 2.22 mmol), derivative (*R*)-(-)-**2 a** was obtained (0.231 g, 89 %): *ee*=94 % (determined from the corresponding methyl ester) [ $\alpha$ ]<sub>D</sub>=-11.3 (*c*=1.00, EtOH), ref. [28]; <sup>1</sup>H NMR (CDCl<sub>3</sub>, 300 MHz):[29]  $\delta$ =5.70 (1 H, bs), 3.75 (1 H, d, *J*=6.0 MHz), 2.74 (1 H, m), 2.10 (1 H, s), 1.22 ppm (3 H, d, *J*=7.4 MHz); <sup>13</sup>C NMR (CDCl<sub>3</sub>, 75 MHz): 180.1, 64.0, 41.6, 13.2 ppm.

#### **(*R*)-2-(Hydroxymethyl)butanoic acid ((*R*)-**2 b**)**

From **1 b** (0.200 g, 1.92 mmol), derivative (*R*)-(-)-**2 b** was obtained (0.057 g, 25 %): *ee*=54 % (determined from the corresponding methyl ester) [ $\alpha$ ]<sub>D</sub>=-2.8 (*c*=0.50, CHCl<sub>3</sub>); <sup>1</sup>H NMR (CDCl<sub>3</sub>, 400 MHz):[30]  $\delta$ =3.90–3.70 (2 H, m, CH<sub>2</sub>OH), 2.56 (1 H, m, CHCOOH), 1.80–1.55 (2 H, m, CHCH<sub>2</sub>), 1.00 ppm (3 H, t, *J*=7.6 Hz, CH<sub>2</sub>CH<sub>3</sub>); <sup>13</sup>C NMR (CDCl<sub>3</sub>, 100.6 MHz):[30]  $\delta$ =180.4, 62.7, 49.0, 21.6, 11.8 ppm.

#### **Methyl (*R*)-2-(hydroxymethyl)butanoate ((*R*)-**5 b**)**

Compound (*R*)-**2 b** (0.050 g, 0.424 mmol) was heated at reflux in MeOH (4 mL) in the presence of a catalytic quantity of H<sub>2</sub>SO<sub>4</sub> to afford, after the usual work-up, the corresponding methyl ester (+)-(*R*)-**5 b** (0.053 g, 95 %): *ee*=54 % (by chiral HPLC of the 3,5-dinitrobenzoate derivative) [ $\alpha$ ]<sub>D</sub>=+2.4 (*c*=1.1, CHCl<sub>3</sub>), ref. [31]; for (*R*)-**5 b** *ee*=88 %

$[\alpha]_{\text{D}}=+4.1$  ( $c=1.0$ ,  $\text{CHCl}_3$ );  $^1\text{H NMR}$  ( $\text{CDCl}_3$ , 400 MHz):[**32**]  $\delta=3.84\text{--}3.66$  (5 H, m+s,  $\text{CH}_2\text{OH}+\text{OCH}_3$ ), 2.52 (1 H, m,  $\text{CHCOOCH}_3$ ), 1.75–1.50 (2 H, m,  $\text{CH}_2\text{CH}_3$ ), 0.95 ppm (3 H, t,  $J=7.4$  Hz,  $\text{CH}_2\text{CH}_3$ );  $^{13}\text{C NMR}$  ( $\text{CDCl}_3$ , 100.6 MHz):  $\delta=175.0$ , 63.0, 51.8, 49.1, 21.8, 11.8 ppm; GC/MS (EI):  $t_{\text{R}}=6.50$  min:  $m/z$  (%)=114 ( $M^+-18$ , 8), 102 (50), 87 (100).

The absolute configuration was confirmed by comparing the HPLC analysis of the 3,5-dinitrobenzoate derivative **7 b** prepared from (+)-(*R*)-**5 b** with a sample of the 3,5-dinitrobenzoate derivative of (*S*)-**5 b** prepared by baker's yeast reduction of ethyl 2-formylbutanoate **6 b**,[22] followed by transesterification with MeOH and a catalytic quantity of  $\text{H}_2\text{SO}_4$ .

Chiral HPLC: Chiralcel OD (*n*-hexane/*i*PrOH 9:1, 0.6 mL min<sup>-1</sup>),  $t_{\text{R}}$  (*R*)-**7 b**=51.30 min,  $t_{\text{R}}$ (*S*)-**7 b**=61.32 min.

#### **1-Methylenebutanoic acid (3 b) and 2-methylbutanoic acid (4 b)**

From **1 b** (0.200 g, 1.92 mmol), besides derivative (*R*)-**2 b** (25%), a 1:1.5 ( $^1\text{H NMR}$ ) mixture of **3 b** and **4 b** (0.097 g) was isolated:  $^1\text{H NMR}$  ( $\text{CDCl}_3$ , 400 MHz), signals of **3 b**: $^{331}$   $\delta=6.27$  (1 H, br s,  $\text{CHH}=\text{C}$ ), 5.65 (1 H, br s,  $\text{CHH}=\text{C}$ ), 2.34 (1 H, q,  $J=7.2$  Hz,  $\text{CH}_2\text{C}=\text{}$ ), 1.10 ppm (3 H, t,  $J=7.2$  Hz,  $\text{CH}_2\text{CH}_3$ ); signals of **4**: $^{341}$   $\delta=2.42$  (1 H, m,  $\text{CHCOOH}$ ), 1.60 (2 H, m,  $\text{CH}_2\text{CH}$ ), 1.18 (3 H, t,  $J=6.9$  Hz,  $\text{CHCH}_3$ ), 0.89 ppm (3 H, t,  $J=7.4$  Hz,  $\text{CH}_2\text{CH}_3$ ); GC/MS (EI): **3 b**  $t_{\text{R}}=5.46$ ,  $m/z$  (%)=100 ( $M^+$ , 78), 85 (52), 55 (100); **4 b**  $t_{\text{R}}=4.99$ :  $m/z$  (%)=87 ( $M^+-15$ , 25), 74 (100), 57 (55).

#### **(R)-2-(Hydroxymethyl)pentanoic acid ((R)-2 c)**

From **1 c** (0.200 g, 1.69 mmol), derivative (*R*)-**2 c** was obtained (0.114 g, 51%):  $ee=68\%$  (determined from the corresponding methyl ester)  $[\alpha]_{\text{D}}=-2.3$  ( $c=2.2$ ,  $\text{CHCl}_3$ ), ref. [**35**]; for (*R*)-**2 c**  $ee=92\%$   $[\alpha]_{\text{D}}=-3.0$  ( $c=10$ ,  $\text{CHCl}_3$ );  $^1\text{H NMR}$  ( $\text{CDCl}_3$ , 400 MHz):[**35**]  $\delta=3.85\text{--}3.70$  (2 H, m,  $\text{CH}_2\text{OH}$ ), 2.62 (1 H, m,  $\text{CHCOOH}$ ), 1.70–1.30 (4 H, m,  $\text{CHCH}_2\text{CH}_2$ ), 0.93 ppm (3 H, t,  $J=7.6$  Hz,  $\text{CH}_2\text{CH}_3$ );  $^{13}\text{C NMR}$  ( $\text{CDCl}_3$ , 100.6 MHz):[**35**]  $\delta=180.0$ , 63.2, 47.5, 30.5, 20.6, 14.1 ppm.

### **Methyl (*R*)-2-(hydroxymethyl)pentanoate ((*R*)-5 c)**

Compound (*R*)-2 c (0.090 g, 0.681 mmol) was heated at reflux in MeOH (4 mL) in the presence of a catalytic quantity of H<sub>2</sub>SO<sub>4</sub> to afford, after the usual work-up, the corresponding methyl ester (*R*)-5 c (0.096 g, 97 %): *ee*=68 % (by chiral HPLC of the 3,5-dinitrobenzoate derivative) [ $\alpha$ ]<sub>D</sub>=-2.4 (*c*=1.5, CHCl<sub>3</sub>); <sup>1</sup>H NMR (CDCl<sub>3</sub>, 400 MHz):[19]  $\delta$ =3.80–3.70 (5 H, m+s, CH<sub>2</sub>OH+OCH<sub>3</sub>), 2.60 (1 H, m, CHCOOCH<sub>3</sub>), 1.70–1.45 (2 H, m, CHCH<sub>2</sub>CH<sub>2</sub>), 1.40–1.30 (2 H, m, CHCH<sub>2</sub>CH<sub>2</sub>), 0.95 ppm (3 H, t, *J*=7.4 Hz, CH<sub>2</sub>CH<sub>3</sub>); <sup>13</sup>C NMR (CDCl<sub>3</sub>, 100.6 MHz):  $\delta$ =175.8, 63.2, 51.6, 47.2, 30.6, 20.4, 13.9 ppm; GC/MS (EI): *t*<sub>R</sub>=8.53 min: *m/z* (%)=128 (*M*<sup>+</sup>-18, 1), 116 (20), 104 (28), 87 (100).

The absolute configuration was confirmed by comparing the HPLC analysis of the 3,5-dinitrobenzoate derivative 7 c prepared from (*R*)-5 c with a sample the of 3,5-dinitrobenzoate derivative of (*S*)-5 c prepared by baker's yeast reduction of ethyl 2-formylpentanoate 6 c,[22] followed by transesterification with MeOH and a catalytic quantity of H<sub>2</sub>SO<sub>4</sub>.

Chiral HPLC: Chiralcel OD (*n*-hexane/*i*PrOH 9:1, 0.6 mL min<sup>-1</sup>), *t*<sub>R</sub> (*S*)-7 c=46.9 min, *t*<sub>R</sub> (*R*)-7 c=57.2 min.

### **2 -Methylenepentanoic acid (3 c) and 2-methylpentanoic acid (4 c)**

From 1 c (0.200 g, 1.69 mmol), besides derivative (*R*)-2 c (51 %), a 4:1 (<sup>1</sup>H NMR) mixture of 3 c and 4 c (0.039 g) was isolated. Only the signals[36] of 3 c are herein reported: <sup>1</sup>H NMR (CDCl<sub>3</sub>, 400 MHz):  $\delta$ =6.27 (1 H, br s, CHH=C), 5.63 (1 H, br s, CHH=C), 2.28 (1 H, t, *J*=7.5 Hz, CH<sub>2</sub>C=C), 1.60–1.40 (2 H, m, CH<sub>2</sub>CH<sub>3</sub>), 0.90 ppm (3 H, t, *J*=7.2 Hz, CH<sub>2</sub>CH<sub>3</sub>); GC/MS (EI): 3 c *t*<sub>R</sub>=6.80: *m/z* (%)=114 (*M*<sup>+</sup>, 25), 99 (31), 86 (42), 69 (100); 4 c *t*<sub>R</sub>=6.10: *m/z* (%)=115 (*M*<sup>+</sup>-1, 1), 101 (5), 87 (15), 74 (100).

### **(*S*)-2-(Hydroxymethyl)pent-4-enoic acid ((*S*)-2 d)**

From 1 d (0.200 g, 1.72 mmol), derivative (*S*)-2 d was obtained (0.143 g, 64 %): *ee*=50 % (determined by conversion into (*S*)-7 c) [ $\alpha$ ]<sub>D</sub>=-0.4 (*c*=2.4, CHCl<sub>3</sub>); <sup>1</sup>H NMR (CDCl<sub>3</sub>, 400

MHz):  $\delta$ =5.84–5.72 (1 H, m, CH=C), 5.16–5.00 (2 H, m, CH<sub>2</sub>=C), 3.80 (2 H, d,  $J$ =6.1 Hz, CH<sub>2</sub>OH), 2.70 (1 H, quintuplet,  $J$ =6.2 Hz, CHCOOH), 2.52–2.40 (1 H, m, CHHC=C), 2.38–2.26 ppm (1 H, m, CHHC=C); <sup>13</sup>C NMR (CDCl<sub>3</sub>, 100.6 MHz):  $\delta$ =179.2, 134.6, 117.6, 62.5, 47.1, 32.5 ppm; GC/MS (EI) as methyl ester:  $t_R$ =8.11 min:  $m/z$  (%)=112 ( $M^+$ -32, 12), 97 (68), 67 (100).

### 3 -Methylpent-4-enoic acid (4 d)

Compound **4 d** was detected by GC/MS analysis of the crude residue, obtained after the work-up of the reaction of diol **1 d**: GC/MS (EI): **4 d**  $t_R$ =5.50 min:  $m/z$  (%)=114 (14), 99 (21), 69 (82), 41 (100).

### (S)-2-(Hydroxymethyl)hexanoic acid ((S)-2 e)

From **1 e** (0.200 g, 1.52 mmol), derivative (S)-**2 e** was obtained (0.157 g, 71 %):  $ee$ =81 % (chiral GC analysis as a methyl ester after diazomethane treatment)  $[\alpha]_D$ =-5.1 ( $c$ =0.75, CH<sub>3</sub>OH), ref. [37]; for (R)-**2 e**  $ee$ =99 %  $[\alpha]_D$ =+6.5 ( $c$ =1.0, CH<sub>3</sub>OH); <sup>1</sup>H NMR (CDCl<sub>3</sub>, 400 MHz):[37]  $\delta$ =3.85–3.75 (2 H, m, CH<sub>2</sub>OH), 2.61 (1 H, quint.,  $J$ =5.9 Hz, CHCOOH), 1.75–1.65 (1 H, m, CHCHHCH<sub>2</sub>), 1.60–1.45 (1 H, m, CHCHHCH<sub>2</sub>), 1.40–1.28 (4 H, m, CHCH<sub>2</sub>(CH<sub>2</sub>)<sub>2</sub>), 0.91 ppm (3 H, t,  $J$ =6.4 Hz, CH<sub>2</sub>CH<sub>3</sub>); <sup>13</sup>C NMR (CDCl<sub>3</sub>, 100.6 MHz):  $\delta$ =180.1, 63.2, 47.9, 29.8, 28.4, 22.7, 14.0 ppm; GC/MS (EI) as methyl ester:  $t_R$ =10.81 min:  $m/z$  (%)=142 ( $M^+$ -18, 1), 130 (20), 104 (54), 87 (100).

Chiral GC: DAcTBSil BetaCDX, 60 °C/0.8 °C min<sup>-1</sup>/90 °C/30 °C min<sup>-1</sup>/220 °C (2 min),  $t_R$  (R)-**2 e**=29.9 min,  $t_R$  (S)-**2 e**=30.6 min.

### 4 -Methylhexanoic acid (4 e)

Compound **4 e** was detected as a methyl ester by GC/MS analysis of the crude residue, obtained after the work-up of the reaction of diol **1 e**: GC/MS (EI): **4 e**  $t_R$ =5.97 min:  $m/z$ (%)=129 ( $M^+$ -15, 2), 113, (8), 101 (25), 88 (100).

### **(S)-2-(Hydroxymethyl)heptanoic acid ((S)-2 f)**

From 1 f (0.200 g, 1.37 mmol), derivative (S)-(-)-2 f was obtained (0.186 g, 85 %):  $ee=92\%$  (determined from the corresponding methyl ester)  $[\alpha]_D=-2.1$  ( $c=2.3$ ,  $\text{CHCl}_3$ );  $^1\text{H NMR}$  ( $\text{CDCl}_3$ , 400 MHz):  $[\mathbf{38}] \delta=3.85-3.70$  (2 H, m,  $\text{CH}_2\text{OH}$ ), 2.59 (1 H, quint,  $J=5.9$  Hz,  $\text{CHCOOH}$ ), 1.70-1.57 (1 H, m,  $\text{CHCHHCH}_2$ ), 1.55-1.42 (1 H, m,  $\text{CHCHHCH}_2$ ), 1.40-1.20 (6 H, m,  $\text{CHCH}_2(\text{CH}_2)_3$ ), 0.88 ppm (3 H, t,  $J=6.5$  Hz,  $\text{CH}_2\text{CH}_3$ );  $^{13}\text{C NMR}$  ( $\text{CDCl}_3$ , 100.6 MHz):  $\delta=179.6, 63.2, 47.9, 31.8, 28.4, 26.9, 22.5, 14.0$  ppm.

### **Methyl (S)-2-(hydroxymethyl)heptanoate ((S)-5 f)**

Compound (S)-(-)-2 f (0.120 g, 0.750 mmol) was heated at reflux in MeOH (4 mL) in the presence of a catalytic quantity of  $\text{H}_2\text{SO}_4$  to afford, after the usual work-up, the corresponding methyl ester (-)-5 f (0.125 g, 96 %):  $ee=92\%$  (chiral HPLC of the 3,5-dinitrobenzoate derivative)  $[\alpha]_D=-8.9$  ( $c=1.1$ ,  $\text{CHCl}_3$ );  $^1\text{H NMR}$  ( $\text{CDCl}_3$ , 400 MHz):  $[\mathbf{38}] \delta=3.80-3.65$  (5 H, m+s,  $\text{CH}_2\text{OH}+\text{COOCH}_3$ ), 2.58 (1 H, m,  $\text{CHCOOH}$ ), 1.70-1.57 (1 H, m,  $\text{CHCHHCH}_2$ ), 1.56-1.47 (1 H, m,  $\text{CHCHHCH}_2$ ), 1.40-1.20 (6 H, m,  $\text{CHCH}_2(\text{CH}_2)_3$ ), 0.88 ppm (3 H, t,  $J=6.4$  Hz,  $\text{CH}_2\text{CH}_3$ );  $^{13}\text{C NMR}$  ( $\text{CDCl}_3$ , 100.6 MHz):  $\delta=176.0, 63.3, 51.8, 47.7, 31.8, 28.6, 27.0, 22.5, 14.0$  ppm; GC/MS (EI):  $t_R=13.83$  min:  $m/z$  (%) = 156 ( $M^+-18$ , 1), 144 (25), 104 (83), 87 (100).

Chiral HPLC: Chiralcel OD ( $n$ -hexane/ $i$ PrOH 9:1,  $0.6 \text{ mL min}^{-1}$ ),  $t_R$  ( $R$ )-7 f = 45.1 min,  $t_R$  ( $S$ )-7 f = 57.0 min.

### **(R)-2-Methylheptan-1-ol ((R)-8)**

Compound (-)-5 f (0.130 g, 0.747 mmol) was treated with mesyl chloride (0.102 g, 0.896 mmol) and  $\text{Et}_3\text{N}$  (0.113 g, 0.112 mmol) in  $\text{CH}_2\text{Cl}_2$  (5 mL). After the usual work-up, the mesylated derivative was isolated and submitted without any further purification to  $\text{LiAlH}_4$  (0.042 g, 1.12 mol) reduction in THF (10 mL) heated at reflux to afford, after the usual work-up, compound ( $R$ )-(+)-8 (0.073 g, 75 %):  $ee=88\%$  (chiral GC of the acetyl derivative)  $[\alpha]_D=+11.5$  ( $c=1.4$ ,  $\text{CHCl}_3$ ), ref.  $[\mathbf{39}]$ ; for ( $S$ )-8  $ee=98\%$   $[\alpha]_D=-13.1$  ( $c=1.15$ ,

CHCl<sub>3</sub>); <sup>1</sup>H NMR (CDCl<sub>3</sub>, 400 MHz):[**40**] δ=3.50 (1 H, dd, *J*=10.4, 5.7 Hz, CHHOH), 3.43 (1 H, dd, *J*=10.4, 6.5 Hz, CHHOH), 1.61 (1 H, m, CHCH<sub>3</sub>), 1.40–1.15 (8 H, m, CH(CH<sub>2</sub>)<sub>4</sub>), 0.95–0.85 ppm (6 H, d+t, CHCH<sub>3</sub>+CH<sub>2</sub>CH<sub>3</sub>); <sup>13</sup>C NMR (CDCl<sub>3</sub>, 100.6 MHz): 68.5, 35.9, 33.3, 32.3, 30.5, 26.8, 22.8, 16.7, 14.2 ppm; GC/MS (EI): *t*<sub>R</sub>=9.2 min (as acetyl derivative): *m/z* (%)=112 (*M*<sup>+</sup>-60, 10), 97 (5), 84 (15), 56 (60), 43 (100).

Chiral GC: Chirasil-DEX-CB, 60 °C/0.8 °C min<sup>-1</sup>/90 °C/90 °C min<sup>-1</sup>/180 °C, *t*<sub>R</sub> (*S*)-**8**=16.48 min, *t*<sub>R</sub> (*R*)-**8**=16.6 min (as acetyl derivative).

### **(*R*)-2-Benzyl-3-hydroxypropanoic acid ((*R*)-2 i)**

From **1 i** (0.200 g, 1.20 mmol), derivative (*R*)-**2 i** was obtained (0.104 g, 48 %): *ee*=92 % (determined from the corresponding methyl ester) [*α*]<sub>D</sub>=+14.2 (*c*=2.1, CHCl<sub>3</sub>), ref. [**41**]; for (*R*)-**2 i** *ee*=86.4 % [*α*]<sub>D</sub>=+13.5 (*c*=3.1, CHCl<sub>3</sub>); <sup>1</sup>H NMR (CDCl<sub>3</sub>, 400 MHz):[**41**] δ=7.35–7.15 (5 H, m, Ar*H*), 3.76 (2 H, m, CH<sub>2</sub>OH), 3.12–3.04 (1 H, m, CHCOOCH<sub>3</sub>), 2.94–2.84 ppm (2 H, m, CH<sub>2</sub>Ph); <sup>13</sup>C NMR (CDCl<sub>3</sub>, 100.6 MHz):[**41**] δ=178.9, 138.4, 129.1, 128.8, 126.8, 62.0, 48.8, 34.2 ppm; GC/MS (EI): *t*<sub>R</sub>=19.11 min (as methyl ester): *m/z* (%)=194 (*M*<sup>+</sup>, 2), 176 (50) 117 (75), 91 (100).

### **Methyl (*R*)-2-benzyl-3-hydroxypropanoate ((*R*)-5 i)**

Compound (*R*)-**2 i** (0.090 g, 0.500 mol) was heated at reflux in MeOH (4 mL) in the presence of a catalytic quantity of H<sub>2</sub>SO<sub>4</sub> to afford, after the usual work-up, the corresponding methyl ester (*R*)-**5 i** (0.087 g, 90 %): *ee*=92 % [*α*]<sub>D</sub>=+23.9 (*c*=1.1, CHCl<sub>3</sub>), ref. [**42**]; for (*S*)-**5 i** *ee*=96 % [*α*]<sub>D</sub>=-25.1 (*c*=0.56, CHCl<sub>3</sub>); <sup>1</sup>H NMR (CDCl<sub>3</sub>, 400 MHz):[**42**] δ=7.32–7.16 (5 H, m, Ar*H*), 3.73 (2 H, m, CH<sub>2</sub>OH), 3.69 (3 H, s, OCH<sub>3</sub>), 3.07–2.98 (1 H, m, CHCOOCH<sub>3</sub>), 2.92–2.80 ppm (2 H, m, CH<sub>2</sub>Ph); <sup>13</sup>C NMR (CDCl<sub>3</sub>, 100.6 MHz):[**42**] δ=175.1, 138.7, 129.1, 128.7, 126.7, 62.4, 51.9, 39.6, 34.6 ppm; GC/MS (EI): *t*<sub>R</sub>=19.11 min: *m/z*(%)=194 (*M*<sup>+</sup>, 2), 176 (50) 117 (75), 91 (100).

Chiral GC: DAcTBSil BetaCDX, 70 °C/10 °C min<sup>-1</sup>/110 °C (60 min)/50 °C min<sup>-1</sup>/220 °C (2 min), (*R*)-**5 i** *t*<sub>R</sub>=51.80 min, (*S*)-**5 i** *t*<sub>R</sub>=53.9 min.

**(*R*)-2-Methyl-3-phenylpropionic acid ((*R*)-**4 i**)**

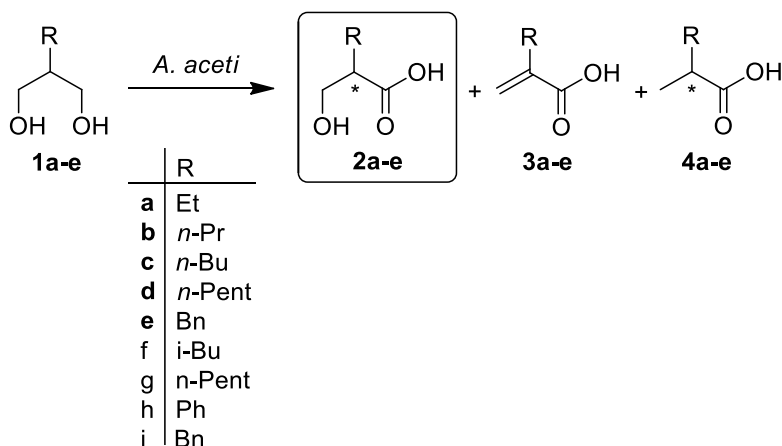
From **1 i** (0.200 g, 1.20 mmol), besides derivative (*R*)-**2 i** (48 %), compound (*R*)-**4 i** (0.020 g, 10 %) was isolated: *ee*=58 % (by chiral GC of the methyl ester) [ $\alpha$ ]<sub>D</sub>=-17.8 (*c*=1.2, CHCl<sub>3</sub>), ref. [**43**]; for (*S*)-**4 i** *ee*=99.2 % [ $\alpha$ ]<sub>D</sub>=+30.2 (*c*=0.82, CHCl<sub>3</sub>); <sup>1</sup>H NMR (CDCl<sub>3</sub>, 400 MHz):[**43**]  $\delta$ =7.35–7.15 (5 H, m, ArH), 3.08 (1 H, dd, *J*=13.4, 6.3 Hz, PhCHH), 2.77 (1 H, m, CHCOOH), 2.67 (1 H, dd, *J*=13.4, 8.0 Hz, PhCHH), 1.18 ppm (3 H, d, *J*=6.9 Hz, CH<sub>3</sub>CH); <sup>13</sup>C NMR (CDCl<sub>3</sub>, 100.6 MHz):[**44**]  $\delta$ =182.4, 139.2, 129.1, 128.6, 126.7, 41.3, 39.5, 16.6 ppm; GC/MS (EI): *t*<sub>R</sub>=16.29 min: *m/z* (%)=164 (*M*<sup>+</sup>, 23), 118 (7), 91 (100).

Chiral GC: Chirasil DEX CB, 65 °C/0.5 °C min<sup>-1</sup>/85 °C/50 °C min<sup>-1</sup>/180 °C (2 min), (*R*)-**4 i** *t*<sub>R</sub>=37.9 min, (*S*)-**4 i** *t*<sub>R</sub>=38.8 min.



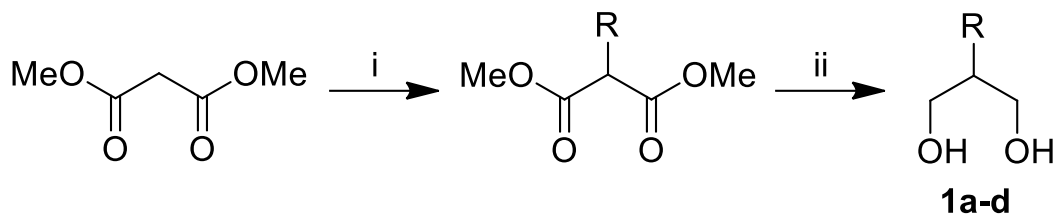
## Results and Discussion

2-Alkyl- and 2-aryl-1,3-diols **1 a-i** reported in Scheme 1 were selected as starting achiral substrates, not only to investigate in a systematic way the effect of the substitution at position 2, but also because of the relevance of the corresponding oxidation products, that is, chiral 1-(hydroxymethyl)alkanoic acids **2**, in the synthesis of chiral APIs. As a matter of fact, most of the known enantioselective syntheses of the resulting hydroxy acids **2** are described in patents filed by pharmaceutical companies, as we will discuss in the following paragraphs.



*Scheme 1. Microbial desymmetrisation of achiral 1,3-diols.*

Compounds **1 a, h** and **i** were commercially available, whereas the remaining diols were prepared by LiAlH<sub>4</sub> treatment of the corresponding 2-substituted malonates, obtained by monoalkylation of dimethyl malonate with the suitable alkyl bromide (Scheme 2).



Scheme 2. Synthesis of 1,3-diol substrates 1a-d. i) NaH, THF, RBr; ii) LiAlH<sub>4</sub>, THF, reflux.

2-(Hydroxymethyl)alkanoic acids **2 a** and **e** have been already obtained by microbial oxidation with acetic acid bacteria of the corresponding diols,[11, 12] thus these biotransformations were chosen as the benchmark for testing the activity of the strains used in this work.

Preliminary investigations were performed with three different acetic acid bacteria, namely *Acetobacter aceti* MIM 2000/28,[7] *Asaia bogorensis* SF2.1[13] and *Gluconobacter oxydans* DSM 2343,[14] known for their oxidative activity on structurally different primary alcohols. Efficient oxidation was achieved only with *A. aceti*, whereas the other two strains showed either scarce or no activity towards substrates **1 a-i**.

Diols **1 a-i** were submitted to *A. aceti* treatment in water at 32 °C with a starting substrate concentration of 1 g L<sup>-1</sup>. The presence of either DMSO or ethanol as a co-solvent (at a concentration as low as 1 % v/v) was found to inhibit the complete conversion of the diol; thus, the oxidative desymmetrisations were carried out by adding the neat diols to the buffer, taking advantage of their partial solubility in aqueous medium. The product distributions and the enantiomeric excess values of the final compounds are reported in Table 1.

Table 1. Data of the biocatalysed desymmetrisation of diols **1** with *A. aceti*.

Substrate	(1)	(2)			(3)	(4)	
	c <sup>a</sup> (%)	c <sup>a</sup> (%)	Yield <sup>[b]</sup> (%)	ee <sup>b</sup> (%)	c <sup>a</sup> (%)	c <sup>a</sup> (%)	ee <sup>b</sup> (%)
<b>1a, R = Me</b>	<1	95	89	94 ( <i>R</i> )	<1	<1	n.d
<b>1b, R = Et</b>	<1	33	25	54 ( <i>R</i> )	20	47	n.d
<b>1c, R = <i>n</i>-Pr</b>	18	62	51	68 ( <i>R</i> )	17	3	n.d.
<b>1d, R = <i>allyl</i></b>	12	85	64	50 ( <i>S</i> )	<1	3	n.d.
<b>1e, R = <i>n</i>-Bu</b>	<1	88	71	80 ( <i>S</i> )	<1	12	n.d.
<b>1f, R = <i>i</i>-Bu</b>	>99	nr <sup>(d)</sup>	-	-	-	-	-
<b>1g, R = <i>n</i>-Pent</b>	<1	98	85	88 ( <i>S</i> )	<1	<1	n.d.
<b>1h, R = <i>Ph</i></b>	>99	nr <sup>(d)</sup>	-	-	-	-	-
<b>1i, R = <i>Bn</i></b>	10	60	48	92 ( <i>R</i> )	5	25	58 ( <i>R</i> )

[a] Conversions calculated by GC analysis of the crude mixture after 72 h reaction time after treatment with CH2N2. [b]

Isolated yield. [c] Enantiomeric excesses calculated by GC or HPLC analysis on a chiral stationary phase after treatment with

CH2N2. [d] n.r.: no reaction product was observed.

Diols **1 f** and **1 h** were recovered unreacted from the reaction medium: the presence either of a branched alkyl chain or of an aromatic ring directly linked to the carbon atom in position 2 seems to sterically hinder the enzymatic activity of *A. aceti*. Nearly quantitative conversions were obtained with diols **1 a** and **1 g**, showing a methyl and a *n*-pentyl substituent in position 2, respectively. The ethyl-substituted diol **1 b** afforded the lowest conversion values.

The effect of substrate loading was investigated for the oxidation of compound **1 g**. After 72 h, conversion was quantitative when the substrate concentration was  $1.0 \text{ g L}^{-1}$ , whereas it decreased to 77 % and 64 % starting from 2.0 and  $3.0 \text{ g L}^{-1}$  of compound **1 g**, respectively.

As for the observed enantioselectivity of the reaction, the (*R*)-enantiomers of compounds **2** were obtained with decreasing *ee* values as the length of the alkyl chain at position 2 increased from methyl to *n*-propyl. An inversion of stereoselectivity was promoted by the reduced flexibility of the three-carbon chain of the 2-allyl derivative **1 d**, affording (*S*)-**2 d** with modest enantiomeric purity. The same (*S*) selectivity was maintained for the *n*-butyl and *n*-pentyl-substituted compounds with higher *ee* values (80 and 88 %, respectively). The presence of a benzyl group was found to promote the oxidation of the primary alcohol affording the (*R*)-enantiomer of **2 i** with *ee*=92 %.

As the reaction is known to occur according to a two-step sequence with an intermediate aldehyde, the enantioselectivity is controlled by the PPQ-ADH acting during the first step. A tentative explanation for the observed inversion of enantioselectivity can be proposed by comparing the steric hindrance of the alkyl substituent R in position 2 and that of the CH<sub>2</sub>OH, which is left unreacted. If R is small (i.e., Me, Et, *n*-Pr), the (*R*)-enantiomer of compound **2** is favoured. When the bulkiness of R increases (i.e., allyl, *n*Bu, *n*-Pent), a switch to (*S*) selectivity is observed. The presence of the aromatic ring in diol **1 i** induces a different orientation of the substrate in the enzyme active site with respect to the other alkyl-substituted diols.

The *ee* values of the desired hydroxymethyl derivatives **2** were found to be rather satisfactory, especially compared with the values reported in the literature, as is hereafter summarized. Compounds (*R*)-**2 a** and (*S*)-**2 e** were obtained with enantiomeric excesses very close to the one previously observed with other strains of *Acetobacter*.[\[11, 12\]](#) Both enantiomers of the ethyl esters of **2 b, e, g** and **2 i** have been previously obtained in enantiomerically enriched form by enzyme-mediated reductions of the corresponding 2-formyl derivatives by the Kaneka corporation,[\[15\]](#) with the following *ee* values being reported: (*R*)-**2 b** 37–89 %, (*R*)-**2 e** 75–97 %, (*R*)-**2 g** 87 % and (*R*)-**2 i** 72–93 %. The Evans

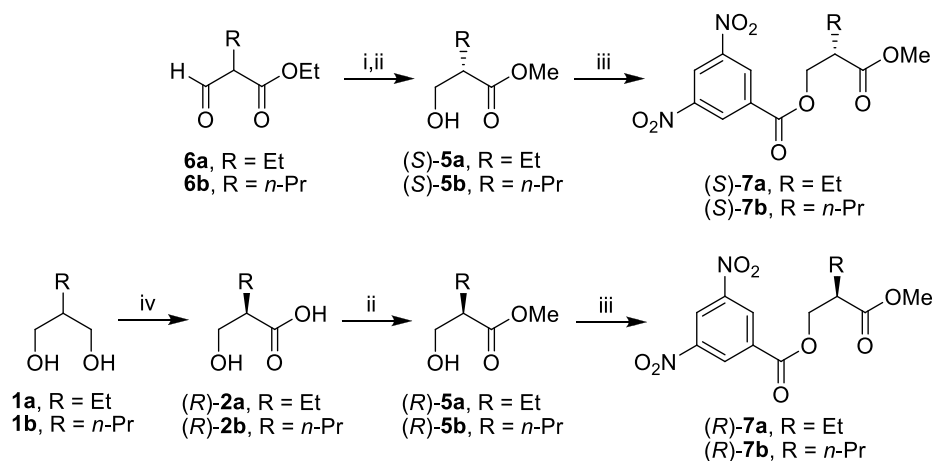
oxazolidinones procedure has been employed by SmithKline Beecham[[16](#)] and Theravance[[17](#)] for the synthesis of derivatives (*R*)-**2 g** and (*R*)-**2 i** to be used in the preparation of antibacterial APIs, although no indication of the enantiomeric purity was provided. The same strategy has been employed by Banyu Pharmaceutical Co. to prepare a suitable derivative of (*R*)-**2 d**[[18](#)] as a single enantiomer for the synthesis of opioid receptor-like 1 antagonists. In 2004, Sibi et al.[[19](#)] reported the radical alkylation of hydroxyacrylates, obtained by Baylis–Hillman reaction, with alkyl iodides in the presence of chiral Lewis acids as catalysts to give hydroxymethyl compounds of type **2**. This procedure afforded both the enantiomers of **2 c** with *ee* values from 40 % to 75 %. The direct enantioselective hydroxymethylation of aldehydes, by using  $\alpha,\alpha$ -diphenylprolinol trimethylsilyl ether as an organocatalyst, has been described to afford  $\alpha$ -substituted- $\beta$ -hydroxyaldehydes, which were further converted to the corresponding hydroxy acids **2** by Pinnick oxidation.[[20](#)] According to this method, (*R*)-**2 c** with 93 % *ee* was obtained. BASF described the opening of racemic oxetan-2-ones by alcohols in the presence of a lipase as a method to obtain enantiopure esters of compounds **2 b**, **c** and **e**,[[21](#)] with the disadvantage that, being a kinetic resolution, it occurred with loss of at least 50 % of the starting material.

The value of the oxidative desymmetrisation herein described is that it represents a biocatalysed enantioselective synthesis, with creation of the stereogenic centre during the reaction under the enzyme control, avoiding the use of external chiral auxiliaries to be introduced and then removed at the end of the procedure.

### **Determination of the absolute configuration of hydroxymethylalkanoic acids**

The absolute configuration of hydroxymethylalkanoic acids **2 a** (the (*R*)-enantiomer of which is commercially available), **b**, **c** and **e**, and of the methyl esters of **2 a** and **b** was known (see the Experimental Section for the corresponding values of optical rotatory power and literature references). In the case of derivatives **2 b** and **c**, showing very low values of optical activity, further confirmation of the (*R*)-configuration was obtained by preparing two samples of the methyl esters of (*S*)-**2 b** and **c**, that is, (*S*)-**5 b** and **c**, respectively, according to a known procedure[[22](#)] based on the reduction of formyl derivatives **6 b** and **c** (Scheme [3](#)) by baker's yeast (BY) in aqueous medium, followed by transesterification in methanol

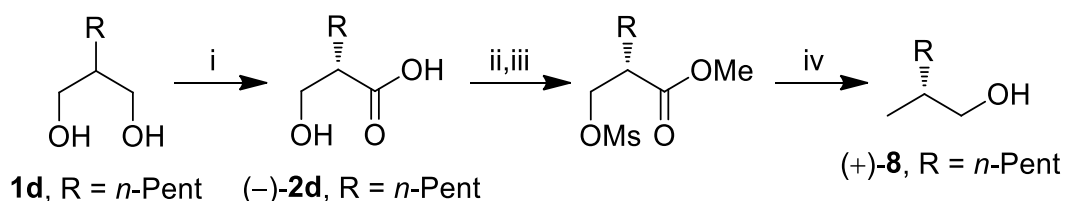
with a catalytic quantity of sulphuric acid. The HPLC analysis on a chiral stationary phase of the 3,5-dinitrobenzoates **7 b** and **c** of compounds **5 b** and **c**, obtained from the products of either *A. aceti* oxidation or BY reduction, were in agreement with the assignment of (*R*)-configuration of those obtained by oxidation of the achiral diols.



*Scheme 3. Assignment of the absolute configuration of (S)-2a-b. i) BY, water, glucose; ii) MeOH, cat. H<sub>2</sub>SO<sub>4</sub>; iii) 3,5-dinitrobenzoyl chloride, Et<sub>3</sub>N, CH<sub>2</sub>Cl<sub>2</sub>; iv) A. aceti, water.*

The absolute configuration of derivative (–)-**2 d** was established by converting it into derivative (*S*)-**7 c** by hydrogenation of the allyl chain (H<sub>2</sub>, Pd/C), esterification (MeOH, cat. H<sub>2</sub>SO<sub>4</sub>) and acylation (3,5-dinitrobenzoylchloride, Et<sub>3</sub>N, CH<sub>2</sub>Cl<sub>2</sub>).

The absolute configuration of derivative (–)-**2 g** was established to be (*S*) by chemical correlation by converting (–)-**2 g** into (+)-(*R*)-**8** according to the reaction sequence reported in Scheme 4.

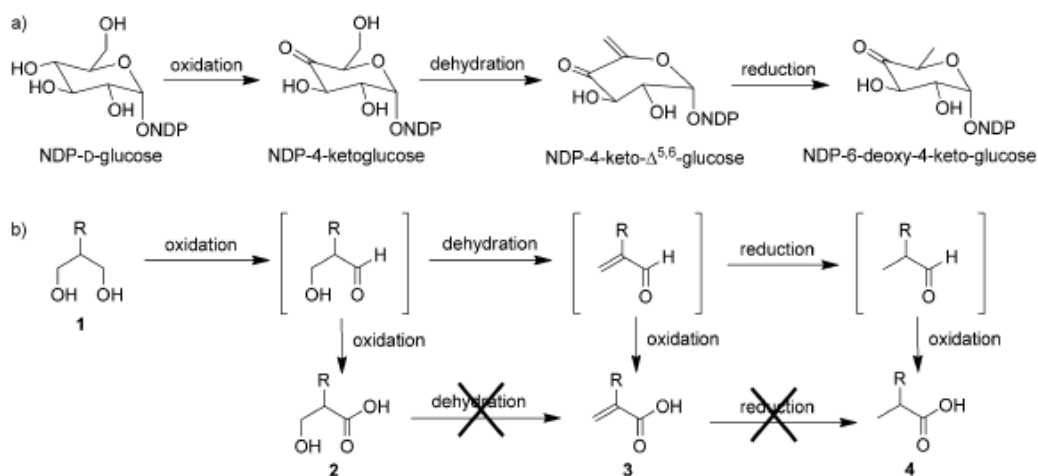


*Scheme 4: Assignment of the absolute configuration of (R)-2d. i) A.aceti, water; ii) MeOH, cat. H<sub>2</sub>SO<sub>4</sub>; iii) MsCl, Et<sub>3</sub>N, CH<sub>2</sub>Cl<sub>2</sub>; iv) LiAlH<sub>4</sub>, THF.*

### Side reactions of the oxidative desymmetrisation

During the oxidation reactions of diols **1 b–e** and **i**, the formation of the dehydrated product **3** and of the corresponding reduced 2-methyl alkanolic acid **4** was observed (Scheme 1 and Table 1), whereas oxidation of **1 a** and **1 g** afforded the corresponding enantiomerically enriched hydroxy acid as the only detectable product. Mixtures of derivatives **3** and **4** were isolated from the reaction medium after the bio-oxidations of diols **1 b** and **1 c**. The two components of each mixture were identified by GC/MS and by <sup>1</sup>H NMR spectroscopy. Compounds **4 d** and **4 e** could be detected only by GC/MS analysis of the corresponding crude residues obtained after the extraction procedure. (*R*)-2-Methyl-3-phenylpropanoic acid (**4 i**) showing an *ee* value of 58 % could be isolated as a pure compound from the reaction mixture when diol **1 i** was the starting substrate.

The formation of these 2-methylalkanoic acids was supposed to involve an enzyme-mediated transformation, which was mainly based on the evidence that compound **4 i** was obtained enriched in the (*R*)-enantiomer form. Carbon–oxygen bond cleavage is a very common reaction in biological systems, and several mechanisms have evolved in nature to promote deoxygenation procedures.[23] Deoxysugars are important examples of compounds obtained by this kind of reaction, through a multi-step sequence that varies according to the position of the OH group to be removed.[24] For example, C-6 deoxygenation of D-hexoses is catalysed by a NAD<sup>+</sup>-dependent nucleotidyldiphosphohexose (NDP-hexose) 4,6-dehydratase (*E*<sub>od</sub>), belonging to the short-chain dehydrogenase/reductase family, and it consists of three sequential steps (Scheme 5 a):[25] i) oxidation of the OH group in position 4 of NDP-D-glucose to give NDP-4-ketoglucose with formation of NADH; ii) elimination of water across C-5 and C-6; iii) final reduction of the 4-keto-Δ<sup>5,6</sup>-glucose intermediate by NADH to afford NDP-6-deoxy-4-keto-glucose.



Scheme 5. Mechanism of the C-6 deoxygenation of *d*-hexoses (a) and an analogous tentative pathway for the explanation of the formation of deoxygenated products 3 and 4 (b).

We hypothesised a similar pathway to explain the formation of deoxygenated compounds **3** and **4** (Scheme 5 b): oxidation of the primary alcohol to the intermediate hydroxymethyl aldehyde, dehydration to  $\alpha$ -methylene aldehyde, reduction of the C=C double bond, and oxidation to acid **4**. The oxidation of the intermediate unsaturated aldehyde can afford derivative **3**.

Because of the highly oxidative character of the culture broth, and the remarkable reactivity of the formyl group towards oxidation, the hypothesised aldehyde intermediates could not be detected during the reactions of diols **1**. To support this dehydration mechanism, feeding experiments (72 h reaction time) were performed by using the unsaturated and saturated aldehydes that are precursors of acids **3 b** and **4 b** (R=Et). When 2-ethylacrolein was added to the *A. aceti* culture in a concentration of  $1.0 \text{ g L}^{-1}$ , a mixture containing 5% saturated acid **4 b** and 95% unsaturated acid **3 b** was recovered. The use of a lower concentration of the aldehyde ( $0.1 \text{ g L}^{-1}$ ) afforded a final reaction mixture containing a higher amount of acid **4 b** (44%) besides **3 b** (56%). When 2-methylbutanal was fed directly into the fermentation medium, either at  $0.1$  or  $1.0 \text{ g L}^{-1}$  concentration, complete oxidation to the



corresponding carboxylic acid **4 b** was observed. The alternative pathway, in which the hydroxy acid **2 b** is dehydrated to **3 b** and then hydrogenated to **4 b**, was excluded on the basis of the fact that no alkene reduction was observed when commercially available acrylic acid **3 b** was added directly to the *A. aceti* culture.

## Conclusions

Acetic acid bacteria are non-pathogenic microorganisms and are readily available owing to their widespread use in the food industry, which makes them ideal candidates for biocatalytic applications. In this case, the *Acetobacter*-mediated desymmetrisation of achiral 1,3-diols has been shown to be an effective procedure for the preparation of enantiomerically enriched hydroxymethyl alkanolic acids. The interest in these derivatives increased considerably in the last few years because they can be converted into  $\alpha$ -substituted- $\beta$ -lactone APIs, [26] currently studied as caseinolytic protease (ClpP) inhibitors, to develop a novel therapeutic strategy to simultaneously sensitize pathogenic bacteria to host defences and pharmaceutical antibiotics. For this purpose, the required hydroxymethyl acid derivative is generally obtained with the use of the Evans chiral oxazolidinones auxiliary. The *Acetobacter*-mediated oxidation occurs under mild operative conditions, in aqueous solution at room temperature, requiring neither the use of complex purpose-made chiral catalysts, nor the assistance of chiral auxiliaries that are to be removed after the creation of the stereocentre. The starting 1,3- diols are readily prepared by a common synthetic sequence, which can be easily extended to the preparation of specific compounds. An interesting change of enantioselectivity from (*S*) to (*R*) was observed when the length of the linear alkyl chain in position 2 of the starting diol increased from three to four carbon atoms. Very few data are reported in the literature on the stereochemical course of the *A. aceti*-mediated oxidation, and most of them refer to the kinetic resolution of racemic secondary alcohols.[27] Thus, this work lays the groundwork for a more detailed investigation of the steric and electronic effects controlling the orientation of the starting diol in the PPQADH active site, and finally influencing the stereochemical outcome of this oxidative desymmetrisation. Further study will be devoted to investigate the hypothesised dehydration pathway and optimise the reaction conditions to inhibit the formation of deoxygenated compounds 3 and 4. Preliminary experiments performed by using immobilized *A. aceti* cells have produced interesting results in terms of increased conversion and reduction of side products.

# Acknowledgements

This work was supported by Fondazione Cariplo, grant no. 2014- 0568.

# References

- [1] M. C. Willis, *J. Chem. Soc. Perkin Trans. 1* 1999, 1765 – 1784.
- [2] H. Fernandez-Perez, P. Etayo, J. R. Lao, J. L. Nfílchez-Rico, A. Vidal-Ferran, *Chem. Commun.* 2013, 49, 10666 – 10675.
- [3] E. García-Urdiales, I. Alfonso, V. Gotor, *Chem. Rev.* 2011, 111, PR110– PR180.
- [4] R. N. Patel, *ACS Catal.* 2011, 1, 1056 – 1074.
- [5] a) D. Romano, R. Villa, F. Molinari, *ChemCatChem* 2012, 4, 739 – 749; b) F. Hollmann, I. W. C. E. Arends, K. Buehler, A. Schallmeyer, B. Behler, *Green Chem.* 2011, 13, 226– 265; N. J. Turner, *Chem. Rev.* 2011, 111, 4073 – 4087.
- [6] O. Adachi, T. Yakushi, *Membrane-bound dehydrogenases of acetic acid bacteria*, in *Acetic Acid Bacteria* (Eds.: K. Matsushita, H. Toyama, N. Tonouchi, A. Okamoto-Kainuma), Springer, Tokyo, 2016.
- [7] a) D. Romano, M. L. Contente, T. Granato, W. Remelli, P. Zambelli, F. Molinari, *Monatsh. Chem.* 2013, 144, 735– 737; b) A. Romano, R. Gandolfi, P. Nitti, M. Rollini, F. Molinari, *J. Mol. Catal. B* 2002, 17, 235 – 240.
- [8] a) A. Sharma, Y. Kawarabayasi, T. Satyanarayana, *Extremophiles* 2012, 16, 1 –19; b) F. Molinari, R. Villa, F. Aragozzini, P. Cabella, M. Barbeni, *J. Chem. Technol. Biotechnol.* 1997, 70, 294 – 298.
- [9] H. Ohta, H. Tetsukawa, N. Noto, *J. Org. Chem.* 1982, 47, 2400 – 2404.
- [10] S. Kara, D. Spickermann, J. H. Schrittwieser, A. Weckbecker, C. Leggewie, I. W. C. E. Arends, F. Hollmann, *ACS Catal.* 2013, 3, 2436 – 2439.
- [11] F. Molinari, R. Gandolfi, R. Villa, E. Urban, A. Kiener, *Tetrahedron: Asymmetry* 2003, 14, 2041– 2043.
- [12] K. Mitsukura, T. Uno, T. Yoshida, T. Nagasawa, *Appl. Microbiol. Biotechnol.* 2007, 76, 61 –65.

- [13] P. Zambelli, A. Pinto, D. Romano, E. Crotti, P. Conti, L. Tamborini, R. Villa, F. Molinari, *Green Chem.* 2012, 14, 2158–2161.
- [14] R. Villa, A. Romano, R. Gandolfi, J. V. S. Gago, F. Molinari, *Tetrahedron Lett.* 2002, 43, 6059 – 6061.
- [15] N. Taoka, D. Maryama, K. Mori, T. Oishi, (Kaneka Corporation), EP1568679 A1, 2005.
- [16] K. M. Aubart, A. B. Benowitz, S. B. Christensen, J. Lee, D. J. Silva, (SmithKline Beecham), US2008/167302 A1, 2008. 2008
- [17] S.-K. Choi, P. R. Fatheree, R. Gendron, R. Hudson, R. M. McKinnell, V. Sasikumar, (Theravance), WO2009/35543, 2009.
- [18] T. Yoshizumi, A. Ohno, T. Tsujita, H. Takahashi, O. Okamoto, I. Hayakawa, H. Kigoshi, *Synthesis* 2009, 1153–1162.
- [19] M. P. Sibi, K. Patil, *Org. Lett.* 2005, 7, 1453 – 1456.
- [20] R. K. Boeckman, K. F. Biegasiewicz, D. J. Tusch, J. R. Miller, *J. Org. Chem.* 2015, 80, 4030 – 4045.
- [21] T. Habicher, R. Stürmer, (BASF), WO2006/015727, 2006.
- [22] Y. Kawai, M. Tsujimoto, S. Kondo, K. Takanobe, K. Nakamura, A. Ohno, *Bull. Chem. Soc. Jpn.* 1994, 67, 524–528.
- [23] D. A. Johnson, H.-W. Liu, A mechanistic analysis of C@O bond cleavage events with a comparison to 3, 6-dideoxysugar formation, in *The Biology – Chemistry Interface: A Tribute to Koji Nakanishi* (Eds.: R. Cooper, J. D. Snyder), Marcel Dekker, New York, 1999, pp. 351 – 396.
- [24] a) D. A. Johnson, H.-W. Liu, Deoxysugars: occurrences, genetics, and mechanisms of biosynthesis, in *Comprehensive Natural Products Chemistry*, Vol. 3 (Eds.: D. Barton, K. Nakanishi, O. Meth-Cohn), Elsevier, Amsterdam, 1999, pp. 311 – 365; b) T. M. Hallis, H.-W. Liu, *Acc. Chem. Res.* 1999, 32, 579–588; X. M. M. He, H.-W. Liu, *Annu. Rev. Biochem.* 2002, 71, 701 – 754.

- [25] X. M. He, H.-W. Liu, *Curr. Opin. Chem. Biol.* 2002, 6, 590– 597.
- [26] M. Gersch, F. Gut, V. S. Korotkov, J. Lehmann, T. Böttcher, M. Rusch, C. Hedberg, H. Waldmann, G. Klebe, S. A. Sieber, *Angew. Chem. Int. Ed.* 2013, 52, 3009 – 3014; *Angew. Chem.* 2013, 125, 3083 – 3088.
- [27] T. Yakushi, K. Matsushita, *Appl. Microbiol. Biotechnol.* 2010, 86, 1257 – 1265.
- [28] S. Wang, Z. Wang, L. Yang, J. Dong, C. Chi, D. Sui, Y. Wang, J. Ren, M. Hung, Y. Jiang, *J. Mol. Catal. A* 2007, 264, 60 –65.
- [29] B. Zupančič, B. Mohar, M. Stephan, *Org. Lett.* 2010, 12, 3022 – 3025.
- [30] G. Guazzelli, S. De Grazia, K. D. Collins, H. Matsubara, M. Spain, D. J. Procter, *J. Am. Chem. Soc.* 2009, 131, 7214– 7215.
- [31] C. H. Senanayake, R. D. Larsen, T. J. Bill, J. Liu, E. G. Corley, P. J. Reider, *Synlett* 1994, 199– 200.
- [32] H. J. Jessen, A. Schumacher, F. Schmid, A. Pfaltz, K. Gademann, *Org. Lett.* 2011, 13, 4368 – 4370.
- [33] Y. Lai, L. Sun, M. K. Sit, Y. Wang, W.-M. Dai, *Tetrahedron* 2016, 72, 664 – 673.
- [34] V. A. Rassadin, Y. Six, *Tetrahedron* 2014, 70, 787– 794.
- [35] R. K. Boeckman, J. R. Miller, *Org. Lett.* 2009, 11, 4544– 4547.
- [36] F. Outurquin, C. Paulmier, *Synthesis* 1989, 690 – 691.
- [37] B. Hu, M. Prashad, D. Har, K. Prasad, O. Repic, T. J. Blacklock, *Org. Process Res. Dev.* 2007, 11, 90 –93.
- [38] J. Lee, (SmithKline Beecham), WO2007/067904 A2, 2007.
- [39] W. Oppolzer, R. Moretti, S. Thomi, *Tetrahedron Lett.* 1989, 30, 5603 – 5606.
- [40] V. Garcia-Ruiz, S. Woodward, *Tetrahedron: Asymmetry* 2002, 13, 2177 – 2180.
- [41] D.-Y. Ma, D.-X. Wang, J. Pan, Z.-T. Huang, M.-X. Wang, *Tetrahedron: Asymmetry* 2008, 19, 322 – 329.

- [42] M. Kim, S. Choi, Y. Lee, J. Lee, K. Nahm, B. Jeong, H. Park, S. Jew, *Chem. Commun.* 2009, 782 – 784.
- [43] S. Li, S.-F. Zhu, C.-M. Zhang, S. Song, Q.-L. Zhou, *J. Am. Chem. Soc.* 2008, 130, 8584– 8585.
- [44] M. J. Aurell, L. R. Domingo, R. Mestres, E. MuÇoz, R. J. Zaragoz#, *Tetrahedron* 1999, 55, 815 – 830.





# Chemoenzymatic synthesis in flow reactors: a rapid and convenient preparation of Captopril

Valerio De Vitis,<sup>[a]</sup> Federica Dall'Oglio,<sup>[b]</sup> Andrea Pinto,<sup>[b]</sup> Carlo De Micheli,<sup>[b]</sup> Francesco Molinari,<sup>[a]</sup> Paola Conti,<sup>[b]</sup> Diego Romano,<sup>\*,[a]</sup> and Lucia Tamborini<sup>\*,[b]</sup>

## Affiliations:

<sup>[a]</sup> Dr. V. De Vitis, Prof. F. Molinari, Dr. D. Romano Department of Food Environmental and Nutritional Science University of Milan Via Mangiagalli, 20133 Milan (Italy) E-mail: [diego.romano@unimi.it](mailto:diego.romano@unimi.it)

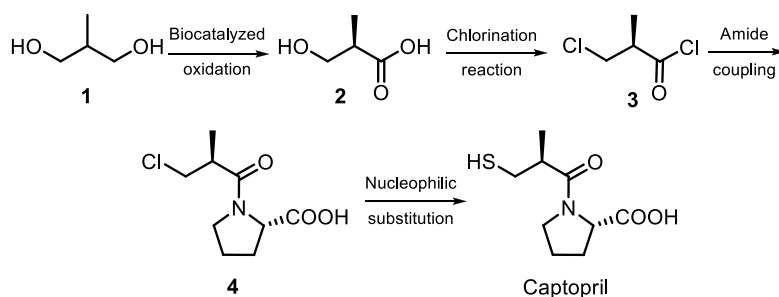
<sup>[b]</sup> Dr. F. Dall'Oglio, Dr. A. Pinto, Prof. C. De Micheli, Prof. P. Conti, Dr. L. Tamborini Department of Pharmaceutical Sciences University of Milan Via Mangiagalli 25, 20133 Milan (Italy)

# Abstract

The chemoenzymatic flow synthesis of enantiomerically pure captopril, a widely used antihypertensive drug, is accomplished starting from simple, inexpensive, and readily available reagents. The first step is a heterogeneous biocatalyzed regio- and stereoselective oxidation of cheap prochiral 2-methyl-1,3-propanediol, performed in flow using immobilized whole cells of *Acetobacter aceti* MIM 2000/28, thus avoiding the use of aggressive and environmentally harmful chemical oxidants. The isolation of the highly hydrophilic intermediate (R)-3-hydroxy-2-methylpropanoic acid is achieved in-line by using a catch-and-release strategy. Then, three sequential high-throughput chemical steps lead to the isolation of captopril in only 75 min. In-line quenching and liquid-liquid separation enable breaks in the workflow and other manipulations to be avoided.

# Introduction

The design and development of reproducible, environmentally benign and economical synthetic routes to drugs is of para-mount importance in the pharmaceutical industry, and, in this context, continuous-flow synthesis is receiving increasing attention.<sup>[1–3]</sup>As a result, in recent years, many new flow-based routes have been designed towards commercially available active pharmaceutical ingredients<sup>[4,5]</sup>. We herein report an efficient chemoenzymatic flow synthesis of captopril [(S)-1-[(S)-3-mercapto-2-methylpropanoyl]pyrrolidine-2-carboxylic acid, **5**, Scheme 1]. Captopril is an angiotensin-converting enzyme (ACE) inhibitor and was discovered and developed at E. R. Squibb & Sons Pharmaceuticals in the 1970s, and is still a widely prescribed drug for the treatment of hyper-tension.



*Scheme 1. Four steps chemoenzymatic synthesis of enantiomerically pure captopril*

Our flow-based synthetic route to obtain captopril includes a first biocatalyzed heterogeneous regio- and stereoselective oxidation reaction starting from a cheap prochiral diol (2-methyl-1,3-propanediol, **1**)<sup>[6,7]</sup> followed, after isolation of carboxylic acid **2**, by three sequential chemical steps. The biocatalyzed flow oxidation offers an efficient alternative for environmentally benign oxidations in answer to the critical economic and environmental issues that urgently demand greener, more atom-efficient and scalable oxidation methods.<sup>[8,9]</sup> The oxidation was performed using *Acetobacter aceti* MIM 2000/28;<sup>[10–12]</sup> this strain is able to completely convert the substrate into (R)-3-hydroxy-2-methylpropanoic acid (**2**) with an excellent *ee* (96–97%) using a conventional batch-mode biotransformation. To exploit all the advantages of performing (bio)catalyzed reactions in flow, in particular the high local concentration of the biocatalyst,<sup>[13–16]</sup> *A. aceti* has been immobilized as dried alginate-

entrapped cells, that are economical, easy to prepare and can be efficiently used in a packed bed column.<sup>[17]</sup> Also, importantly, the use of whole cells in biocatalytic oxidation has the great advantage of not requiring an additional cofactor regeneration system. The following three chemical steps that yield captopril under continuous flow conditions are depicted in Scheme 1. To achieve this continuous-flow synthesis, the reactions have been designed so that the excess of reagents and reaction by-products from each reaction were compatible with the down-stream reactions, in order to perform steps in sequence without breaks in the workflow and manipulation. The risks associated with exothermic reactions and quenches (i.e., the use and neutralization of thionyl chloride) were mitigated owing to two of the advantages of continuous flow over batch synthesis: 1) only a small amount of material relative to the overall output of the system is utilized at any given time, and 2) the large surface-area-to-volume ratios that allow precise reaction control through rapid heat transfer and mixing. Moreover, in-line liquid–liquid extractions safely neutralized and removed problematic reagents and by-products.

# Experimental Section

All reagents and solvents were purchased from Sigma–Aldrich. The continuous flow reactions were performed using a commercial R2C/R4 flow reactor (Vapourtec, Bury St. Edmunds, Suffolk, UK) equipped with Omnifit glass columns (15 mm i.d. x 100 mm length) and PFA reactor coils (2 and 10 mL, respectively). The R2C unit is the pumping unit that contains two adapted Knauer pumps, which are able to pump highly concentrated and corrosive acids. R4 is the heating unit with four heating positions. The additional HPLC pumps necessary to perform the overall synthesis were provided by another R2 + /R4 flow reactor (Vapourtec) and by two external pumps (ThalesNano). The temperature sensor sits on the wall of the PFA tubing. The pressure was controlled by using two 100 psi BPRs. In-line liquid–liquid extractions were performed using a Zaiput separator. <sup>1</sup>H NMR and <sup>13</sup>C NMR spectra were recorded with a Varian Mercury 300 (300 MHz) spectrometer. Chemical shifts ( $\delta$ ) are expressed in ppm, and coupling constants (J) are expressed in Hz. The molar conversion of the biotransformation was determined by HPLC analysis using a Luna NH<sub>2</sub> 100 Å column (250 mm x 4.6 mm, particle size 5  $\mu$ m, Phenomenex, Aschaffenburg, Germany) and a Biorad refractor index detector with an acidic aqueous KH<sub>2</sub>PO<sub>4</sub> buffer (20 mm, pH 2.7) as the mobile phase (flow rate 0.2 mL min<sup>-1</sup>). The samples (40 mL) were injected as soon as collected and without further treatment. The enantiomeric composition of **2** was determined by gas chromatographic analysis of the corresponding methyl ester [methyl (*R*)-3-hydroxy-2-methylpropionate: *tr* = 3.6 min], obtained after treatment with diazomethane, using a chiral capillary column (diameter 0.25 mm, length 25 m, DMCPeBeta-CDX-PS086, MEGA, Legnano, Italy). Optical rotation determinations were performed using a Jasco P-1010 spectropolarimeter coupled with a Haake N3-B thermostat. MS analyses were performed on a Varian 320-MS triple quadrupole mass spectrometer with an electrospray ionization (ESI) source. Microanalyses (C, H, N) were within  $\pm$  0.4% of theoretical values.

## Strain Preparation

The *A. aceti* MIM 2000/28 strain was routinely maintained on GYC agar plates [glucose (50 g L<sup>-1</sup>), yeast extract (10 g L<sup>-1</sup>), CaCO<sub>3</sub> (30 g L<sup>-1</sup>), agar (15 g L<sup>-1</sup>), pH 6.3] at 28 °C. Strain was inoculated into 100 mL Erlenmeyer baffled flask containing GLY medium [yeast extract (10

g $L^{-1}$ ) and glycerol (25 g $L^{-1}$ ), pH 5; 20 mL]. After growth for 24 h (shaking at 150 rpm, 28 °C), the liquid culture was entirely used to inoculate a 1 L Erlenmeyer baffled flask containing GLY medium (150 mL). Flasks were grown for 24 h at 28 °C, with shaking at 150 rpm. Preparation of Dry Alginate Beads Gel beads were prepared by ionotropic gelation, by following a protocol previously developed by us:<sup>[17]</sup>a 4% (w/v) sodium alginate solution was prepared in distilled water and stirred until a homogeneous clear solution was formed. The solution was allowed to settle for 2 h in order to eliminate the air bubbles. The alginate solution was then gently mixed in a 1:1 (w/w) ratio with a suspension of *A. aceti* cells (40 ODm $L^{-1}$ ) in sodium acetate buffer (20 mM, pH 6). The resulting mixture was then pumped drop wise into a slightly agitated CaCl $_2$  solution (0.2 M). Calcium alginate beads were agitated for 20 min, then filtered, washed with deionized water and dried at 25 °C for 16 h.

### Synthesis of (R)-3-Hydroxy-2-methylpropanoic Acid (2)

Dry alginate beads (400 mg) were packed into a glass column (i.d. 15 mm) and swelled until their volume tripled by flowing acetate buffer (20 mM, pH 6) through the column (flow rate: 400 mL $min^{-1}$ , 60 min). The final volume of the bed was 5.1 mL. Air was delivered at 17 psi; its flow was measured using the method described in Ref. [20]. To ensure a constant flow, a BRP (40 psi) was applied before the air tank. An aqueous solution of **1** (1 g $L^{-1}$ , 40 mL) was pumped at 60 mL $min^{-1}$ , joining the airflow at the T-junction, before entering the column in which the oxidation occurs in approximately 10 min. The exiting flow stream was directed into a decompression column. A BPR (5 psi) ensured a constant and controlled flow of aqueous phase leaving the column. The aqueous stream was directed into a column filled with Ambersep 900 OH resin (2 g) and, after washing the column with water (20 mL, 0.5 mL $min^{-1}$ ), the trapped acid was released by flowing HCl (1 N, 5 mL). After lyophilization, compound **2** was isolated as pale yellow oil (42 mg). To obtain a larger amount of **2**, 1.6 g of alginate beads were used, with a reactor volume of 20 mL. At this scale, 170 mg of compound **2** was isolated (91% yield).  $[\alpha]_D^{25} = -11.55$  (c=1.00 in EtOH);  $^1H$  NMR (300 MHz, CDCl $_3$ ):  $\delta$  = 1.22 (d, J=7.4 Hz, 3 H), 2.10 (s, 1 H), 2.68–2.80 (m, 1 H), 3.75 (d, J=6.0 Hz, 2 H), 5.70 ppm (br s, 1 H);  $^{13}C$  NMR (75 MHz, CDCl $_3$ ):  $\delta$  = 13.2, 41.6, 64.0, 180.1 ppm; MS (ESI): m/z: 102.9 [M–H] $^-$ ; [21] HPLC analysis: **1**,  $t_r$ =22 min; **2**,  $t_r$ =18 min.

### Synthesis of (R)-3-Chloro-2-methyl propanoyl Chloride (3)

A solution of **2** (52 mg, 0.5 mmol) was prepared in anhydrous toluene (410 mL). Imidazole (3.5 mg, 0.1 equiv) and DMF (50  $\mu$ L) were added to the solution. A second solution of thionyl chloride (125 mL, 3.5 equiv) was prepared in anhydrous toluene (375 mL). The two solutions were mixed into a T-piece and flowed through a 10 mL reactor coil according to the conditions reported in Table 1. A 200 psi backpressure regulator was applied to the system. The exiting solution was collected, the solvent was evaporated under reduced pressure to yield **3** as a crude oil, which was analyzed by  $^1\text{H}$  NMR spectroscopy.  $^1\text{H}$  NMR (300 MHz,  $\text{CDCl}_3$ ):  $\delta$  = 1.42 (d, 3 H), 3.20–3.31 (m, 1H), 3.66–3.80 ppm (m, 2 H).

### Synthesis of (S)-1-[(S)-3-Chloro-2-methylpropanoyl]pyrroli-dine-2-carboxylic Acid (4)

A solution of compound **3** (70 mg, 0.5 mmol) in toluene (0.5 mL) was prepared. A second solution of l-proline (115 mg, 2 equiv) and NaOH (60 mg, 3 equiv) was prepared in water (0.5 mL). The two solutions were flowed at a total rate of 2 mL  $\text{min}^{-1}$  through a 2 mL reactor coil, that had been washed with a mixture of toluene and water, at room temperature. The aqueous phase was acidified to pH 2 by introducing a flow of HCl (6 N, 1 mL  $\text{min}^{-1}$ ) and the resulting biphasic system was mixed using a T-junction into an EtOAc stream (1 mL  $\text{min}^{-1}$ ) to perform in-line extraction. The two phases were separated in-line using a Zaiput liquid-liquid separator. A 200 psi backpressure was applied to the system. The organic solvent was dried over anhydrous  $\text{Na}_2\text{SO}_4$  and evaporated under reduced pressure to yield **4** as a crude solid, which was analyzed by  $^1\text{H}$  NMR spectroscopy.  $[\alpha] = -103.6$  ( $c=1$  in EtOH);  $^1\text{H}$  NMR (300 MHz,  $\text{CDCl}_3$ ):  $\delta$  = 1.24 (d, 3 H,  $J=7.0$ ), 2.02–2.18 (m, 4 H), 2.96–3.08 (m, 1 H), 3.44–3.51 (m, 1 H), 3.57–3.72 (m, 2 H), 3.81 (t, 1 H,  $J=10.4$ ), 4.62–4.69 (m, 1 H), 11.30 (br s, 1 H);  $^{13}\text{C}$  NMR (75 MHz,  $\text{CDCl}_3$ ):  $\delta$  = 15.8, 24.9, 27.7, 41.3, 45.8, 47.7, 59.6, 173, 175 ppm; MS (ESI):  $m/z$ : 217.9  $[\text{M}-\text{H}]^-$ ; elemental analysis calcd (%) for  $\text{C}_9\text{H}_{14}\text{ClNO}_3$ : C 49.21, H 6.42, N 6.38; found: C 49.00, H 6.31, N 6.50.

### Synthesis of (S)-1-[(S)-3-Chloro-2-methylpropanoyl]pyrroli-dine-2-carboxylic Acid (Captopril, 5)

A solution of compound **4** (22 mg, 0.1 mmol) in toluene (0.1 mL) was prepared. A second solution of NaSH (21 mg, 3 equiv) was prepared using degassed water (0.1 mL). The two solutions were flowed through a 10 mL reactor coil. A 200 psi backpressure was applied to

the system. Reaction time and temperature were optimized, as reported in Table 2. The aqueous phase was acidified at pH 2 by introducing a flow of HCl (2 N) and the resulting biphasic system was mixed using a T-junction into an EtOAc stream to perform inline extraction. The two phases were separated inline using a Zaiput liquid–liquid separator. The organic solvent was dried over anhydrous Na<sub>2</sub>SO<sub>4</sub> and evaporated under reduced pressure to yield **5** as a pale yellow crude solid, which was analyzed by <sup>1</sup>H NMR spectroscopy. [ $\alpha$ ] = -128.5 (c=1 in EtOH); lit=-129.4 (c=1.35 in EtOH at 22 °C);[18] <sup>1</sup>H NMR (300 MHz, CDCl<sub>3</sub>):  $\delta$ =1.24 (d, J=7.0 Hz, 3 H), 1.58 (t, J=9.2 Hz, 1 H), 2.02–2.18 (m, 4 H), 2.43–2.51 (m, 1 H), 2.79–2.90 (m, 2 H), 3.55–3.71 (m, 2 H), 4.62–4.69 (m, 1 H), 11.30 ppm (br s, 1 H); <sup>13</sup>C NMR (75 MHz, CDCl<sub>3</sub>):  $\delta$ =17.0, 20.8, 24.7, 27.4, 42.5, 47.4, 59.2, 173.0, 175.0 ppm; MS (ESI): m/z: 215.9 [M-H]<sup>-</sup>; elemental analysis calcd (%) for C<sub>9</sub>H<sub>15</sub>NO<sub>3</sub>S: C 49.75, H 6.96, N 6.45; found: C 49.60, H 6.89, N 6.52.

### Three-Step Continuous-Flow Synthesis of Captopril (**5**)

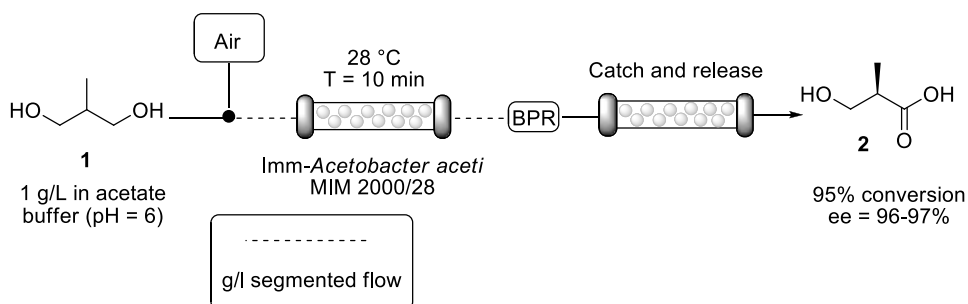
A solution of **2** (156 mg, 1.5 mmol) in anhydrous toluene (1.23 mL) was prepared. Imidazole (10.5 mg, 0.1 equiv) and DMF (150  $\mu$ L) were added to the solution. A second solution of thionyl chloride (375  $\mu$ L, 3.5 equiv) was prepared using anhydrous toluene (1.12 mL). The two solutions were flowed through a 10 mL coil reactor that was maintained at 110 °C, with a residence time of 30 min (total flow rate 0.33 mLmin<sup>-1</sup>). Then, the exiting flow was merged at a T-junction with an aqueous solution (1.5 mL) of l-proline (2 equiv) and NaOH (7 equiv). This then entered a 2 mL reactor coil, maintained at room temperature with a residence time of 3 min (total flow rate 0.66 mLmin<sup>-1</sup>). The aqueous phase was acidified to pH 2 by adding a flow stream of HCl (6 N, 0.33 mLmin<sup>-1</sup>) and the resulting biphasic system was mixed using a T-junction into an EtOAc stream (0.33 mL min<sup>-1</sup>) to perform an in-line extraction. The two phases were separated in-line using a Zaiput liquid–liquid separator. The organic phase was collected in a vial acting as a substrate reservoir for the final nucleophilic substitution reaction. The organic phase was pumped and mixed with a solution of NaSH (c = 1.5 M, 3 equiv) in degassed water, and entered a 10 mL coil reactor maintained at 125 °C for 30 min (total flow rate 0.66 mL min<sup>-1</sup>). A 200 psi backpressure was added to the whole system. The exiting flow was then acidified to pH 1 with HCl (2 N) and a continuous extraction with the Zaiput liquid–liquid separator was performed. The organic solvent was dried over anhydrous Na<sub>2</sub>SO<sub>4</sub> and evaporated under reduced pressure to yield a crude material that was purified



by column chromatography (dichloro-methane/methanol 98:2) to yield captopril, which was crystallized from ethyl acetate/hexane (1:1, total volume 1 mL; 160 mg, 50 %).

## Results and Discussion

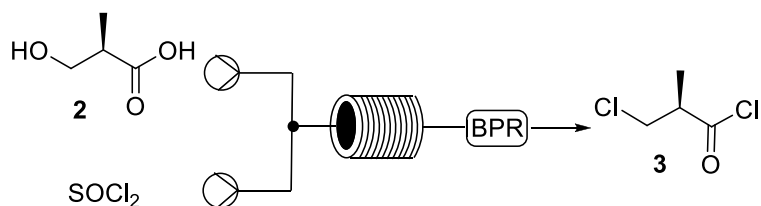
First, commercially available diol **1** (1 gL<sup>-1</sup> in 20 mm acetate buffer, pH 6) was successfully oxidized with dried alginate beads of *Acetobacter aceti* MIM 2000/28 with high enantio and regioselectivity. The immobilized cells were prepared according to a protocol recently reported by us,<sup>[17]</sup> packed into a glass column (inner diameter 15 mm) and swelled by flowing buffer through the column until their volume tripled. No release of catalyst in the exiting flow stream was observed. The oxygen supply, essential for cofactor recycling, was ensured by means of a segmented air–liquid flow stream (for details, see the Experimental Section) formed before contact with the immobilized biocatalyst (Scheme 2).



*Scheme 2. Biocatalyzed heterogeneous oxidation of prochiral 2-methyl-1,3-propanediol, (1) and in line purification of the product through a catch and release protocol.*

The reaction reached 95% conversion in only 10 min with an excellent *ee* (96–97%), as determined by chiral gas chromatography. The stability of the biocatalyst under continuous work was assessed by performing the biotransformation under the conditions reported in the Experimental Section. Using 400 mg of immobilized biocatalyst, a total volume of approximately 50 mL was collected. Samples collected at different times were analyzed by HPLC and the results obtained in terms of conversion were comparable over time, indicating good stability under continuous work conditions. The maximum conversion (95%) was observed for the first 35 mL of collected solution. Then, the conversion slowly decreased to 80% in the following fractions. Therefore, the use of dried alginate beads in flow offers good stability over the time, giving 95% conversion for approximately 10h of continuous work.

However, the buffer flow stream, even if characterized by low ionic strength (20 mM), might interfere with the alginate bead structure, which could slowly release the biocatalyst and consequently decrease the conversion. Attempts to perform in-line acidification and extraction with an organic solvent (e.g., EtOAc) using a liquid–liquid separator were not successful due to the high hydrophilicity of the obtained carboxylic acid **2**. Consequently, we exploited a catch- and-release strategy using a column packed with Ambersep 900 OH resin that trapped the acid, leaving unreacted starting material in the exiting flow stream. Compound **2** was then released from the resin by using 1 N HCl and lyophilized. Then, starting from the isolated compound **2**, we studied the chlorination reaction with thionyl chloride with heating in a pressurized system to effect both the formation of the acid chloride and the direct chlorination of the primary alcohol (Scheme 3). A 200 psi backpressure regulator (BPR) was used to prevent outgassing. The possibility of conducting such an exothermic reaction under heating conditions demonstrates one of the operational advantages and capabilities of continuous flow synthesis over analogous batch processes that require cooling during the addition of thionyl chloride.



*Scheme 3. The chlorination reaction using a 10 mL reactor coil. BPR: 200 psi. Solvent, temperature and residence time were optimized as summarized in Table 1.*

The reaction was tested in anhydrous toluene, THF, and CH<sub>2</sub>Cl<sub>2</sub>; the reaction proceeded similarly with all the selected solvents. Therefore, toluene was selected and a 1 mM solution of compound **2** was used. An excess of thionyl chloride (3 equiv, 3 mM solution in toluene) was necessary to drive the reaction to completion. A catalytic amount of imidazole and 10% DMF (v/v) were added to the solution of **2**. The use of DMF has a double effect: first, it

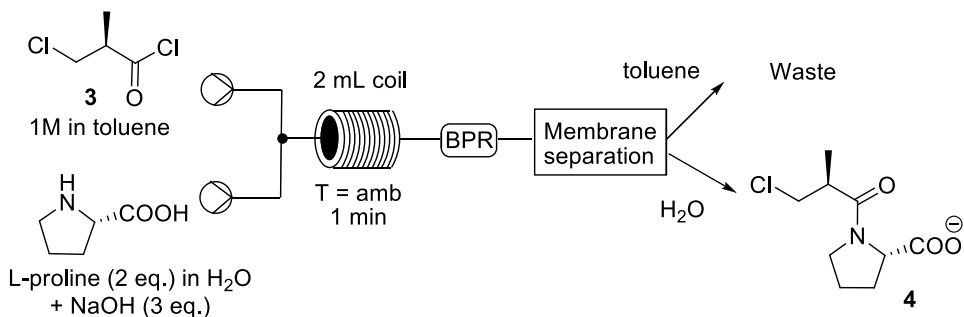
favored the reaction due to the formation of the Vilsmeier reagent and, second, it increased the solubility of the starting material in toluene. Different reaction conditions were then tested and they are summarized in Table 1. The outcome was monitored by  $^1\text{H}$  NMR spectroscopy after evaporation of the solvent. If no complete conversion was observed, the starting material **2** and/or the acid chloride (without substitution of the hydroxy group) were identified as the only impurities. We also tried the reaction using only DMF to prepare the solution of **2** (Table 1, entries 6 and 7) and observed complete conversion at  $100\text{ }^\circ\text{C}$  in 30 min.

*Table 1. Conditions tested for the chlorination reaction.[a]*

Entry	T [ $^\circ\text{C}$ ]	tr [min]	Yield <b>3</b> <sup>[b]</sup> (%)
1 <sup>[c]</sup>	85	60	80
2 <sup>[c]</sup>	100	60	100
3 <sup>[c]</sup>	110	30	100
4 <sup>[c]</sup>	125	15	70
5 <sup>[c]</sup>	150	15	70
6 <sup>[d]</sup>	100	30	100
7 <sup>[d]</sup>	100	15	85

[a] See the Experimental Section for the reaction conditions. [b] Conversions were determined by  $^1\text{H}$  NMR, after evaporation of the solvent. [c] Flow stream A: **2** (1 M) in toluene/DMF (9:1) containing 0.1 equiv imidazole; flow stream B:  $\text{SOCl}_2$  in toluene (3 M). [d] Flow stream A: **2** in DMF containing 1 % imidazole; flow stream B: neat  $\text{SOCl}_2$ .

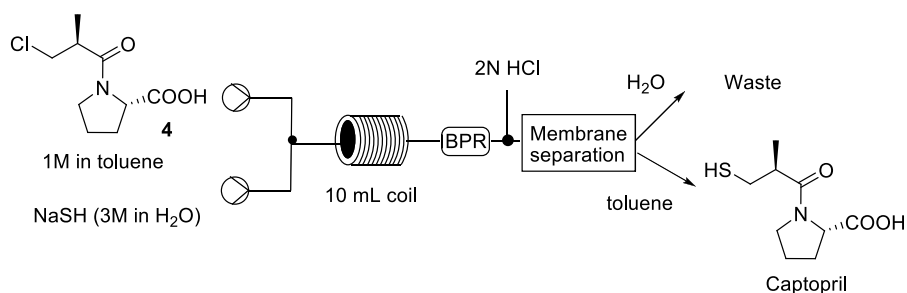
Intermediate **3** was then submitted to amide coupling with l-proline (Scheme 4). Because the final goal was to have all the synthetic steps in-line, without a break in the workflow, we decided to use for this reaction the same solvent as in the previous step.



*Scheme 4. The coupling reaction using a 2 mL reactor coil. Pressure: 200 psi*

Thus, **3** was dissolved in toluene (1 M solution), mixed with an aqueous basic (NaOH, 3 equiv) solution of L-proline (2 M solution, 2 equiv) and flowed into a 2 mL perfluoroalkoxy alkane (PFA) reactor coil. The reaction was performed at room temperature, without cooling, and was rapid, giving full conversion within only 1 min of residence time. In-line acidification to pH 2 followed by a liquid–liquid separation using a Zaiput separator were performed, affording the desired product **4**.

The final step was the nucleophilic substitution of the chlorine with the thiol group (Scheme 5). Again, we used toluene as an organic solvent and the reaction was studied in a biphasic system toluene/degassed water, used to reduce the possible formation of oxidized byproducts.



*Scheme 5. The nucleophilic substitution using a 10 mL reactor coil. Pressure: 200 psi*

To perform the substitution, an excess of NaSH (3 equiv) was efficiently used. An in-line acidification followed by a liquid–liquid separation allowed captopril to be obtained from the organic phase that was evaporated and analyzed by <sup>1</sup>H NMR spectroscopy. Temperature

and residence time were optimized and the results are summarized in Table 2. The reaction was complete in 30 min at 125 °C (Table 2, entry 4).

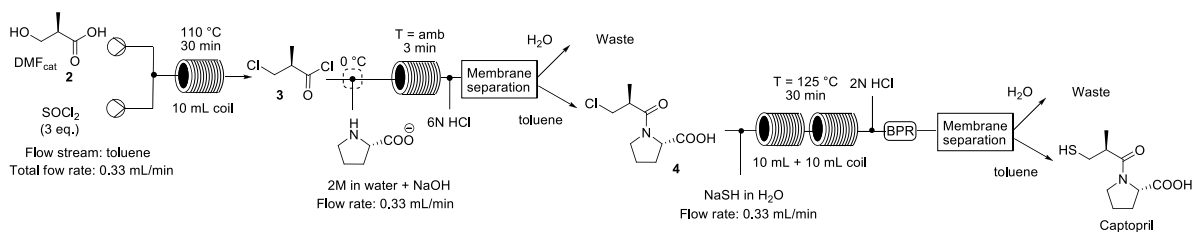
Table 2. Conditions tested for the nucleophilic substitution.<sup>[a]</sup>

Entry	T [°C]	tr [min]	Yield <b>3</b> <sup>[b]</sup> (%)
1	50	60	70
2	80	60	90
3	100	60	93
4	125	30	100
5	125	15	75

[a] See the Experimental Section for the reaction conditions. [b] Conversions were determined by <sup>1</sup>H NMR spectroscopy after evaporation of the solvent.

Once the reactions were separately optimized, we next developed a continuous multistep production of captopril that would be sufficiently robust for multiple hours of continuous work (Scheme 6). We assembled the system such that the product stream from the chlorination reaction, obtained using the conditions reported in Table 1 (entry 3), was immediately submitted to the coupling reaction in a toluene/water biphasic system, as described above. To this end, first we evaluated the amount of NaOH necessary to neutralize the excess acid from the chlorination step. The T-junction was cooled to 0 °C for the neutralization and, in this way, the uncontrolled exothermic neutralization and the release of large quantities of HCl vapors were avoided. In this set-up, the residence time for the coupling reaction in the 2 mL reactor coil was approximately 3 min (Scheme 6). After separation of the two phases, the exiting organic solution of compound 4 was collected in a

vial, acting as a reservoir, and then directly used for the substitution reaction. The solution was pumped into a 10 mL reactor coil after mixing with the solution of NaSH in degassed water and heated at 125 °C.



*Scheme 6. Three-step flow chemical synthesis of captopril. BPR: 200 psi*

After in-line acidification, extraction and evaporation of the solvent, the resulting crude material was purified by column chromatography to yield pure captopril as a white solid. The  $^1\text{H}$  NMR spectrum and the optical rotation matched those reported in the literature.<sup>[18]</sup>

## Conclusions

The multistep flow synthesis presented here enabled captopril to be obtained in an overall yield of 50% after crystallization. Biocatalytic oxidation facilitated the conversion of a prochiral substrate into a chiral intermediate with high enantiomeric excess. Three chemical transformations were performed without isolation of the intermediates. The separation of co-products, by-products, and excess reagents was achieved inline. These results clearly highlight the benefits of performing multi-step chemical synthesis in a flow environment. As a further advantage, our synthetic protocol benefits from the use of an environmentally friendly biocatalytic oxidation, avoiding the use of toxic chemical oxidants. The bioprocess might be further linked to the chemical transformations by optimizing the extraction of acid (**2**) with organic solvents, for example, using specific organic-acid-complexing carriers.<sup>[19]</sup> In light of a future scale-up, whereas none of the chemical steps have foreseen limitations, further efforts should be directed toward increasing the productivity of the first biocatalyzed step, which at present represents a bottleneck in the process. The new proposed protocol for the synthesis of captopril represents a powerful integration of biocatalysis and flow-chemistry technology.



# Reference

- [1] T. Tsubogo, H. Oyamada, S. Kobayashi, *Nature* 2015, 520, 329– 332.
- [2] D. Webb, T. F. Jamison, *Chem. Sci.* 2010, 1, 675 – 680.
- [3] R. L. Hartman, J. P. McMullen, K. F. Jensen, *Angew. Chem. Int. Ed.* 2011,50, 7502–7519; *Angew. Chem.* 2011, 123, 7642 – 7661.
- [4] M. Baumann, I. R. Baxendale, *Beilstein J. Org. Chem.* 2015, 11, 1194 –1219.
- [5] R. Porta, M. Benaglia, A. Puglisi, *Org. Process Res. Dev.* 2016, 20, 2– 25.
- [6] F. Molinari, R. Gandolfi, R. Villa, E. Urban, A. Kiener, *Tetrahedron: Asym-metry* 2003, 14, 2041 –2043.
- [7] E. Brenna, F. Cannavale, M. Crotti, V. De Vitis, F. G. Gatti, G. Migliazza, F. Molinari, F. Parmeggiani, D. Romano, S. Santangelo, *ChemCatChem* 2016, 8, 3796– 3803.
- [8] F. Hollmann, I. W. C. E. Arends, K. Buehler, A. Schallmeyer, B. B • hler, *GreenChem.* 2011, 13, 226 – 265.
- [9] D. Romano, R. Villa, F. Molinari, *ChemCatChem* 2012, 4, 739– 749.
- [10] A. Borrometi, A. Romano, R. Gandolfi, J. V. Sinister ra, F. Molinari, *Tetrahe-dron: Asymmetry* 2002, 13, 2345 –2349 .
- [11] A. Romano, R. Gandolfi, P. Nitti, M. Rollini, F. Molinari, *J. Mol. Catal. B* 2002, 17, 235 –240.
- [12] D. Romano, M. Contente, T. Granato, W. Remelli, P. Zambelli, F. Molinar i, *Monatsh. Chem.* 2013, 144 , 735 – 737.
- [13] S. G. Newman, K. F. Jensen, *Green Chem.* 2013, 15, 1456 – 1472.
- [14] L. Tamborini, D. Romano, A. Pinto, M. Contente, M. C. Iannuzzi, P. Conti, F. Molinari, *Tetrahedron Lett.* 2013, 54, 6090 – 6093.

- [15] L. Tamborini, D. Romano, A. Pinto, A. Bertolani, P. Conti, F. Molinari, *J. Mol. Catal. B* 2012, 84, 78–82.
- [16] M. Planchestainer, M. L. Contente, J. Cassidy, F. Molinari, L. Tamborini, F. Paradisi, *Green Chem.* 2017, 19, 372–375.
- [17] P. Zambelli, L. Tamborini, S. Cazzamalli, A. Pinto, S. Arioli, S. Balzaretto, F. J. Plou, L. Fernandez-Arrojo, F. Molinari, P. Conti, D. Romano, *Food Chem.* 2016, 190, 607–613.
- [18] G. Bashiardes, S. G. Davies, *Tetrahedron Lett.* 1987, 28, 5563–5564.
- [19] R. Leão, F. Molinari, D. M. F. Prazeres, J. M. S. Cabral, *J. Chem. Technol. Biotechnol.* 2000, 75, 617–624.
- [20] S. Wang, Z. Wang, L. Yang, J. Dong, C. Chi, D. Sui, Y. Wang, J. Ren, M. Hung, Y. Jiang, *J. Mol. Catal. A* 2007, 264, 60–65.
- [21] B. Tomaszewski, A. Schmid, K. Buehler, *Org. Process Res. Dev.* 2014, 18, 1516–1526.

Bioprocess intensification using flow  
reactors: stereoselective oxidation of  
achiral 1,3-diols with immobilized  
*Acetobacter aceti*

# Abstract

A scalable process for the stereoselective desymmetrisation of achiral 2-alkyl-1,3-diols to chiral 2-hydroxymethyl alkanolic acids was developed using a continuous-flow approach based on an immobilized whole cells-packed bed reactor. The use of immobilized cells of *Acetobacter aceti* MIM 2000/28 caused dramatically change substrate and product diffusion and thus affecting reaction rates and inhibition effects. The technological transfer from a classical batch system to an innovative flow system based on the use of a segmented gas-liquid flow regime (Taylor flow) guaranteeing high mass transfer between the gaseous and the liquid phase allowed a significant improvement of the productivity.

# Introduction

Biocatalytic oxidations are attractive reactions for the organic chemist, since they often occur with regio- and stereoselectivity under mild conditions, utilizing environmentally benign oxidants (i.e., O<sub>2</sub>)<sup>1-2</sup> and dehydrogenases of acetic acid bacteria are versatile and selective enzyme for alcohol oxidation;<sup>3-5</sup> production of structurally diverse aldehydes,<sup>5-6</sup> aldoximes,<sup>7</sup> lactones,<sup>8</sup> and carboxylic acids<sup>9-11</sup> has been achieved using whole cells of acetic acid bacteria, often with high enantioselectivity.<sup>12-13</sup> The stereoselective oxidation of achiral 2-alkyl-1,3-diols has been previously performed using free whole cells of acetic acid bacteria to afford the corresponding chiral 2-hydroxymethyl alkanolic acids.<sup>14-15</sup> Oxidation of one of the two enantiotopic primary alcohol allowed for desymmetrization of the achiral substrates, furnishing the desired 2-hydroxymethyl alkanolic acids with medium-to-high enantiomeric excesses. This microbial oxidation occurs under mild conditions, in aqueous solution at room temperature. Low productivity and side products formation were the main drawbacks of this biotransformation; in fact, concurrent formation of the corresponding  $\alpha$ -methylenic alkanolic acids and  $\alpha$ -methyl alkanolic acids, when the substituent in 2-position was ethyl, *n*-propyl or benzyl.<sup>15</sup>

Different strategies can be undertaken for improving the productivity and selectivity of a biotransformation.<sup>16</sup> Biocatalysts can be immobilized for enhancing stability and easy reuse; moreover, immobilization may dramatically change substrate and product diffusion and thus affecting reaction rates and inhibition effects.<sup>17</sup> Packed bed flow micro- and meso-reactors can ensure high surface-to-volume ratios, thus providing high heat and mass transfer rates; flow packed bed reactors generally ensure that the substrate stream flows at the same velocity through all the reactor volume with no back-mixing.<sup>18-19</sup> Flow-based biocatalysis has been recently applied for improving applications such as peptide condensation,<sup>20</sup> hydrolysis and formation of esters,<sup>21-26</sup> stereoselective carbonyl reduction,<sup>27</sup> formation of C-C bonds,<sup>28</sup> nucleoside, monosaccharide and oligosaccharide production,<sup>29-31</sup> interconversion of carbonyls and amines using transaminases.<sup>32-33</sup>

Transfer of the gas (air or pure O<sub>2</sub>) to the liquid phase is often the factor limiting the efficiency of liquid phase oxidations and a solution to increase the reaction rate is to facilitate mass transfer by increasing the interfacial area by applying a segmented gas-liquid flow

regime.<sup>34</sup> A segmented gas-liquid flow regime (Taylor flow) is characterized by gas bubbles alternating with short liquid slugs and recirculation occurs within segments of the two-phase segmented flow, providing an efficient mass transfer between the gaseous and the liquid phase.<sup>34-35</sup>

In this work, we have used immobilized cells of *Acetobacter aceti* MIM 2000/28 for the continuous flow oxidation of 2-alkyl-1,3-diols to chiral 2-hydroxymethyl alkanolic acids. The aim of the work was to intensify these bioconversions using a flow reactor.<sup>36</sup> Continuous flow-based oxidation with immobilized cells was carried out under a segmented air-water flow regime for guaranteeing high mass transfer between the gaseous and the liquid phase.

# Material and method

## General methods

$^1\text{H}$  and  $^{13}\text{C}$  NMR spectra were recorded with a 400 or 500 MHz spectrometer in  $\text{CDCl}_3$  solution at room temperature. The chemical shift scale was based on internal tetramethylsilane.

GC/MS analyses were performed by using a HP-5MS column (30 m $\times$ 0.25 mm $\times$ 0.25  $\mu\text{m}$ , Agilent). The following temperature program was employed: 60  $^\circ\text{C}$  (1 min)/6  $^\circ\text{C min}^{-1}$ /150  $^\circ\text{C}$  (1 min)/12  $^\circ\text{C min}^{-1}$ /280  $^\circ\text{C}$  (5 min).

Chiral GC analysis was performed on a Chirasil-DEX-CB (25 m $\times$ 0.25 mm $\times$ 0.25  $\mu\text{m}$ , Chrompack) column or on a DAcTBSil BetaCDX column (25 m $\times$ 0.25 mm $\times$ 0.25  $\mu\text{m}$ , Mega), installed on a gas chromatograph equipped with FID (carrier gas  $\text{H}_2$ , constant flow 3.7 mL  $\text{min}^{-1}$ ,  $t_{\text{injector}}=250$   $^\circ\text{C}$ ,  $t_{\text{detector}}=250$   $^\circ\text{C}$ ). Chiral HPLC analysis was performed on a Chiralcel OD column (4.6 mm $\times$ 250 mm, Daicel) installed on an HPLC instrument with UV detector ( $\lambda=220$  nm).

## Strain Preparation

The *A. aceti* MIM 2000/28 strain was routinely maintained on GYC agar plates [glucose (50 gL $^{-1}$ ), yeast extract (10 g L $^{-1}$ ),  $\text{CaCO}_3$  (30 g L $^{-1}$ ), agar (15 gL $^{-1}$ ), pH 6.3] at 28  $^\circ\text{C}$ . Strain was inoculated into 100 mL Erlenmeyer baffled flask containing GLY medium [yeast extract (10 gL $^{-1}$ ) and glycerol (25 gL $^{-1}$ ), pH 5; 20 mL]. After growth for 24 h (shaking at 150 rpm, 28  $^\circ\text{C}$ ), the liquid culture was entirely used to inoculate a 1 L Erlenmeyer baffled flask containing GLY medium (150 mL). Flasks were grown for 24 h at 28  $^\circ\text{C}$ , with shaking at 150 rpm. Preparation of Dry Alginate Beads Gel beads were prepared by ionotropic gelation, by following a protocol previously developed by us:<sup>[17]</sup> a 4% (w/v) sodium alginate solution was prepared in distilled water and stirred until a homogeneous clear solution was formed. The solution was allowed to settle for 2 h in order to eliminate the air bubbles. The alginate solution was then gently mixed in a 1:1 (w/w) ratio with a suspension of *A. aceti* cells (40 ODmL $^{-1}$ ) in sodium acetate buffer (20 mM, pH 6). The resulting mixture was then pumped

drop wise into a slightly agitated  $\text{CaCl}_2$  solution (0.2 M). Calcium alginate beads were agitated for 20 min, then filtered, washed with deionized water and dried at 25 °C for 16 h.



# Results

## Biotransformations with immobilized cells

*Acetobacter aceti* MIM 2000/28 was immobilized in dried alginate beads, which proved suited for preparing packed bed reactor used under flow conditions. Firstly, immobilized cells were used for the oxidation of different 2-alkyl-1,3-diols. Commercially available 2-methyl-1,3-propanediol **1a** was firstly used as current substrate for optimizing the biotransformation. Substrate concentration, buffer pH, and immobilized cells concentration were used as control parameters and optimization was carried out using a Multisimplex approach; conversion and enantiomeric excess of the product were the response variables. Optimized batch conditions (substrate 12mM in acetate buffer 20 mM pH 6.0, 40 mg/mL of alginate beads containing 10 mg dry weight of cells) gave (*R*)-3-hydroxy-2-methylpropanoic acid **3a** with >95% molar conversion and ee = 94% after 120 minutes. Minor amounts of the aldehyde **2a** (>10 %) were transiently observed during the reaction.

Considering the good result obtained with **1a** and the general advantages related to immobilized cells, it was decided to investigate the biotransformation of other achiral 2-alkyl-1,3-diols with alginate-immobilized *A. aceti* under the conditions optimized for **1a** (Table 1).

Table 1 Oxidation of achiral 2-substituted 1,3-diols **1a–e** with immobilized cells of *Acetobacter aceti* 2000/28. <sup>[a]</sup> Conversions calculated by <sup>1</sup>HNMR of the crude mixture after the indicated reaction time. <sup>[b]</sup> Enantiomeric excesses measured by chiral GC or HPLC analysis after treatment with CH<sub>2</sub>N<sub>2</sub>.

entry	Substrate	R	<b>2</b> (%) <sup>[a]</sup>	<b>3</b> (%) <sup>[a]</sup>	ee ( <b>3</b> ) (%) <sup>[b]</sup>	Time (h)
1	<b>1a</b>	Me	5	86	94 ( <i>R</i> )	1
2	<b>1a</b>	Me	-	> 95	94 ( <i>R</i> )	2
4	<b>1b</b>	Et	-	> 97	60 ( <i>R</i> )	5
5	<b>1c</b>	<i>n</i> -Bu	-	> 97	61( <i>R</i> )	5

7	<b>1d</b>	<i>n</i> -Pent	-	> 97	88 ( <i>S</i> )	6
8	<b>1e</b>	Bn	-	86	34 ( <i>R</i> )	24

All the tested substrates gave the desired chiral 2-hydroxymethyl alkanolic acid as major product and only small amounts of the intermediate aldehydes were observed during the reaction; reaction rates show a strong dependence on the steric hindrance of that C2. Interestingly, immobilized cells were much more chemoselective, since only traces (< 2%) of  $\alpha$ -methylenic alkanolic acids and  $\alpha$ -methyl alkanolic acids (the by-products observed with free cells) were detected, even at prolonged times (72 h). Compared with the biotransformation performed with the free cells,<sup>15</sup> higher selectivity was observed. These results can be justified considering that cells entrapment alters substrate and product diffusion through the solid support, as already observed in literature using similar systems.<sup>5,17</sup>

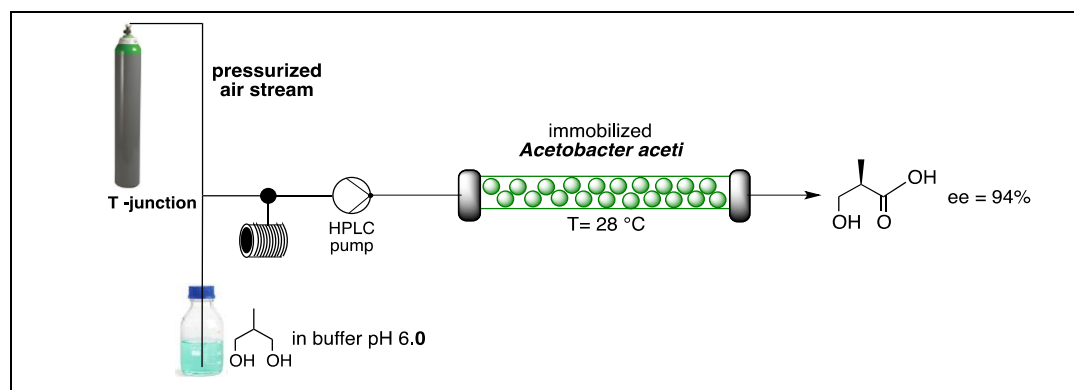
### Oxidation in a flow reactor

Dry alginate beads (400 mg containing 100 mg of dry cells) were packed into a glass column (i.d. 15 mm) and swelled until they triplicate their volume by flowing a 20 mM acetate buffer (pH 6) through the column (flow rate: 400  $\mu$ L/min, 60 min). The final volume of the bed was 5.3 mL. Optimization of the conditions in the flow reactor was carried out using compound **1a**. No traces of biotransformation were found when the column was simply fed with 1 g/L solution of **1a** in acetate buffer, no matter the flow rate employed. This failure was ascribed to lack of available oxygen in the flow stream, since in *A. aceti*, PQQ-dependant alcohol dehydrogenases need molecular oxygen to regenerate the reducing potential of the cells. Actually, while in batch conditions the continuous agitation allows oxygen availability through air-liquid mixing, in the flow reactor buffer solution is confined inside microtubes and the initial oxygen content was insufficient to accomplish the reaction. In order to feed oxygen and buffer solution simultaneously and to favour oxygen dissolution in the aqueous phase, a segmented gas-liquid flow was applied. Pressurized air was directed to a T junction, where it merged with the liquid phase containing the substrate. Oxidation of **1a** run with segmented gas-liquid regime was successfully performed through the flow reactor containing the DALGE-immobilized cells. Temperature was kept constant at 28 °C, while flow rate and substrate concentration were varied (Table 2). The reaction rate  $r_f$  for the flow reactions was calculated from the concentration of the formed product (P expressed

as  $\mu\text{mol/mL}$ ), the flow rate of the liquid phase ( $F$  expressed as  $\text{mL/min}$ ), and the mass of the biocatalyst expressed as dry weight of the cells employed ( $m$  expressed as  $\text{g dry weight}$ ) according to Eq. 1.

$$r_{flow} = \frac{[P] \cdot F}{m} \left( \frac{\mu\text{mol}}{\text{min} \cdot \text{g}} \right)$$

*Table 2 Continuous enantioselective oxidation of 1a with immobilized Acetobacter aceti MIM 2000/28 in flow reactor. <sup>[a]</sup> Specific reaction rate was calculated according to Eq. 1. <sup>[b]</sup> Conversions calculated by 1HNMR of the crude mixture after the indicated reaction time.*



Entry	[1a] (mM)	Flow rate (mL/min)	$r^{[a]}$ ( $\mu\text{mol/min g}_{\text{dry cells}}$ )	Molar conversion (%) <sup>[b]</sup>
1	12	0.015	1.80	> 97
2	12	0.030	3.60	> 97
3	12	0.060	4.68	65
4	24	0.015	3.60	> 97
5	24	0.030	7.20	> 97
6	24	0.060	7.34	51
7	48	0.015	4,32	60
8	48	0.030	5.09	41
9	48	0.060	8.07	28

Total conversion was obtained with substrate concentration of 12-24 mM (entries 2 and 5) with flow rates between 15-30  $\mu\text{L/min}$ , whereas at higher substrate concentrations and low

flow rate (entry 7) satisfactory rates were observed but without complete conversion of the substrate.

The continuous flow reaction was performed over 24 hours using 24 mM 1a (Figure 1). Biocatalyst productivity was calculated as mmol of (*R*)-3-hydroxy-2-methylpropanoic acid **3a** produced per g of dry cells employed. Enantioselectivity was checked, showing the same enantiomeric excess (94%) observed in the batch reaction.

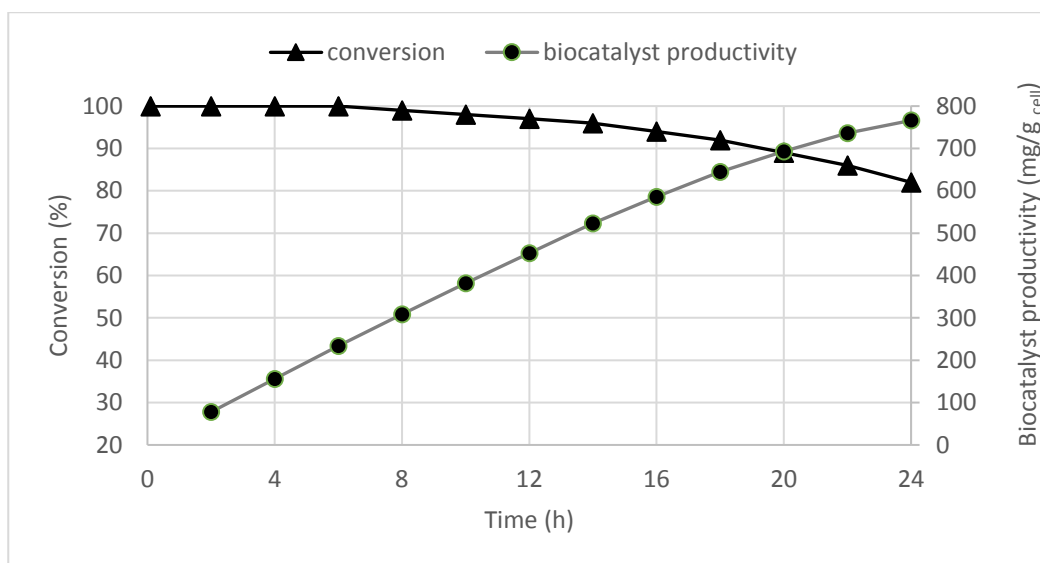


*Figure 1 Continuous enantioselective oxidation of 1a (24 mM in the flow stream) with immobilized Acetobacter aceti MIM 2000/28 in flow reactor. Biocatalyst productivity is defined as the amount of product (mmol) formed per dry weight of biocatalyst*

An in-line purification step was applied, consisting of a Ambersep 900 OH- resin, able to quantitatively catch the acid contained in the outstream (Figure 2).

## Conclusions

Desymmetrisation of achiral 1,3-diols with *Acetobacter aceti* has been previously shown to be an effective procedure for the preparation of enantiomerically enriched hydroxymethyl alkanolic acids. Batch reaction with free cells carried out in conventional shake flasks showed also formation of the corresponding  $\alpha$ -methylenic alkanolic (**3**) and  $\alpha$ -methyl alkanolic (**4**) acids. Immobilization in Ca-alginate, beyond the advantages of easier work up and potential catalyst reusability, was found to be an excellent tool for improving the selectivity of the reactions with respect to the use of cell free systems. As further improvement, the oxidation of diols **1a** was developed under continuous-flow conditions, exploiting the application of alginate beads in a packed-bed reactor. A segmented air-water flow regime (which ensured high mass transfer between the gaseous and the liquid phase) was applied allowing for high rates. The overall bioprocess was strongly intensified, since a remarkable reduction of the reactor size was achieved, while yields and biocatalyst productivity were improved. In order to evaluate the efficiency of the air flow-system, the immobilized cells of *Acetobacter aceti* will be used with the other 2-alkyl-1,3-diols already tested in batch system.

# References

- 1 F. Hollmann, I. W. C. E. Arends, K. Buehler, A. Schallmeyer, B. Bühler, *Green Chem.* 2011, 13, 226-265; N.J. Turner, *Chem. Rev.* 2011, 111, 4073– 4087.
- 2 D. Gamemara, G. A. Seoane, P. Saenz-Mendez, P. Dominguez de Maria, *Redox Biocatalysis*, John Wiley & Sons, Hoboken New Jersey, 2012.
- 3 N. Saichanaa, K. Matsushita, O. Adachi, I. Frébort, J. Frebortova, *Biotechnol. Adv.* 2015, 33, 1260-1271.
- 3 T. Yakushi, K. Matsushita, *Appl. Microbiol. Biotechnol.* 2010, 86, 1257-1265.
- 4 D. Romano, R. Villa, F. Molinari, *ChemCatChem* 2012, 4, 739-749.
- 5 O. Adachi, T. Yakushi, *Membrane-bound dehydrogenases of acetic acid bacteria*, in *Acetic Acid Bacteria* (Eds.: K. Matsushita, H. Toyama, N. Tonouchi, A. Okamoto-Kainuma), Springer, Tokyo, 2016.
- 5 R. Gandolfi, K. Cavenago, R. Gualandris, J. V. Sinisterra Gago, F. Molinari, *Process Biochem.* 2004, 39, 747-751.
- 6 R. Villa, A. Romano, R. Gandolfi, J. V. Sinisterra Gago, F. Molinari, *Tetrahedron Lett.* 2002, 43, 6059-6061.
- 7 P. Zambelli, S. Pinto, D. Romano, E. Crotti, P. Conti, L. Tamborini, R. Villa, F. Molinari, *Green Chem.* 2012, 14, 2158-2161.
- 8 D. Romano, M. Contente, T. Granato, W. Remelli, P. Zambelli, F. Molinari, *Monatsh Chem.* 2013, 144, 735-737.
- 9 J. Svitel, E. Sturdik, *Enzyme Microb. Technol.* 1995, 17, 546- 550.
- 10 F. Molinari, R. Villa, F. Aragozzini, P. Cabella, M. Barbeni, *J. Chem. Technol. Biotechnol.* 1997, 70, 294-298.

- 11 H. Habe, T. Shimada, T. Yakushi, H. Hattori, Y. Ano, T. Fukuoka, D. Kitamoto, M. Itagaki, K. Watanabe, H. Yanagishita, K. Matsushita, K. Sakaki, *Appl. Environ. Microbiol.* 2009, 75, 7760-7766.
- 12 A. Romano, R. Gandolfi, P. Nitti, M. Rollini, F. Molinari, *J. Mol. Catal. B* 2002, 17, 235-240.
- 13 G. Keliang . W. Dongzhi, *Appl. Microbiol. Biotechnol.* 2006, 70, 135-139.
- 14 F. Molinari, R. Gandolfi, R. Villa, E. Urban, A. Kiener, *Tetrahedron: Asymmetry* 2003, 14, 20141-2043.
- 15 E. Brenna, F. Cannavale, M. Crotti, V. De Vitis, F. G. Gatti, G. Migliazza, F. Molinari, F. Parmeggiani, D. Romano, S. Santangelo *ChemCatChem* 2016, 8, 3796-3803
- 16 C. Garcia-Galan, A. Berenguer-Murcia, R. Fernandez-Lafuente, R. C. Rodrigues, *Adv. Synth. Catal.* 2011, 53, 2885-2904.
- 17 L. Mignot, G. A. Junter, *Appl. Microbiol. Biotechnol.* 1990, 32, 418-423.
- 18 C. Wiles, P. Watts, *Green Chem.* 2012, 14, 38-54.
- 19 J.M. Bolivar, J. Wiesbauer, B. Nidetzky, *Trends Biotechnol.* 2011, 29, 333-342.
- 20 P. Falus, L. Cerioli, G. Bajnoczi, Z. Boros, D. Weiser, J. Nagy, D. Tessaro, S. Servi, L. Poppe, *Adv. Synth. Catal.* 2016, 358, 1608-1617.
- 21 C. Csajagi, G. Szatzker, E. R. Toke, L. Urge, F. Darvasa, L. Poppe, *Tetrahedron: Asymmetry* 2008, 19, 237-246.
- 22 I.I. Junior, M.C. Flores, F.K. Sutili, S.G.F. Leite, L.S. de M. Miranda, I.C.R. Leal, R.O.M.A. de Souza, *Org. Process Res. Dev.* 2012, 16, 1098-1101.
- 23 L. Tamborini, D. Romano, A. Pinto, A. Bertolani, F. Molinari and P. Conti, *J. Mol. Catal. B Enzym.* 2012, 84, 78-82.
- 24 I. Itabaiana, L.S. de M. Miranda, R.O.M.A. De Souza, *J. Mol. Catal. B: Enzym.* 2013, 85-86, 1-9.

- 25 L. Tamborini, D. Romano, A. Pinto, M. Contente, M. C. Iannuzzi, P. Conti, F. Molinari, *Tetrahedron Lett.* 2013, 54, 6090-6093.
- 26 S.S. Wang, Z. J. Li, S. Sheng, F. A. Wu, J. Wang, *J. Chem. Technol. Biotechnol.* 2016, 91, 555-562.
- 27 F. Dall'Oglio, M. L. Contente, P. Conti, F. Molinari, D. Monfredi, A. Pinto, D. Romano, D. Ubiali, L. Tamborini, I. Serra, *Cat. Commun.* 2017, 93, 29-32.
- 28 J. Lawrence, B. O'Sullivan, G.J. Lye, R. Wohlgemuth, N. Szita, *J. Mol. Catal. B Enzym.* 2013, 95, 111-117.
- 29 E. Calleri, G. Cattaneo, M. Rabuffetti, I. Serra, T. Bavaro, G. Massolini, G. Speranza, D. Ubiali, *Adv. Synth. Catal.* 2015, 357, 2520-2528.
- 30 L. Babich, A.F. Hartog, L.J.C. van Hemert, F.P.J.T. Rutjes, R. Wever, *ChemSusChem* 2012, 5, 2348-2353.
- 31 P. Zambelli, L. Tamborini, S. Cazzamalli, A. Pinto, S. Arioli, S. Balzaretto, F.J. Plou, L. Fernandez-Arrojo, F. Molinari, P. Conti, D. Romano, *Food Chem.* 2016, 190, 607-613.
- 32 L.H. Andrade, W. Kroutil, T.F. Jamison *Org. Lett.* 2014, 16, 6092-6095.
- 33 M. Planchestainer, M.L. Contente, J. Cassidy, F. Molinari, L. Tamborini, F. Paradisi, *Green Chem.* 2017, 19, 372-375.
- 34 H. P. L. Gemoets, Y. Su, M. Shang, V. Hessel, R. Luque, T. Noel, *Chem. Soc. Rev.*, 2016, 45, 83-117
- 35 A. Gunther, M. Jhunjhunwala, M. Thalmann, M. A. Schmidt, K. F. Jensen, *Langmuir* 2005, 21, 1547-1555.
- 36 J. M. Bolivar, J. Wiesbauer, B. Nidetzky, *Trends Biotechnol.* 2011, 29, 333-342.



# Biotransformation of limonene from citrus peel into food relevant additives

Work in progress

# Abstract

(*R*)-limonene is an abundant component of citrus peel and its modification into compounds with higher commercial value seems very attractive. Biocatalytic hydroxylation of (*R*)-limonene into (*R*)-perillyl alcohol is interesting, since the product is a promising candidate for chemo prevention and cancer therapy; moreover, perillyl alcohol can be used as substrate for preparing flavours (perillaldehyde) and sweeteners (perillartine) by applying chemoenzymatic techniques. Hydroxylation of (*R*)-limonene into (*R*)-perillyl alcohol will be studied using recombinant whole cells harbouring an optimized redox gene operon (CYP153A6) which encodes a cytochrome P450, a ferredoxin, and a ferredoxin reductase from *Mycobacterium* sp. strain HXN-1500 by using the broad-host-range vector pET100. Selective and cost-effective methods for the modification of (*R*)-perillyl alcohol into perillaldehyde and perillartine will be developed. Finally, the bioprocesses will be intensified applying continuous flow chemistry reactors.

# Introduction

Limonene is one of the most common terpenes in nature, being a major component of several citrus oils and therefore a cheap by-product of the citrus processing industry. Depending on the source, the enantiomeric composition of limonene may vary: (*R*)-limonene (*D*-limonene) is largely predominant in orange, lemon, grapefruit, mandarin, and bergamot, whereas, citronella and lemongrass oils mostly contain (*S*)-limonene (*L*-limonene). Concentration of (*R*)-limonene in orange and grapefruit oils may reach 95%. (*R*)-Limonene is a thin and transparent oil obtained from the manufacturing of citrus pulp pellets, used in the biodegradable solvents and cleaning products and in the manufacturing of synthetic resins and adhesives. Citrus peel is an important food supply chain waste occurring in Italy in high volumes and it is suited for the combined extraction of known marketable chemicals such as (*R*)-limonene, pectin, and flavonoids<sup>1</sup>. Therefore, valorization of (*R*)-limonene by its transformation into high value-added compounds interesting for the food and pharmaceutical industries is a valid economical option. One way to conveniently valorise limonene is to perform selective hydroxylations by enzymatic means<sup>2</sup>.

Enzymatic hydroxylation of limonene may occur at different position (Fig 1): monooxygenation of the double bonds at position 1,2 and 8,9 gives the corresponding epoxides, endocyclic hydroxylations are reported at position 3 and 6 furnishing isopiperitenol and carveol, respectively, whilst hydroxylation of the C7 methyl affords perillyl alcohol. The latter hydroxylation is attractive from a preparative point of view, since perillyl alcohol is a promising candidate for chemoprevention and cancer therapy<sup>3</sup>.

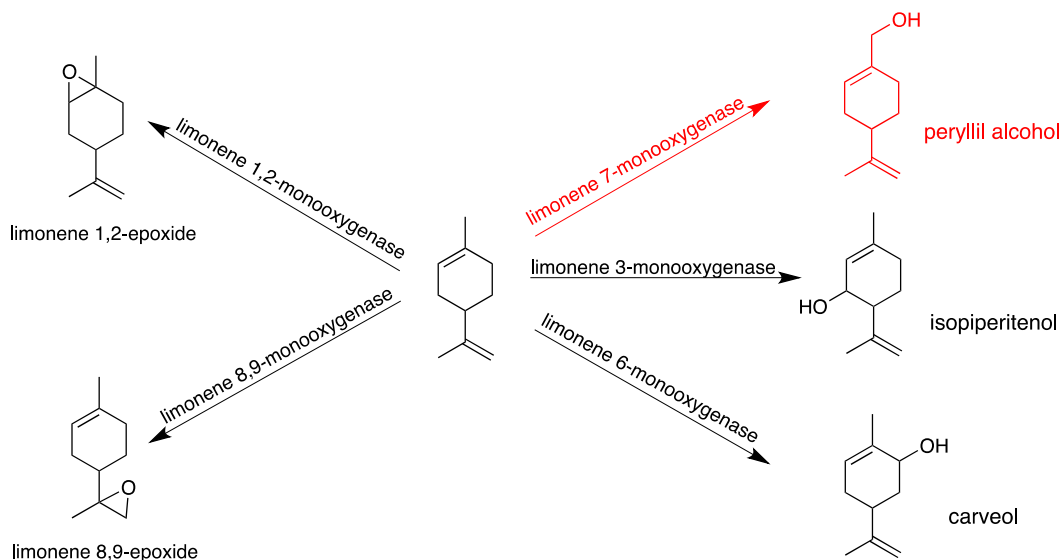


Fig. 1 Possible route for limonene oxidation

Cytochrome P450 (CYP) monoxygenases are a group of enzymes able to selectively introduce a hydroxyl group into an unfunctionalized C–H-bonds under mild reaction conditions, using molecular oxygen as oxidizing agent; The set-up of CYP-based bioprocesses in industry is hampered by low space- time yields<sup>4</sup>, since problems like protein solubility, co-expression of different proteins for efficient cofactor recycling, and toxic effects of substrates/products must be circumvented.

Whole wild-type cells of bacteria and fungi have been used for performing hydroxylation of limonene, but recovery of the corresponding alcohols or epoxides is complicated by further modifications, where the intermediate alcohol is further oxidized to perillic acid through the action of unspecific alcohol and aldehyde dehydrogenases<sup>5</sup>. Screening of 1800 bacterial strains showed limonene 7-monoxygenases have been found in different alkane degraders<sup>6</sup>.

Not always the limonene 7-monoxygenases found in nature are totally selective concerning the position of hydroxylation. A limonene hydroxylase containing 444 amino acid residues has been isolated from *Bacillus stearothermophilus* BR388 (now *Geobacillus stearothermophilus*) and cloned in *E. coli*; this enzyme shows limited regioselectivity, being able to hydroxylate limonene at C6 (giving carveol) and C7 (giving perillyl alcohol)<sup>7</sup>.

Biocatalytic limonene oxidation using CYP153A6 provides an alternative and selective method for 7-hydroxylation of limonene. This cytochrome P450 system from *Mycobacterium* HXN 1500, including catalytic domain (CYP153; *ahpG*), ferredoxin reductase (FdR; *ahpH*), and ferredoxin (Fd; *ahpI*), has proved very selective and has been used for obtaining recombinant whole cells suited for the biotransformation of limonene into perillyl alcohol<sup>6</sup>.

Hydroxylation of (*S*)-limonene to (*S*)-perillyl alcohol was obtained using recombinant bacterial cells harbouring the cytochrome P450 CYP153A6 from *Mycobacterium* sp. strain HXN-1500; among the different expression systems used, *E. coli* W3110 harbouring both CYP153A6 and the alkane transporter *AlkL* showed good limonene hydroxylation activities, giving (*S*)-perillyl alcohol with high selectivity<sup>8</sup>. With a different approach, Alonso-Gutierrez et al. (2013)<sup>9</sup> engineered a strain of *E. coli* with a heterologous mevalonate pathway and limonene synthase for production of limonene followed by coupling with a cytochrome P450, which specifically hydroxylates limonene to produce perillyl alcohol.

In this project, we will employ the chemically competent strain of *Escherichia coli* BL21 Star™ (DE3), which has been transformed by co-expression of the redox gene operon which encodes a cytochrome P450, a ferredoxin, and a ferredoxin reductase from *Mycobacterium* sp. strain HXN-1500 by using the broad-host-range vector pET100. This T7 expression vector allowed for high-level expression because the T7 RNA polymerase is more processive than native *E. coli* RNA polymerase and is dedicated to the transcription of the genes of interest. The recombinant strain so far obtained appears to be like a suited biocatalyst for the selective hydroxylation of (*S*)- and (*R*)-limonene into (*S*)- and (*R*)-perillyl alcohol. We will use the immobilized recombinant whole cells system (*E. coli*) for the selective hydroxylation of limonene in a flow reactor for the preparation of perillyl alcohol.

Two products of the oxidation of perillyl alcohol have great interest in the food industry: perillyl aldehyde (or perillaldehyde used as a flavor component)<sup>10</sup> and perillyl aldehyde oxime (or perillartine, a sweetener that is about 2000 times as sweet as sucrose). Perillyl alcohol can be further oxidize to perillyl aldehyde using alcohol dehydrogenases both as isolated enzymes or whole cells (Scheme 2). A green synthetic method for the one-pot preparation of aldoximes in water was developed<sup>11</sup>; the method is based on the combination

of the enzymatic oxidation of primary alcohols to aldehydes using different alcohol dehydrogenase of acetic acid and *in situ* condensation of the aldehydes with hydroxylamine.

The main aims of this project is the preparation of recombinant strains of *E. coli* able to efficiently convert limonene into perillyl alcohol: with the following set-up of cascade reactions using *Acetobacter aceti* MIM 2000/28 for the preparation of food-valuable molecules such as perillaldehyde and perillartine from limonene in a continuous system.

The overall result of the project will be a platform of chemoenzymatic transformations for the preparation of different molecules of practical interest starting from limonene.

# Material and Method

## **CYP153A6 cloning**

The synthetic gene encoding CYP153A6 operon has been designed and amplified using the following primer:

Forward: 5'-CACCATATGACCGAAATGACCGTGGC-3'

Reverse: 5'-ATTGCTCGAGTCAATGCTGCGCGGC-3'

The amplified gene was then cloned into the pET100/D-TOPO<sup>®</sup> vector (Invitrogen) and correct construct sequence was confirmed by DNA sequencing (Eurofins Biolab Srl).

## **Expression of recombinant CYP153A6**

Expression of the recombinant CYP153A6 operon was performed using BL21(DE3)Star E. coli strain harboring pET100-CYP53A6 expression vectors. Starter cultures were prepared growing 0,2 mL of glycerol stock of recombinant strain for overnight at 37 C in Erlenmeyer flasks containing 20 mL of broth with 100 mg/mL ampicillin added. Cultures were diluted with the same media to a starting OD<sub>600 nm</sub> of 0.1 and then incubated at 37 C on a rotatory shaker at 180 rpm. Cells were grow until 0.8 OD/mL and induced with 0.5 mM of IPTG and further incubated for 4h or 16 h at 28 °C on rotatory shaker at 180 rpm.

The following liquid media were used: Luria–Bertani (LB: 10 g/L bacto-tryptone, 5 g/L yeast extract, 10 g/L NaCl), Super Broth (SB: 32 g/L bacto-tryptone, 20 g/L yeast extract and 5 g/L NaCl), Terrific Broth (TB: 12 g/L bacto-tryptone, 24 g/L yeast extract, 8 g/L glycerol, 17 mM KH<sub>2</sub>PO<sub>4</sub> and 72 mM K<sub>2</sub>HPO<sub>4</sub>). . Experiments were carried out in 1 L baffled Erlenmeyer flasks containing 200 mL of liquid media.

## **Crude extract preparation**

Cell pellets were re-suspended in freshly prepared sodium phosphate buffer (5 mL per gram of wet cells) 100 mM, pH 7, and sonicated for five cycles of 30 s each, on ice. The insoluble fraction was removed by centrifugation at 13,000 rpm for 1 h at 4 °C.

### **Biotransformation condition**

Biotransformations were carried out in 5 mL screw capped tube, in a final volume of 1 mL of sodium phosphate buffer 100 mM, pH 7 using 9 mg of crude extract and adding 100  $\mu$ L of stock solution of NADH (5 mg/mL). The substrates were added at the final concentration of 7 mM, dissolved in ethanol at the final concentration of 1%. Incubations were carried out with magnetic stirring at 30 °C.

### **Analytical methods**

The conversion and stereochemical outcome of the biotransformations were determined by gas chromatographic analyses using a chiral capillary column (DMePeBeta-CDX- PS086, MEGA, Legnano, Italy), having 0.25 mm-diameter, 25 m-length and 0.25  $\mu$ m-thickness. With the following thermal gradient: starting from 80 °C increase until 110 °C in 3 minutes, maintain 110 °C for 9 minutes and then increase until 180 °C in 7 minutes and maintain 180 °C for 10 minutes.



## Result and discussion

The chemically competent strain of *Escherichia coli* BL21 Star™ (DE3) has been transformed by expression of the redox synthetic gene operon (CYP153A6) which encodes a cytochrome P450, a ferredoxin, and a ferredoxin reductase from *Mycobacterium* sp. strain HXN-1500 by using the broad-host-range vector pET100. This strain *Escherichia coli* BL21 Star™ (DE3) harbouring CYP153A6 will be used in this project.

### **Optimization of recombinant *E. coli* for the transformation of limonene into perillyl alcohol**

The expression of the genes of interest will be indirectly analysed evaluating the perillyl alcohol production using the whole growing cells of the recombinant *E.coli* in the biotransformation of limonene, followed by gas-chromatography, since their differentiation in gel electrophoresis is difficult. Particular attention has been dedicated to the highly volatile limonene; for this purpose, the screening for the optimized conditions will be carried out using septum-sealed vials. These biotransformation have allowed to obtain a good amount of perillyl alcohol (between 90 mg/L and 140 mg/L after 24h) but with low reproducibility, may be due to highly volatility of substrate coupled with the long biotransformation time. In order to resolve this problem, the possibility to use the crude extract to perform the limonene conversion has been evaluated; this approach has allowed to obtain a lower biotransformation time (1h compared to 24h of the growing cells) reducing the evaporation effect ensure availability of substrate for all reaction time. Therefore, the induction study has been performed using directly crude extract as biocatalyst in the bioconversion of limonene.

Initially, the recombinant CYP153A6 was expressed in standard condition: LB broth induced by addition of 0.5 mM IPTG at an OD<sub>600</sub> nm of 0.8–1 (mid-exponential growth phase). Then, *E. coli* cells transformed with harbouring plasmid cells were incubated for an additional 4 h at 28 °C. Under these conditions, limonene monooxygenase specific activity of 1.6 mU/mg, corresponding to a volumetric productivity of 0.4 U/L and a specific productivity of 0.7 U/g of dry cells.

In order to improve the productivity of the laboratory-scale microbial process for the recombinant limonene monooxygenase, we first investigated the effect of medium composition on the growth both non-induction and induction culture at 28 °C and on their enzyme productivity. Growth curve evaluation was carried out monitoring the increase in the absorbance every hour. Three different media containing various combinations of carbon (glycerol) and nitrogen sources (yeast extract and tryptone), NaCl and phosphate buffer were analysed.

The observed specific growth rates is higher in SB (0.45/h) respect compared to results obtained with LB and TB (respectively 0.38/h and 0.31/h); no significant difference was found making the comparison between the non-induced and induced culture. Moreover, SB media has allowed to get the higher biomass level in comparison to LB and TB, in particular high biomass production of 2.9 g/L were achieved in SB while were obtained 0.6 g/L and 1.8 g/L respectively in LB and TB.

Beside higher biomass production, SB medium also sustained the higher limonene monooxygenas expression, measured as volumetric productivity and specific productivity. Growing the cells using the standard induction condition, in SB medium gave up a 4-fold increase, in comparison to the enzyme produced under standard conditions while the specific activity achieved in LB and SB medium, is comparable (Fig.1).

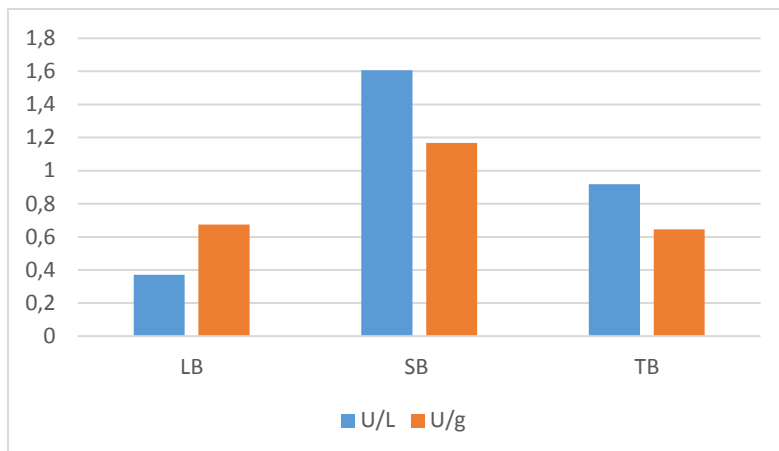


*Fig. 1 Production of limonene monooxygenase using different media, expressed as U/L (blue bars) and U/g dry weight cell (orange bars) after induction with 0.5 mM IPTG at middle-exponential phase (cells collected after 4 h at 28 °C).*

Since *E. coli* transformed cells grew with a different kinetics and reached variable level of biomass production depending on medium composition, limonene monooxygenase expression was studied with extend growth and induction time (collecting the cells after 16 h of induction). The results, in term of volumetric productivity and specific activity, confirm that the higher activity in the crude extract was achieved using SB medium, but without obtain an improvement compared the previous condition.

## Conclusion and future perspectives

The induction study will be continue evaluating different parameters such temperature, IPTG concentration and induction in different grow phase. The best induction condition will be used for immobilization study on the whole cell but also on the crude extract since has shown comparable results in term of perillyl alcohol production (between 100 mg/L and 130 mg/L after 1h). Using the immobilized whole cells guarantee the recycling of the cofactor essential for the reaction, but at the same, the antimicrobial effect of limonene, limit its use in high concentration in bioconversion. On the other hand, using the immobilized crude extract the main problem will be to find a method to recycle the cofactor, since the continue addition is too expensive in development of bioprocess.

To ensure the continuous supply of oxygen to the reaction the continuous process will be developed using the air flow system previously described in the second chapter. To permanently ensure the availability of the hydrophobic and volatile substrate in the liquid phase, loss of limonene, will be avoided by using limonene-saturated air.

Once, the flow reactor for the production of perillyl alcohol will be optimized, it will be studied the possibility to obtain perillaldehyde and perillartine as well. The recovered perillyl alcohol will be flown in a packed-bed reactor containing immobilized acetic acid bacteria, able to oxidize the substrate into the corresponding aldehyde.

Alternatively, the corresponding aldoxime (perillartine) will be prepared using a one-pot chemo-enzymatic reaction which combines the oxidation of perillyl alcohol by acetic acid bacteria with condensation of the produced aldehyde with hydroxylamine.

The continuous reactors will be optimized evaluating best conditions of flow streams, residence times and substrate concentrations. In these cases, an aqueous stream will be use, since perillyl alcohol is partially soluble in water.



## References

1. Pfaltzgraff, L. A., De bruyn, M., Cooper, E. C., Budarin, V. & Clark, J. H. Food waste biomass: a resource for high-value chemicals. *Green Chem.* **15**, 307 (2013).
2. Duetz, W. A., Bouwmeester, H., Beilen, J. B. & Witholt, B. Biotransformation of limonene by bacteria, fungi, yeasts, and plants. *Appl. Microbiol. Biotechnol.* **61**, 269–277 (2003).
3. Da Fonseca, C. O. *et al.* Efficacy of monoterpene perillyl alcohol upon survival rate of patients with recurrent glioblastoma. *J. Cancer Res. Clin. Oncol.* **137**, 287–293 (2011).
4. Julsing\_et\_al-2012-Biotechnology\_and\_Bioengineering.pdf.crdownload.
5. Ferrara, M. A. *et al.* Bioconversion of R- (+)-limonene to perillic acid by the yeast *Yarrowia lipolytica*. *Brazilian J. Microbiol.* **1080**, 1075–1080 (2013).
6. Van Beilen, J. B. *et al.* Biocatalytic production of perillyl alcohol from limonene by using a novel *Mycobacterium* sp. cytochrome P450 alkane hydroxylase expressed in *Pseudomonas putida*. *Appl. Environ. Microbiol.* **71**, 1737–1744 (2005).
7. Cheong, T. K. & Oriel, P. J. Cloning and expression of the limonene hydroxylase of *Bacillus stearothermophilus* BR388 and utilization in two-phase limonene conversions. *Appl. Biochem. Biotechnol.* **84–86**, 903–915 (2000).
8. Cornelissen, S. *et al.* Whole-cell-based CYP153A6-catalyzed (S)-limonene hydroxylation efficiency depends on host background and profits from monoterpene uptake via AlkL. *Biotechnol. Bioeng.* **110**, 1282–1292 (2013).
9. Alonso-Gutierrez, J. *et al.* Metabolic engineering of *Escherichia coli* for limonene and perillyl alcohol production. *Metab. Eng.* **19**, 33–41 (2013).
10. Pyo, S.-H. *et al.* A new route for the synthesis of methacrylic acid from 2-methyl-1,3-propanediol by integrating biotransformation and catalytic dehydration. *Green Chem.* **14**, 1942 (2012).

11. Zambelli, P. *et al.* One-pot chemoenzymatic synthesis of aldoximes from primary alcohols in water. *Green Chem.* **14**, 2158–2161 (2012).





# Products

# List of publication

1-**De Vitis, V.**, Dall'Oglio, F., Pinto, A., De Micheli, C., Molinari, F., Conti, P., Tamborini, L. (2017). Chemoenzymatic synthesis in flow reactors: A rapid and convenient preparation of captopril. *ChemistryOpen*, doi:10.1002/open.201700082

2-Romano, D., Valdetara, F., Zambelli, P., Galafassi, S., **De Vitis, V.**, Molinari, F., Vigentini, I. (2017). Cloning the putative gene of vinyl phenol reductase of *dekkera bruxellensis* in *saccharomyces cerevisiae*. *Food Microbiology*, 63, 92-100. doi:10.1016/j.fm.2016.11.003

3-Brenna, E., Cannavale, F., Crotti, M., **De Vitis, V.**, Gatti, F. G., Migliazza, G., Santangelo, S. (2016). Synthesis of enantiomerically enriched 2-hydroxymethylalkanoic acids by oxidative desymmetrisation of achiral 1,3-diols mediated by *acetobacter acetii*. *ChemCatChem*, 8(24), 3796-3803. doi:10.1002/cctc.201601051

4-Contente, M. L., Guidi, B., Serra, I., **De Vitis, V.**, Romano, D., Pinto, A., Molinari, F. (2016). Development of a high-yielding bioprocess for 11- $\alpha$  hydroxylation of canrenone under conditions of oxygen-enriched air supply. *Steroids*, 116, 1-4. doi:10.1016/j.steroids.2016.09.013

5-Contente, M. L., Serra, I., Brambilla, M., Eberini, I., Gianazza, E., **De Vitis, V.**, Romano, D. (2016). Stereoselective reduction of aromatic ketones by a new ketoreductase from *pichia glucozyma*. *Applied Microbiology and Biotechnology*, 100(1), 193-201. doi:10.1007/s00253-015-6961-y

6-**De Vitis, V.**, Guidi, B., Contente, M. L., Granato, T., Conti, P., Molinari, F., Romano, D. (2015). Marine microorganisms as source of stereoselective esterases and ketoreductases: Kinetic resolution of a prostaglandin intermediate. *Marine Biotechnology*, 17(2), 144-152. doi:10.1007/s10126-014-9602-z

7-Contente, M. L., Molinari, F., Zambelli, P., **De Vitis, V.**, Gandolfi, R., Pinto, A., & Romano, D. (2014). Biotransformation of aromatic ketones and ketoesters with the non-conventional yeast *Pichia glucozyma*. *Tetrahedron Letters*, 55(51), 7051-7053. doi:10.1016/j.tetlet.2014.10.133

## Congress proceedings

1-Guidi B., Ferraboschi P., Ciceri S., Contente M.L., **De Vitis V.**, Molinari F. *Biocatalytic approach for the preparation of pramipexole*. Biotrans. Wien, Austria, July 2015.

2-**De Vitis V.**, Romano D., Molinari F. *Biocatalysis in seawater*, Biotrans. Wien, Austria, July 2015.

3-**De Vitis V.**, Romano D., Molinari F. *Acetic acid bacteria cell factories*, XX Workshop on the Developments in the Italian PhD Research on Food Technology and Biotechnology, Perugia, Italy, September 2015

4-**De Vitis V.**, Tamborini L, Romano D., Brenna E., Crotti M., and Molinaria F. *Desymmetrization of achiral 2-alkyl-1,3-diols by microbial oxidation and development of a flow-based strategy for its continuous application*, GRC, Biddeford, Maine, USA, July 2016.

5-**De Vitis V.** *Acetic acid bacteria cell factories*, XX Workshop on the Developments in the Italian PhD Research on Food Technology and Biotechnology, Perugia, Italy, Settembre 2016

6-**De Vitis V.**, Romano D., Dall'Oglio F., Tamborini L., Molinari F. *BIOCATALYTIC OXIDATION IN A FLOW SYSTEM*, Biotrans. Budapest, Hungary, Luglio 2017